COMPOSITIONAL ANALYSIS OF GLASS SURFACES AND THEIR REACTION IN AQUEOUS ENVIRONMENTS

By

CARLO GEORGE PANTANO, JR.

A DISSERTATION PRESENTED TO THE GRADUATE COUNCIL OF
THE UNIVERSITY OF FLORIDA
IN PARTIAL FULFILLMENT OF THE REQUIREMENTS FOR THE
DEGREE OF DOCTOR OF PHILOSOPHY

UNIVERSITY OF FLORIDA

1976

Engng.

To Jackie

5-77

ACKNOWLEDGEMENTS

The author wishes to express his gratitude to three extremely capable advisors, G. Y. Onoda, Jr., D. B. Dove and L. L. Hench. Each in his own way has offered invaluable encouragement and advice throughout the course of this work. The research training and experience provided by their involvement is most appreciated.

In addition, thanks are extended to A. E. Clark and D. E. Clark for helpful discussions about glass surfaces. The technical assistance of F. Ohuchi, S. Gould and B. Molnar is also acknowledged.

Finally, the author acknowledges the Glass Container Industry Research Corporation for providing a portion of the initial equipment grant which made this work possible.

TABLE OF CONTENTS

LIST OF FIGURES

Abstract of Dissertation Presented to the Graduate Council of the University of Florida in Partial Fulfillment of the Requirements for the Degree of Doctor of Philosophy

COMPOSITIONAL ANALYSIS OF GLASS SURFACES AND THEIR REACTION IN AQUEOUS ENVIRONMENTS

By

Carlo George Pantano, Jr.

June, 1976

Chairman: George Y. Onoda, Jr.
Major Department: Materials Science and Engineering

Of particular concern in the study of glass surface reactions is the analysis for chemical and structural information at the outermost atomic layers and to depths of the order of 1000 Å beneath the surface. This work describes a method of investigating the surface composition of multicomponent silicate glasses with Auger electron spectroscopy (AES). Subsequently, the method is applied to study particular aspects of the glass-water reaction.

Special problems arise when AES is applied to these electrically insulating materials due to the accumulation of electrical charge upon the sample. While Auger spectra may usually be obtained by utilizing a glancing angle of incidence for the exciting electron beam, nevertheless significant electric fields may be developed at the

surface of the glass sample and this commonly produces a significant migration of mobile cations.

In order to investigate the behavior of alkali ions in the surface region of primarily soda-lime-silicate glasses, measurements were made using a beam current of a few microamps and the sample temperature was lowered to about 100°K. Using these conditions, quite stable measurements of sodium ions could be obtained. By removing surface layers during the AES measurement by Ar-ion bombardment, composition profiles of the outer region of the glass were determined.

It has been found that for soda-lime-silicate glass surfaces which have not undergone special surface treatments, the presence of an alkali-enriched layer at the surface appears to be a common characteristic. By producing clean glass surfaces in vacuum by ion bombardment and subsequently reacting them in situ, it was shown that exposure of a bulk glass surface to air containing water vapor induces sodium segregation at the surface. Depth profiles indicated that under the sodium-enriched surface existed a relatively sodium-depleted region. This supported the hypothesis that the increased sodium concentration on the surface resulted from ion exchange between the sodium at the surface and in the subsurface with hydrogen from the adsorbed water vapor. Hence, it has been concluded that soda-lime-silicate glass is capable of reacting rapidly with water vapor in air to

produce the characteristic surface composition profile observed initially.

Upon reaction of the glass with static aqueous solution, depth profiles clearly indicated regions at the surface depleted of alkali and alkaline earth species. The effects of composition, temperature and solution pH were interpreted on the basis of these profiles. By means of an empirical calibration method, the measured profiles have been put on a semiquantitative level. Solution analysis results correlated with the interpretation of these surface compositional profiles. It has been determined that surface composition profiles of this kind must be interpreted with regard to the dynamic equilibrium they represent between leaching and dissolution.

The peculiar surface compositional behavior of "bioglass," a specially designed invert soda-lime-silicate glass containing a small addition of phosphorous, was also investigated. It was found that in aqueous solution a film formed on the surface rich in calcium and phosphorous oxides. It has been suggested that this is an important phenomenon responsible for the biocompatibility of this material with bone hydroxyapatite structures.

CHAPTER I

INTRODUCTION

Overview

Reactions between alkali-alkaline earth-silicate glass and an aqueous phase (gas or liquid) have been studied for many years. This class of chemical reactions has been of particular importance with regard to the practical corrosion properties of commercial soda-lime-silicate glasses [1]. Although it is generally believed that glass is relatively chemically inert, the multi-component glass-water interaction is found to be a complex phenomenon capable of significantly altering the glass surface chemistry. The most widespread method for investigation of this reaction monitors changes in the composition of the solution which is in contact with the glass surface. This provides a direct measure of the glass decomposition products. Extensive studies of this kind have characterized the effects of time, temperature, solution composition, glass composition, pH, etc., upon the rate of reaction [2]. Recently, the technique of infrared reflection spectroscopy (IRRS) has been applied [3] to

measure directly the structural changes which occur at the reacted glass surface. It is clear, however, that compositional effects at the glass surface are not readily measured by either of these methods, and perhaps not at all in the early stages of reaction. Over the years, the absence of this information has hampered the confirmation (or exclusion) of theories proposed for glass surface reactions, particularly when the aqueous phase is gaseous. Presently, this compositional information should be obtainable using recently developed surface analytical techniques [4] such as Auger electron spectroscopy (AES), electron spectroscopy for chemical analysis (ESCA), secondary ion mass spectroscopy (SIMS), ion scattering spectroscopy (ISS), and photon emission induced during ion etching. The technique of Auger electron spectroscopy has been chosen for the present investigation owing to its applicability, availability, speed of data aquisition, and capability for at least semiquantitative analysis. Unfortunately, AES does not detect hydrogen, a significant reactant at glass surfaces. Although SIMS can detect hydrogen, it has particular problems with regard to quantitative analysis.

Auger electron spectroscopy [5] has been used extensively to analyze the surface composition and surface impurities of a variety of thin films [6, 7] and metals [8, 9]. The method probes a solid surface with sensitivity

to surface layers whose thickness is in the 10-50Å range. When combined with *in situ* ion-milling [10], composition versus depth information (i.e., a surface composition profile) can be obtained. Due to certain difficulties encountered when analyzing insulating materials with AES, however, investigations of multicomponent glass surfaces are lacking [4].

The purpose of this research, therefore, is two-fold. First, an AES technique is developed which is suitable for the compositional analysis of, primarily, alkali-alkaline earth-silicate glass surfaces. Clearly, the method developed is generally applicable to glass surface investigations. The major obstacle to overcome in that development is associated with mobile ion migration induced by electron irradiation [11]. Subsequently, the technique is applied to the compositional analysis of soda-lime-silicate glass which has reacted with an aqueous environment. Experiments are designed to test existing theories of the glass-water reaction which have been formulated in the absence of such data.

Compositional Effects at Glass Surfaces

In general, differences in composition may occur between the bulk and the surface or near surface region of a multicomponent glass [12-14]. In many cases these

compositional variations are initiated, and in some cases limited, within angstroms of the surface. Hence, the requirement for a sufficiently surface-sensitive tool, such as AES, is apparent.

This is undoubtedly true with regard to simple adsorption phenomena at a glass surface. Exposure of a freshly formed glass surface to a gaseous environment containing water vapor is known to result in chemisorption of hydroxyl ions and physisorption of water [12]. If the glass is multicomponent, reactions can occur between the adsorbed water layers and components of the glass. This effect is particularly evident when the glass contains alkali ions. Presently utilized surface techniques observe this effect only after extensive reaction. IRRS and electron microprobe analysis (EMP) require reacted surface layers thousands of angstroms thick. Scanning electron microscopy (SEM) requires at least the formation of surface precipitates. Hence, these techniques observe these weathering phenomena [15] after long exposure to severe conditions, e.g., high temperature, high relative humidity, etc. The reaction products which form in the very early stages of interaction have not been experimentally determined but are believed to be of importance in the mechanism of subsequent attack. It has been suggested by Charles [16] that the triggering reaction for

this attack is a sodium-hydrogen ion-exchange at the surface. The hydrogen ion is presumably derived from water adsorbed on the glass surface. The hydroxyl ion liberated by the dissociation of water then acts to break down the silicate network. This mechanism suggests, therefore, that segregation of sodium at the glass surface may occur upon exposure to water vapor. He points out that although this hypothesis is only qualitatively based, it does explain many experimental observations, particularly the accelerated attack of soda-lime-silicate glass exposed to super-heated steam. Tichane [17] attempted to measure the initial stages of this reaction using replica electron microscopy. Using high temperature treatments, morphological changes at the surface were observed. He interpreted these changes to be a result of soda segregation at the surface as predicted by the Charles theory. In view of the severe treatments employed in these studies, it is not clear whether the theory is applicable under ambient conditions. Since this reaction may be of critical importance to the static fatigue and general degradation of soda-lime-silicate glass, the compositional changes which accompany the proposed reaction should be verified. AES should have sufficient sensitivity to detect the surface compositional changes which accompany the initial stages of reaction, even at room temperature and under ambient humidity conditions.

Likewise, exposure of multicomponent glass surfaces to static aqueous solution results in corrosive reaction. A number of workers have investigated this phenomenon in great detail [18-20]. Almost exclusively, those studies utilized solution analysis to measure the glass decomposition products. Sanders and Hench have combined IRRS with solution analysis to deduce surface structural changes [3]. In general, the results of these studies are interpreted on the basis of surface composition changes.

Clearly, the reaction between soda-lime-silicate glass and water is extremely complex and is not completely understood. Most theories are based on an initial ion exchange reaction between hydrogen ions in the water and sodium ions in the glass (diffusion-limited process). The sodium-deficient surface layer then grows thicker, thereby retarding the further extraction of sodium. Depending upon the solution pH and temperature, the silica-rich surface layer may or may not be subject to breakdown and hence determines to some extent the overall glass solubility. Because the solution pH changes with time at a rate dictated by the glass reactivity (composition, temperature, etc.), the effect is most complex. One study suggested that above 80°C network breakdown is dominant while below 80°C the diffusion process dominates

[21]. Also, the role of calcium is not clear. Wang and Tooley [22] hypothesized that calcium is released into solution only through silicate network breakdown. Zagar and Schillmoller [21], however, suggest that removal of alkaline earth ions may also take place by diffusion. It is the author's belief that these studies of the glass-water reaction have been hampered by a lack of the surface compositional information necessary to resolve the uncertainties pointed out above. AES analysis, however, provides a direct means of measuring the composition of the surface which had been in contact with solution from time zero until equilibrium (if any) is reached. When AES is combined with *in situ* ion-milling, it is possible to measure directly a surface compositional profile for the reacted surface.

The recent development of a large range of biomaterials has demanded suitable techniques for research investigations of biomaterial surfaces. The discovery of a surface-active, invert soda-lime-silicate "bioglass" which bonds to living bone in animals has provided a biomaterial surface of great interest [23, 24]. Presently, this bioglass is being studied extensively with regard to chemical and mechanical properties in the aqueous physiological environment. Chemical effects at the surface are critically important [25]. The first interaction between

a biomaterial and physiological environment undoubtedly involves the outermost layer of atoms within the material surface. This outer layer of atoms usually interacts first with the physiological solution environment, perhaps involving the adsorption of various ions or charged species from solution. Conversely, this atom layer may preferentially release certain material species into solution. In either case, the initial condition of the outermost atom layer of the biomaterial may be of critical importance. Likewise, changes in that layer in the early stages of (simulated) physiologic exposure is of importance, particularly as it relates to subsequent chemical reactions of the material and histo-chemical reactions of the tissue. Hence, it is crucial that biomaterial surface reactions be investigated on this scale. Compositional surface analysis with sensitivity to such thin layers is possible using AES.

In addition to these largely academic interests in the AES analysis of aqueous reactions at glass surfaces, there exist a number of commercially important phenomena. The fabrication of glasses, and in particular their surfaces, results in compositional effects within thin surface layers. Conventional press and blow processing of glass containers results in exposure of a hot, freshly formed surface to the factory environment. In most cases, this

environment contains water vapor and sulfur gases. Since these species are known to react chemically with multi-component glasses, changes in surface composition are expected [26]. The actual changes which do occur, however, have not been characterized. Likewise, the specific treatment of these container surfaces in order to provide increased chemical [27] and mechanical [28] durability results in surface composition changes. The treatment of hot inside container surfaces with sulfur [26] or fluorine [29] containing gases is believed to improve chemical durability via a change in composition at and near the surface. Also, treatment of the outside surface of the containers with $SnCl_4$ or $TiCl_4$ results in the formation of an ultrathin metal-oxide coating which improves scratch resistance [30]. Treatment with an organic emulsion leads to the production of an ultrathin organic film on the surface which provides increased lubricity to the glass container [31]. These commercially significant surface treatments are certainly amenable to investigation using the method developed.

Research Plan

The research carried out is an initiatory effort in the sense that AES has not previously been applied to a complete analysis of alkali-alkaline earth-silicate

glass surfaces. Therefore, a large portion of the work is devoted to developing appropriate techniques specific to the analysis of multicomponent glass surfaces, as well as accomplishing composition analyses of general surfaces of interest.

Goldstein and Carlson [32] have measured Auger spectra for an alkali-strontium-silicate glass while Rynd and Rastogi [33] have used AES to characterize glass fiber surfaces. Chappell and Stoddart [34] have investigated the effect of the float glass process upon surface composition using AES. Recently, Anderson, Bacon and Byrum [35] have attempted a study of sulfur and fluorine surface treatments using AES. Finally, the author has applied AES to examine a sequence of chemical reactions at a "bio-glass" surface upon aqueous attack [36, 37]. A common result of the above studies was the absence of sodium at the surface. This result, by itself, could suggest that the surfaces of soda-containing glasses are depleted of sodium. However, the experience of these and other [38-40] workers has been that mobile ions such as sodium are difficult to measure in a glassy matrix using electron beam techniques.

Chapter II provides a brief introduction to the AES technique and discusses some AES spectra for both fused silica and multicomponent alkali silicate glass. The peculiar difficulties associated with AES analysis of

glass are discussed. Critical conditions for the technique are defined. These experimental conditions are maintained throughout the remainder of the work.

Because of the importance attributed to sodium in surface reactions of soda-lime-silicate glass, it is necessary to develop suitable methods for its measurement during AES analysis. Hence, Chapter III is devoted to the investigation of mobile ion migration during AES measurements. Although the investigation is specific to sodium migration, the qualitative results should apply to mobile alkali ions in general. In addition to defining appropriate measures for carrying out mobile ion AES analysis, a mechanism for this migration effect is presented. The results are also discussed with regard to similar migration effects reported during EMP analysis.

On the basis of the work presented in Chapters II and III, an analytical procedure for analysis of mobile ions at glass surfaces is developed. This completes the first objective of this work.

Chapter IV considers the effect of the ambient environment upon the surface composition of soda-lime-silicate glass of commercial composition. The previous section discussed the importance of such data in light of the existing theory of water vapor attack. Furthermore, since all glass specimens must be exposed to the

ambient prior to AES analysis, all surfaces are subject to possible reaction. In fact, the author and others have reported the observation of particular composition profiles at soda-lime-silicate surfaces prepared or exposed in the ambient environment. The present investigation is accomplished by preparing clean glass surfaces in vacuum by ion bombardment and subsequently reacting them in situ.

A method for semiquantitative analysis of the measured AES spectra and AES composition profiles is presented. A discussion concerning the interpretation of the composition profiles with regard to the ion-milling process is also included. These methods of data analysis are utilized, where applicable, throughout the remainder of the work.

Chapter V is devoted to a presentation of surface composition profiles which result upon reaction of soda-lime-silicate glass with static aqueous solution. The effects of temperature, pH and buffering action upon the surface composition profile are discussed. The effect of glass-water reaction upon the glass surface composition has long been of interest, particularly with regard to corrosion. Crucial experiments are designed which address the points raised in the last section. In particular, the proposed ion-exchange reactions at the glass surface are investigated. This ionic transfer should produce

gradients in composition at and in the surface of the glass after reaction. In general, depletion of the modifying ions (Na and Ca) is expected. This work provides a direct measurement of such composition profiles. The breakdown of the resulting silica-rich surface is also studied. Silica-rich surface films produced by the sodium release are subsequently reacted at a higher temperature and in a replenished solution. Previous work has suggested that breakdown of the film depends upon both temperature and the concentration of reaction products released to solution [18]. Hence, this work represents an attempt to isolate those effects.

Finally, Chapter VI applies the techniques and concepts developed above to a specially designed invert soda-lime-silicate glass ("bioglass"). Initial studies by the author have established that the formation of a multilayer surface film [36] on the glass surface occurs upon exposure to a buffered aqueous solution. The previous work, however, did not include sodium AES analysis owing to the difificulties already pointed out. In the absence of that data, the mechanism of film formation could not clearly be deduced. The present study is aimed at characterizing the evolution of surface composition for bioglass in pure water and buffered solution. A model which describes the formation and role of the surface films which

develop is presented. Although the scope of the bioglass investigation is by no means exhaustive, an identification of potentially important surface reactions should provide a framework for future studies.

CHAPTER II

APPLICATION OF AES TO GLASS SURFACES

Auger Electron Spectroscopy: Review of Theory and Technique

The theory and technique of AES analysis has been extensively developed over several years [4]. When a surface is bombarded with energetic electrons (or other particles) some electrons are ejected from the inner shell levels of atoms in the excited surface region. Deexcitation may then occur by an outer shell electron dropping to the vacant inner level with the ejection of another electron. Thus the ejection energy of an Auger electron involves the difference in energy between three electronic states and is therefore readily estimated from known X-ray energies. Figure 1 shows schematically the sequence of events in the Auger electron effect.

The measurement of Auger electron energies, therefore, provides a direct method of identification of atomic species at or within a few atomic layers of the surface. The surface sensitivity is determined primarily by the Auger electron escape probability. All elements

AUGER TRANSITION

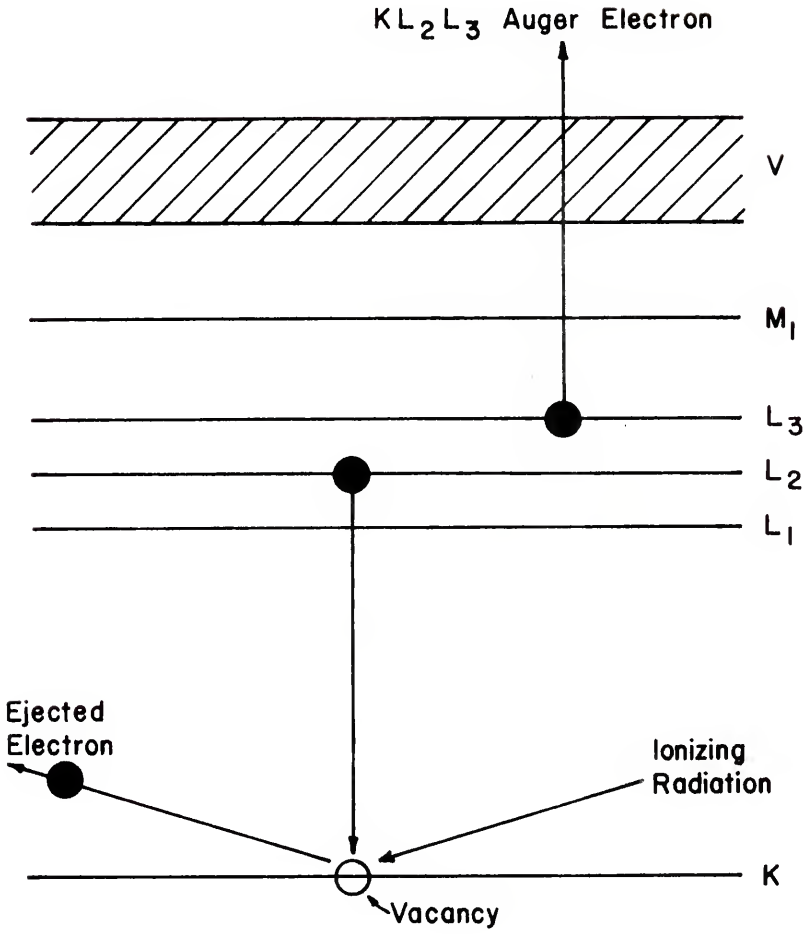

Figure 1. Schematic representation of the sequence of events during Auger transition.

except hydrogen and helium can be detected by the presence of one or many Auger electron peaks at particular characteristic energies.

An Auger spectrum is obtained by bombarding the surface with an electron beam, typically a few keV in energy. Electrons leaving the surface enter an electron spectrometer commonly of retarding grid or cylindrical dispersive analyzer type. The dispersive analyzer [41] has a considerably superior signal to noise ratio than the retarding grid system and offers better sensitivity and resolution at both low and high electron energies. Owing to the presence of a large background of secondary and back-scattered electrons the Auger peaks are most easily resolved by operating the analyzer in a mode which yields a series of differentiated peaks. AES spectra are therefore differential spectra.

Once the Auger spectrum for the sample has been obtained, identification of atoms in the surface region is straightforward. Comparison of the measured Auger peak energies recorded in the spectrum with a table [42] of principal Auger electron energies provides a means of atomic identification. Since most elements undergo a number of Auger transitions, each of which is recorded in the spectrum, peak overlap seldom presents a problem in identification. Hence, the extraction of qualitative information from the AES spectrum is clear.

The extraction of quantitative information from the measured Auger spectrum is somewhat less straightforward [43]. The current measured for a particular Auger transition is directly proportional to the number of those atoms in the detected surface region. Thus, the integrated area under the Auger peak is proportional to the surface concentration. If the analyzer constants (transmission, acceptance, angle, etc.), primary beam current, ionization cross-section and back-scattering factors are known, these together with the measured Auger current (integrated area under the peak) can be used to obtain absolute concentration for monolayer surface coverages. For greater than monolayer coverages, the escape depth function for Auger electrons must also be known. The Auger current may be obtained from the usual "differential" Auger spectrum using integration techniques [44] and background subtraction [45].

In many cases, making an evaluation of relative concentration for a particular element from one specimen to another is of primary interest. Such semiquantitative information can be obtained more easily than absolute concentration. Since the surface concentration is proportional to the area under the Auger peak in the secondary electron energy spectrum, peak-to-peak heights of the differentiated Auger signals are also proportional to concentration, provided the peak shapes are identical. Hence,

under certain circumstances, peak-height interpretation can provide quantitative information. In the simplest case, the mere comparison of peak-heights can yield information about relative concentrations. A method using Auger peak-heights for semiquantitative analysis of alkali-alkaline earth-silicate glass surface composition is presented in detail in Chapter IV.

In some investigations, it is of interest to know the manner in which the composition varies as a function of depth into the surface. This surface compositional profile indicates the gradients in chemical composition from the surface into the bulk of the material. This profiling can be accomplished by simultaneously measuring AES spectra and removing surface material to expose atom layers below the original surface [10]. Removal of surface material is carried out utilizing inert ion bombardment. This procedure is described schematically in Figure 2. In this instance, monitoring peak-to-peak heights as a function of ion-milling time provides an indication of the concentration gradients in the surface. If the peak-heights are quantitatively interpreted and the ion-milling rate is known, a surface compositional profile, i.e., a composition versus depth plot, can be obtained. This method is also described in Chapter IV for an alkali-alaline earth-silicate glass.

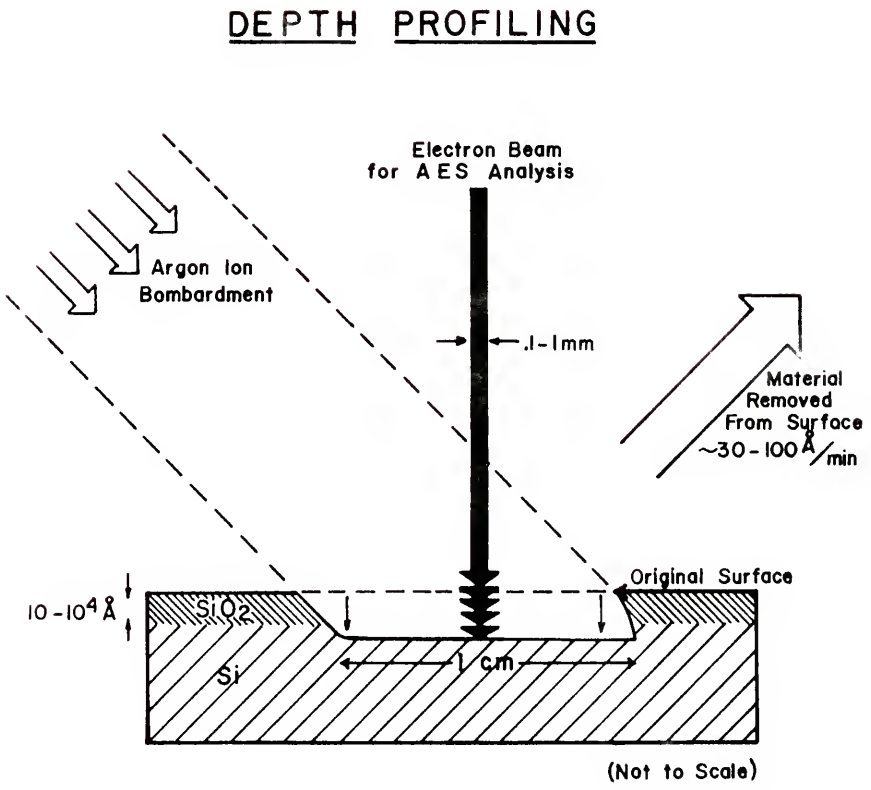

Figure 2. Schematic description of simultaneous AES analysis and inert gas sputtering for obtaining in-depth composition profiles.

Present Experimental Arrangement

The AES technique probes a solid surface with electron and ion beams and hence must be carried out in vacuum. Although the vacuum requirements for electron and ion beam production are not critical, maintainence of the sample surface is of importance. AES analysis, therefore, is carried out in high vacuum.

The working chamber is a stainless steel cylinder having a 20 inch diameter and 25 inch length. It contains 28 flanged parts through which various components can be inserted into the working area. All flange gaskets are metal type. Likewise, the valves operate with metal seats.

The system has three gas adsorption pumps* for rough-pumping of the chamber. A 110 litre-per-second metal ion pump** is used to attain high vacuum. The ion pump is of the noble type so that inert gases such as Argon may also be pumped. The system also contains a titanium sublimation pump*** mounted within a liquid nitrogen shroud. When the chamber is filled with Argon for ion bombardment, this pump is utilized to remove active gases liberated during ion profiling. The system is also equipped with

---

*Varian, Model 941-6001

**Varian, Model 912,7007

***Varian, Model 916-0017

resistance heaters mounted upon the outside of the chamber. Baking the system accelerates the pumping time by driving adsorbed species off the inner walls.

The Auger electron spectrometer, ion gun, and sample manipulator comprise the heart of the system. Figure 3 shows schematically the geometrical arrangement of these components within the working chamber. The spectrometer* has an electron gun mounted along the axis of its cylinder. The gun can be operated at up to 5 keV and can provide a beam of up to 50 μA at a diamter of 100 μm. The electron energy analyzer is situated around and concentric to the electron gun within the spectrometer structure. This particular Auger electron spectrometer is a dispersive analyzer of the cylindrical mirror type which operates similar to a band pass filter. The electrons enter the analyzer and are filtered according to energy via their passage through two concentric cylinders between which an electric field exists. The electric field, or pass energy, is scanned from zero volts up to the primary energy. Those electrons which pass completely through the analyzer strike an electron multiplier for measurement. Differentiation is accomplished electronically by superimposing a small ac-modulation on the

*Physical Electronics Ind., Model 10-150

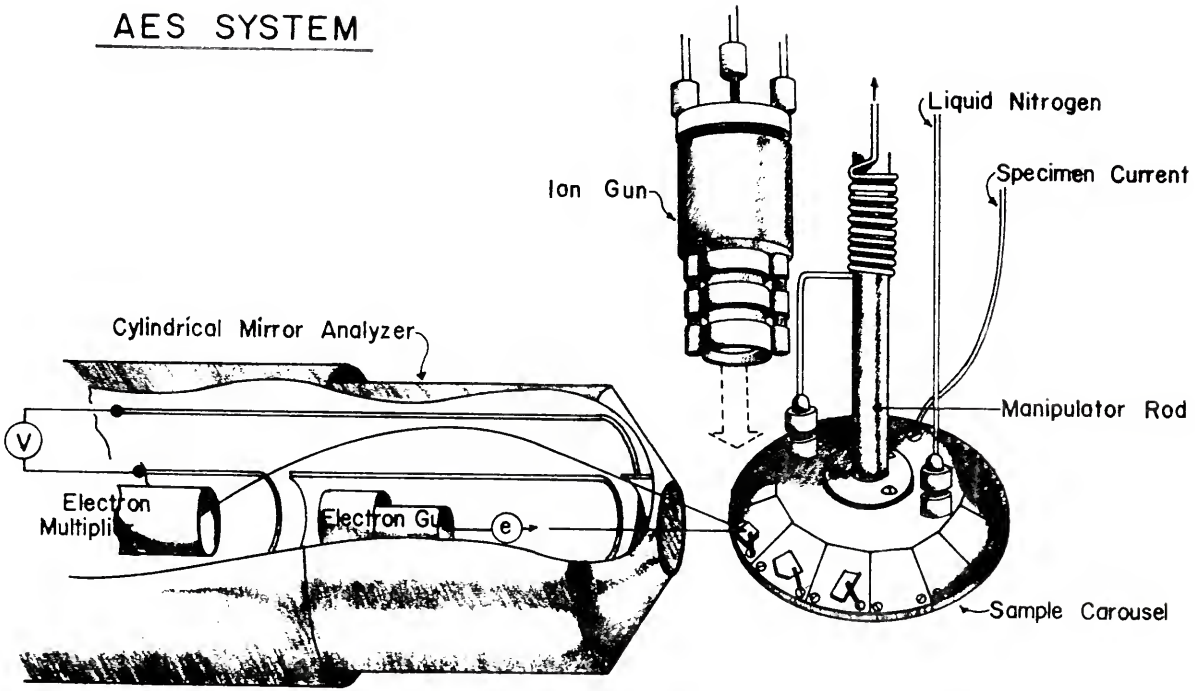

Figure 3. Experimental arrangement for AES analysis and depth profiling.

field plates. By detecting the out-of-phase component of the signal in a lock-in amplifier, the first derivation of the secondary electron energy distribution is obtained [5], i.e., the usual Auger spectrum.

Proper operation of the Auger electron spectrometer requires that the sample be situated at the focal point of the analyzer. The focal point is approximately .25 inches in front of the spectrometer structure. This point is most conveniently located by displaying the Auger spectrum upon the oscilloscope and adjusting the sample position so as to bring the elastic peak in the spectrum to the primary energy.

Ion bombardment is accomplished using an ion gun* which is directed upon the sample surface. The vacuum system is backfilled to 5×10^{-5} torr of Argon during ion milling. Under this condition, the ion gun can be operated at 2 keV to yield a beam of Ar ions with a current of 200 $\mu A/cm^2$ at a diameter of 5 mm.

To accomplish depth profiling requires simultaneously measuring Auger spectra and removing surface material by ion bombardment. It is crucial, therefore, that the most intense region of the ion beam be directed precisely at the point on the sample surface being analyzed by the

---

*Physical Electronics Ind., Model 04-161

electron beam. This ion beam focal point alignment is facilitated through the use of aluminum thin films ($\sim$500Å) deposited upon glass slides. The sample is first situated at the focal point of the analyzer using the method described above. The intersection of the electron beam and sample surface then fixes the point at which the ion beam must be directed. Upon removing the aluminum film by ion bombardment a region of the glass substrate approximately the diameter of the ion beam is exposed. If the initial direction of the ion beam was approximately correct, the focal point will be within this sputtered region. The point can be located by noting fluorescence of the electron beam upon the glass substrate surface. (This is best carried out using a microscope which can be mounted outside the vacuum chamber for examination of the sample surface in vacuum.) Suitable adjustments are then made in the ion beam direction. If the above procedure is carried out repetitively, the ion beam direction can be adjusted so as to bring the sputtered region concentric with the fluorescing beam spot. Depth profiling is best carried out under this condition.

The specimen manipulator* has a carousel sample stage permitting multiple sample loading. The face of the

*Physical Electronics Ind., Model 10-502

sample stage is situated at an angle of 45° with respect to both the electron and ion beams. This geometric arrangement is necessary for the analysis of glasses. Maintaining this proximity for all experiments adds to the consistency of the experimental results. The sample stage can be heated internally up to 300°C or be cooled by liquid nitrogen.

Development of a General Procedure: Fused Silica

Theoretically, the general process of Auger deexcitation is independent of the matrix in which an atom is contained. However, because atomic excitation is carried out using electron bombardment, the electrical characteristics of the matrix may be of importance. In particular, difficulties may arise when AES is applied to glasses owing to their insulating nature. Since AES and ion milling involve the bombardment of the surface with electrons and positive ions, atomic species at the surface are subject to local electrical fields, thermal excitation, and atomic collisional processes. These effects may then induce the migration of mobile nonnetwork cations present in multicomponent glasses. Obviously such perturbations not only make difficult the measurement of accurate AES spectra, but may also obscure the compositional profile which is under measurement.

Impingement of the electron beam at normal incidence to the glass surface leads to unstable charging. This charging condition at the glass surface is a result of the build-up of electrons in the nonconducting matrix. As a result, the surface increases in potential (negative), perhaps as high as the main beam, and may then spontaneously discharge. Hence, the surface potential varies sporadically. As a result, the energy of emitted secondary electrons and Auger electrons vary with the surface potential in an unstable way. Under these conditions, measurement of the AES spectra is not possible. When viewed on the oscilloscope, the AES spectra appears to consist of many strong signals moving in an unstable fashion along the energy coordinate.

This unstable charging condition may be prevented by maintaining the electron beam at a low angle to the sample surface. As the angle between the electron beam and sample surface is decreased, the incident electron collision cascade is confined closer and closer to the surface. This causes a large increase in the secondary electron emission which provides a positive surface potential. The potential is held stable because the surface can charge only positive enough to compensate the negative space-charge of the incident electrons. This represents a condition of dynamic equilibrium and hence, although

secondary emission is stabilized, significant electric fields may still exist in the surface. These fields may then induce the migration of charged, mobile species present in the surface; this effect is considered in a later section. Nonetheless, utilizing an angle of incidence of 45°, stable AES spectra may be measured for fused silica, as well as for a variety of multicomponent glasses.

Figure 4 provides some spectra for a fused silica glass slide* whose surface is examined in the as-received condition. The beam energy was 3 keV at .03 A/cm^2. The upper spectrum, recorded immediately upon exposure of the glass to the electron beam, should represent the original surface composition. Auger peaks are observed at 75eV (Si-LMM), 263eV (C-KLL), 510eV (O-KLL) and 1620eV (Si-KLL).

The Si signal at 75eV is due to Auger electrons whose escape range is of the order 8-9Å [5], and is referred to as the low-energy Si peak. Since this peak arises from a valence-band associated Auger transition, it may reflect changes in the chemical environment of silicon atoms in the surface region. Hence, Si in the form of SiO_2 produces an Auger peak at 75eV; Si in the form of

*Thermal American Fused Quartz Co., Montvale, N.J.

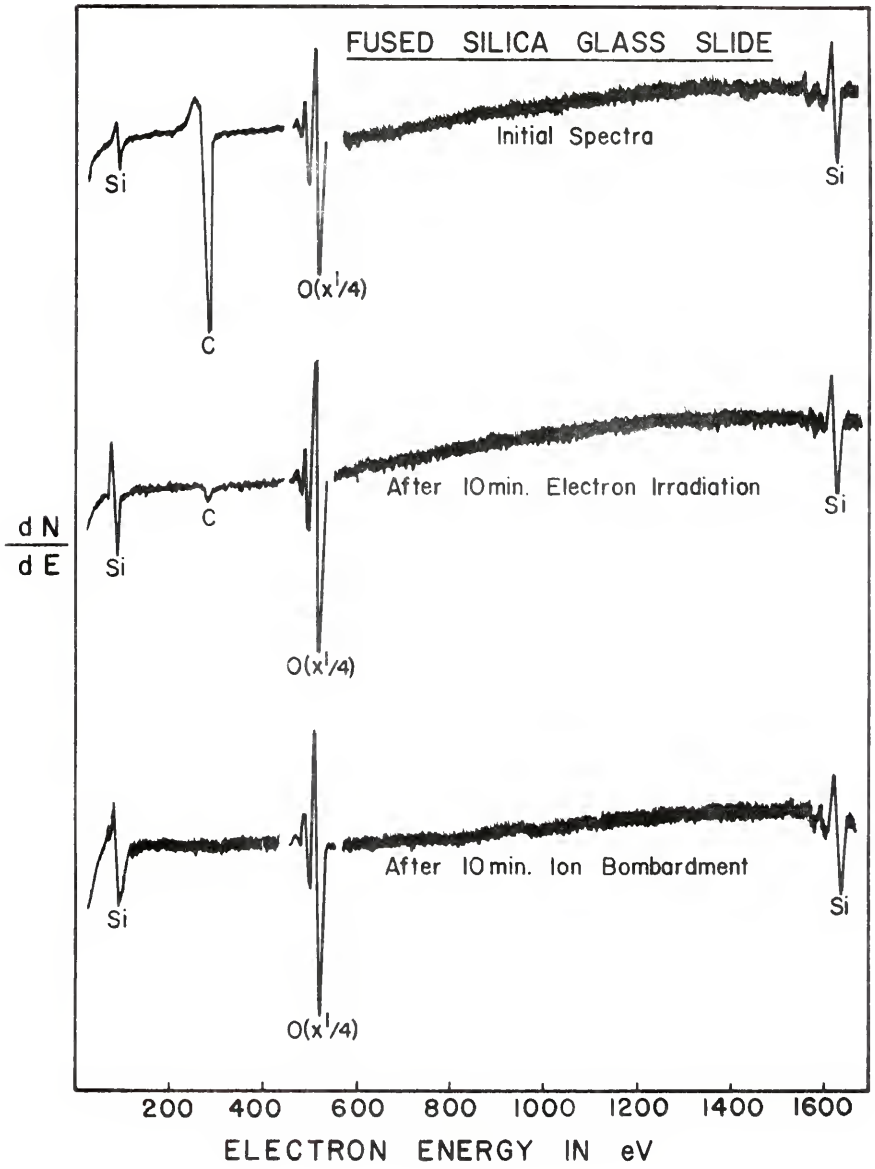

Figure 4. AES spectra of a fused silica surface as received and after both electron and ion bombardment.

Si (metallic-crystal) produces a peak at 92eV. The Si signal at 1620eV is due to electrons whose escape range is of the order 40A [5], and is referred to as the high-energy Si peak. This peak arises from a core-level Auger transition, and is relatively insensitive to chemical environment. In this case, a significant peak shift is not observed upon changing the oxidation state of silicon. It is apparent that, in general, careful monitoring and subsequent comparison of these two Si peaks can yield additional information concerning depth distribution and chemical effects for Si.

The middle spectrum in Figure 4 represents the fused silica surface composition after approximately 10 minutes of electron bombardment. While the carbon peak has disappeared, the low-energy silicon and oxygen peaks have increased in magnitude. The carbon has presumably been desorbed from the surface by electron irradiation. The loss of this surface carbon has exposed more of the silica surface, evidenced by the increased magnitudes of the Si and O peaks. The low-energy Si peak responds most dramatically. In any event, exposure to electron irradiation during analysis has altered the original surface composition of this fused silica slide. It is to be emphasized that analysis be carried out as quickly as possible to prevent such experimental perturbation. The

glass surface should not be electron irradiated except while recording the AES spectra.

The lower spectrum in Figure 4 represents the fused silica surface composition after 10 minutes of 2keV Ar ion bombardment. A change in peak shape is observed for the low-energy Si peak. This is probably a result of surface structural damage and charging inflicted by ion bombardment. This valence-band associated Auger transition is clearly affected. It is suggested that the low-energy silicon peak-to-peak height not be utilized to extract quantitative information after ion bombardment.

Comparison of the middle and lower spectra in Figure 4 indicates no change in surface composition after ion bombardment, except for the removal of residual carbon. This is best seen by comparing the high-energy Si to O peak-height ratios. In both cases, this ratio is approximately .1. After removing the carbon contamination the surface and bulk of this fused silica slide are compositionally identical. More importantly, however, this implies that ion milling does not adversely affect the measured surface composition; i.e., preferential milling is not observed. Careful measurements of the Si to O peak-height ratios by Dove [46] has revealed a knock-on effect due to ion bombardment of thermally grown SiO_2 thin films. He observed a slight decrease (<10%) in the ratio indicating

a knock-on of oxygen due to prolonged ion bombardment. The effect is not easily measured under normal operating procedures (Figure 4) and hence is assumed negligible for the present purposes.

The beam current density utilized when analyzing glass surfaces is an important parameter. Higher beam current density provides increased sensitivity but can cause changes in the surface species under analysis. Figure 5 shows the changes in the low-energy Si peak as a function of electron irradiation time for a fused silica surface. The electron beam current density was approximately .1 amps per cm^2. The progressive appearance of a peak on the high-energy side of the 75eV Si peak is apparent. This new peak appears at 92eV. The Auger transition corresponding to this peak is due to silicon atoms in the metallic state. Thomas [47] has observed a similar phenomenon for thin SiO_2 films thermally grown on silicon single crystal surfaces. He has interpreted this peak modification phenomenon as electron-induced dissociation of SiO_2 to Si at the surface. Probably, this same effect gives rise to the Si-peak modification observed for fused silica. This same phenomenon has also been observed by the author for multicomponent silicate glasses.

The effect discussed above must be prevented during analysis of multicomponent silicate glasses, particularly

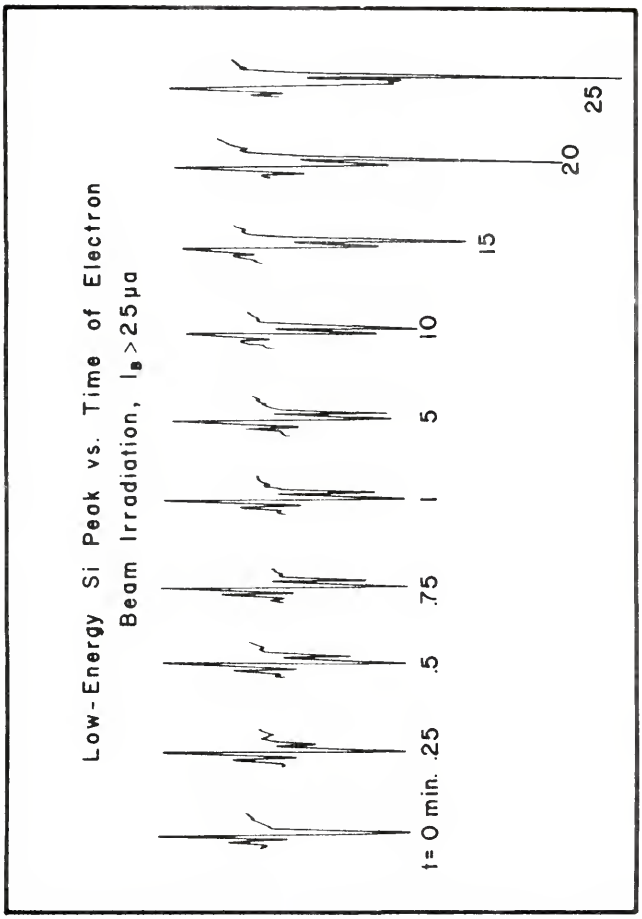

Figure 5. Effect of electron irradiation (.1 A/cm^2) upon the shape of the Si (LMM) Auger peak.

if a quantitative analysis is desired. Reduction of SiO_2 to Si changes the chemical nature of the surface, as well as the composition. If in situ surface reactions are being carried out during AES analysis the results are subject to doubt. If electron irradiation is carried out simultaneously with ion bombardment, the etch rate will be representative of the removal of Si rather than SiO_2 [48]. Also the development of a peak at 92eV affects the peak-to-peak magnitude for the 75eV peak. This makes quantitative peak-height interpretation of the 75eV peak imprecise.

It has been found that electron beam induced dissociation of SiO_2 at the surface of a silicate glass may be prevented by maintaining the beam current density below some critical value. This critical value of beam current depends upon both glass composition and electron beam energy. Figure 6 portrays a more plausible configuration for the low-energy Si peak from SiO_2 and is obtained by operating at a beam current density equal to or less than .06 amps per cm^2. At this lower beam current density, peak shape modification is not observed for up to 25 minutes of electron irradiation. As pointed out above, this critical value depends upon beam energy and glass composition. For multicomponent silicate glasses, one must operate below .05 amps per cm^2. Careful selection

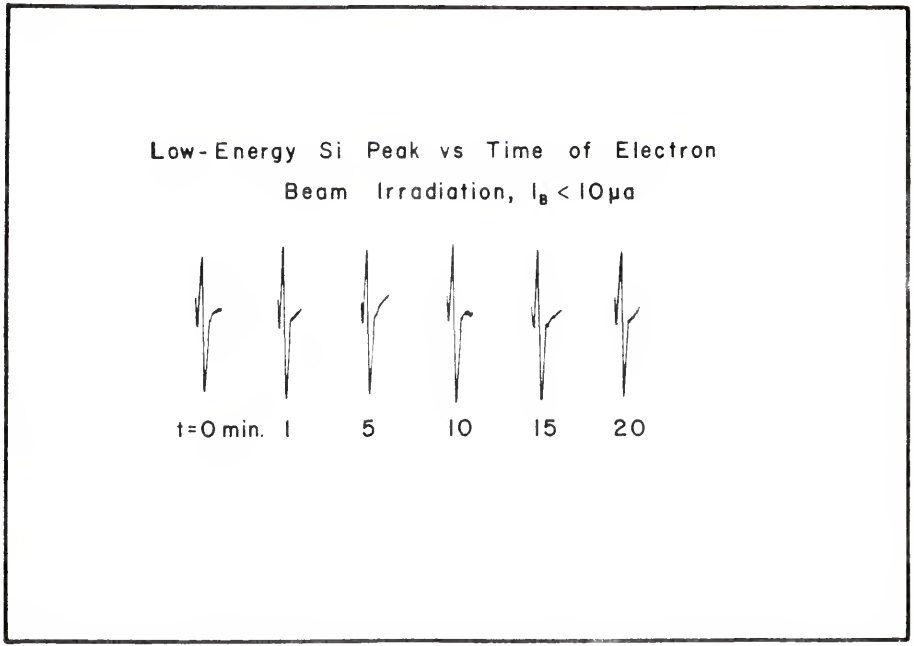

Figure 6. Preservation of Si (LMM) Auger peak shape by maintaining electron-beam current density below the critical value.

of electron beam conditions is required to prevent electron induced desorption, in general.

The high-energy Si peak does not reflect this surface reduction of SiO_2 to Si. This is due both to the insensitiveness of the KLL Auger transition to oxidation state and also to the high escape range of these electrons. Under conditions where this effect must be tolerated, the high-energy Si peak should remain a good measure of surface silicon content.

Analysis of a Soda-Lime-Silicate Glass

The glass utilized in this measurement was obtained from a commercial soda-lime-silicate container.* The upper portion of Figure 7 shows the spectrum obtained. The spectrum was recorded under the conditions found most suitable for fused silica. Namely, the angle of incidence of the electron beam was 45° while the beam current density was approximately .025 amps per cm^2; beam energy was 3keV. In addition to the oxygen and silicon peaks, a peak at 292eV is observed, due to a Ca-KLL Auger transition.

Sodium is known to be present in this glass but is not detected in this spectrum. The Na-KLL Auger

*Brockway Glass Co., Inc., Brockway, Pa.

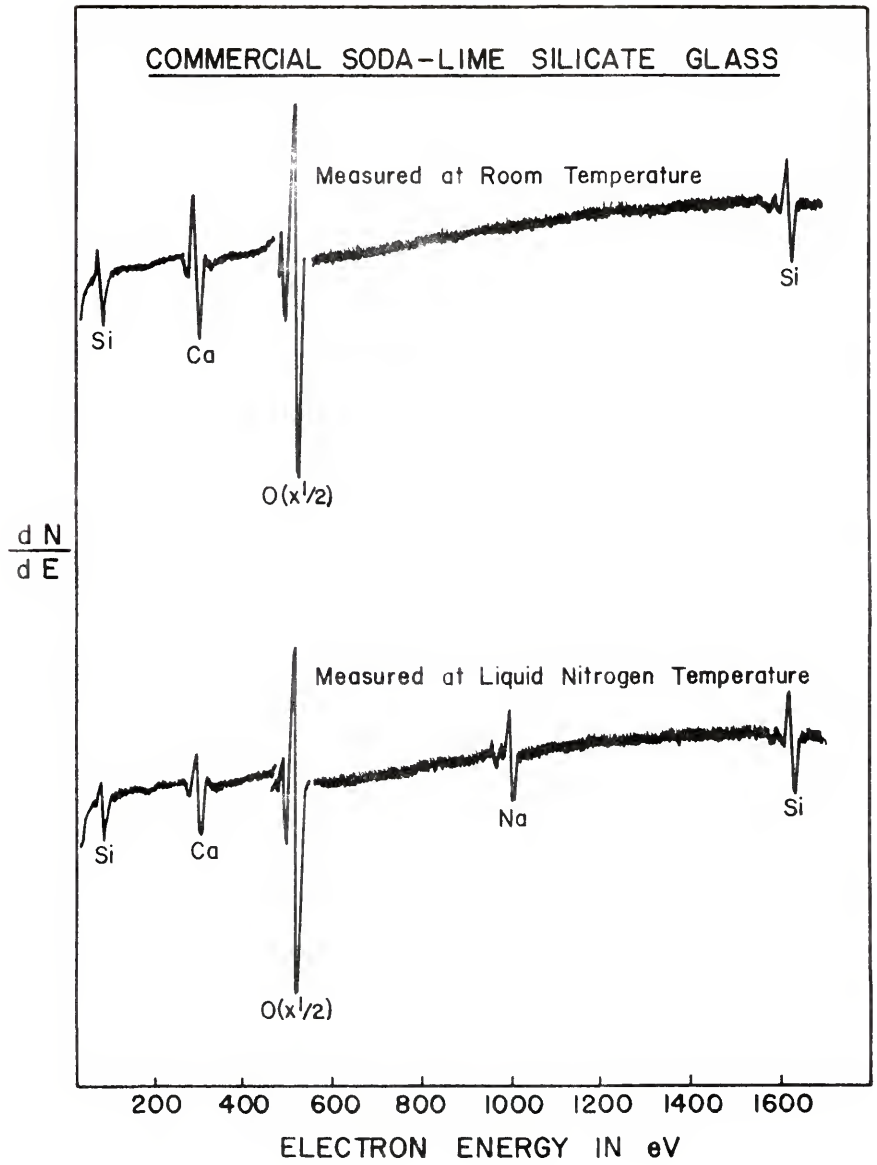

Figure 7. AES spectra for a multicomponent glass illustrating the effect of temperature upon the "measured" composition.

transition would produce a peak at 990eV. The absence of a peak at 990eV in this spectrum could suggest that the surface is originally depleted of sodium or alternatively that the sodium is caused to leave the region of investigation due to the effects of electron irradiation. The alternative hypothesis was tested on this soda-lime-silicate glass in the following manner. The Auger spectrum was displayed on the oscilloscope and the beam current was set at a minimal value. Upon translating the sample under the electron beam, a sodium peak was observed on the oscilloscope. When the sample was held stationary, the sodium peak rapidly decayed away. This observation indicated that sodium was originally present, but perturbing effects of the electron beam caused it to leave the surface region rapidly. Because of the much slower scan rate used for charting the spectrum on the x-y recorder, the sodium peak could never be recorded.

Two possible causes for this sodium effect at the surface are (1) the electron irradiation creates electrostatic force fields at and below the surface which drives sodium ions toward the interior, or (2) sodium is volatized from the surface by localized heating or direct desorption caused by the impinging electron beam. In either case, if sodium is originally present at the surface, the rate at which sodium leaves should decrease

with decreasing current density of electron irradiation and with decreasing temperature of the glass. Less severe electron beam conditions would reduce the driving force for sodium diffusion or volatilization, while lower temperatures would reduce the mobility or reaction rate constant.

The lower portion of Figure 7 shows a spectrum for this soda-lime-silicate glass measured at 110°K (liquid nitrogen cooled). All other conditions were identical to those used for the room temperature spectrum. For this low temperature measurement, a sodium peak at 990eV is observed in the spectrum. Continual monitoring of the sodium peak indicated that even at low temperature, the concentration of sodium at the surface is constantly decreasing with time. However, the rate of decay is much slower than that observed on the oscilloscope at room temperature. Similar to the case for carbon on the fused silica surface, these results show that the closest indication of the true sodium peak-to-peak height is a measurement taken as rapidly as possible after turning on the electron beam. Utilizing a minimal beam current density is extremely beneficial. Comparison of the room temperature and low temperature results clearly demonstrates that lower temperatures reduce the rate at which sodium Auger peaks decay. The comparison also proves that

sodium is present at the surface, and the absence of sodium in normal room temperature measurements is not representative of the original surface composition. Because most multicomponent glasses have loosely bound, nonnetwork ions, such as sodium, it is anticipated that similar problems would arise in measuring Auger spectra of other glasses at room temperature. The low temperature, low beam current technique described above should prove useful for indicating the presence of mobile species at the surface. The mechanism for the perturbing effect observed during AES analysis of soda-lime-silicate glass is considered in detail in Chapter III.

Summary

1. Stable AES spectra may be obtained for glasses utilizing a 45° angle of incidence between the electron beam and sample surface.
2. Beam current density must be kept below .05 amps per cm^2 to prevent electron-induced dissociation of the SiO_2 network.
3. Volatile species such as adsorbed CO, organics, etc. are subject to desorption by electron irradiation. AES analysis, therefore, should utilize minimal beam current densities and minimal measurement times.

4. Ion milling with 2keV argon does not significantly alter the Si to O ratio for fused silica.
5. AES analysis of soda-lime-silicate glass at room temperature perturbs the original surface composition, and in most cases, indicates the absence of sodium on the surface.
6. AES analysis of a soda-lime-silicate glass cooled by liquid nitrogen provides a more accurate measure of surface composition although the sodium signal is time dependent.
7. Mobile ions at the surface are, in general, subject to perturbation by the electron beam.

CHAPTER III

BEHAVIOR OF MOBILE SURFACE IONS UNDER ELECTRON IRRADIATION

The difficulty associated with the measurement of sodium (and mobile ions in general) within a glassy SiO_2 matrix using electron beam techniques has been noted by a number of workers [11]. The measurements described in the last section indicated that this difficulty is also encountered with soda-lime-silicate glasses. Under the influence of electron irradiation upon the glass surface, the sodium ions have sufficient mobility at room temperature to quickly leave the region of investigation. At room temperature, therefore, sodium is not detected in the AES spectra. Measurements carried out at low temperature, however, revealed that the effect could be retarded enough to detect and record a sodium Auger peak.

It was also pointed out in the last section that even at low temperature, a slow decay of the sodium peak is observed. Also, comparison of the spectra in Figure 7 reveals that the presence of sodium at the surface leads to a change in the relative magnitude of the peak-to-peak heights for the other glass constituents. Theoretically,

this is a predictable result since any sodium atoms at the surface must attenuate the Auger current from other constituents. However, one could not predict the magnitude of attenuation (i.e., matrix effect) without a direct measurement of the sodium level. From a quantitative point of view, the detection of sodium is of particular importance to the accuracy of analysis.

Because of the importance attributed to sodium in surface reactions of soda-lime-silicate glass, it is very desirable to be able to accurately measure sodium concentrations and sodium concentration profiles using AES. The low temperature measurement described in the last section offers a method of at least qualitatively detecting the presence of sodium at the surface. However, to make accurate, quantitative measurements of sodium concentration requires a more detailed understanding of the ion-migration effect. This section compares the influence of electron irradiation on the sodium AES signal measured from a soda-lime-silicate glass between liquid nitrogen temperature and room temperature. A mechanism of interaction between the electron beam and soda-lime-silicate glass surface is suggested.

Experimental Method

The measurements reported in this section were carried out on two different soda-lime-silicate glasses,

one of commercial composition and the other of invert composition. The commercial glass composition was approximately 74% SiO_2, 13% Na_2O, 12% CaO, 1% other (molar). The invert glass composition was approximately 46% SiO_2, 24% Na_2O, 27% CaO, 3% P_2O_5 (molar). This latter glass was known to be phase separated (Chapter VI). The samples were mounted on a low temperature stage that could be cooled by liquid nitrogen. A thin film thermocouple deposited on the surface of a soda-lime-silicate glass slide indicated the attainment of 110°K when mounted on the liquid nitrogen cooled sample stage.

It was found that a reproducible surface condition characterized by the AES spectra could be obtained by prolonged ion bombardment with 2 keV Ar ions at the low temperature. The ion bombardment was carried out in the presence of thermal electrons which flooded the glass surface to minimize possible charging effects due to the bombarding ions. This procedure gave a surface that was stable in vacuum for many hours and did not change with further ion bombardment. In this way a reproducible surface composition was achieved which proved convenient for certain types of investigation. It was assumed that the AES spectrummeasured for this surface was characteristic of the bulk composition of the glass.

In investigating the migration of sodium ions, the electron beam was held at 3 keV and a particular current

value while the Na peak was measured repetitively using the cylindrical mirror analyzer. The beam current was set by positively biasing the sample holder and measuring the current passing through it to ground.

Results

Figure 8 shows a plot of the peak-to-peak heights, normalized to the peak-to-peak height at zero time, for the Na signal from the commerical soda-lime-silicate glass (surface prepared as described above) as a function of the time of exposure to the exciting electron beam and for several values of beam current. The beam diameter was approximately 250 μm. At ∿1 μA of beam current and with the sample at room temperature, the Na signal decreased markedly within a few seconds although some sodium could be detected even after approximately one minute of electron beam exposure. At higher current levels at room temperature, the Na signal decreased much more rapidly and could not be readily recorded with the present XY-recorder arrangement.

With the sample mounted on the stage cooled with liquid nitrogen, it was found that the Na peak remained essentially unchanged and could be repetitively measured for a period of 80 seconds using a beam current of ∿1 μA. Thereafter the signal level decreased slowly reaching about half its initial level after a few minutes. At higher

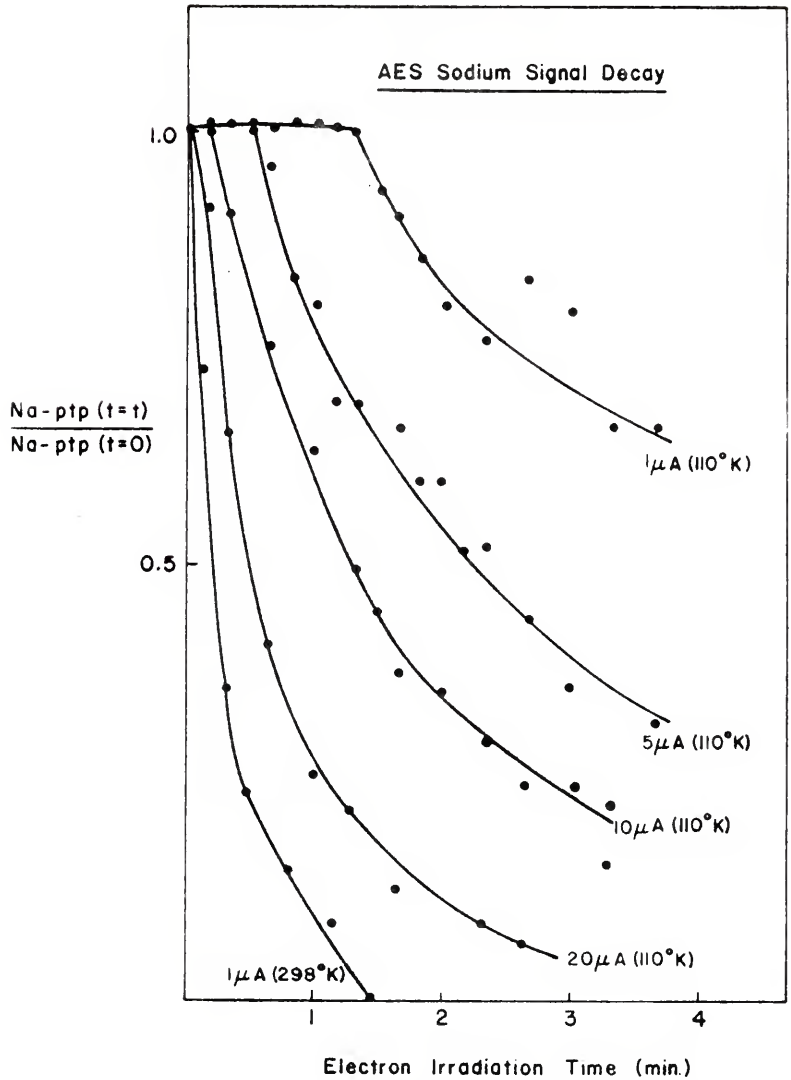

Figure 8. The decay at 110°K of the sodium peak-to-peak height, normalized to the peak-to-peak height at zero time, as a function of the time of electron irradiation for beam currents of 1, 5, 10 and 20 μA. A decay curve measured at room temperature and 1 μA is also shown.

current levels, the signal remained constant for a much shorter period and then decreased with time as can be seen in the curves of Figure 8.

It was found that the curves could be represented by an equation of the form,

$$(Na)_t = (Na)_o \quad \text{for } t < t_o \quad (1)$$

$$(Na)_t = (Na)_o \, [1 - 0.3 \ln(t/t_o)] \quad \text{for } t > t_o \quad (2)$$

where $(Na)_o$ is the sodium peak-to-peak height at zero time, $(Na)_t$ is the sodium peak-to-peak height at time t, and t_o is the residence time during which no change in Na signal is observed. The values of t_o deduced from the curves of Figure 8 are 80, 30, 15 and 7 seconds for beam currents, I, of ∿1, 5, 10 and 20 μA, respectively. It can be noted that with this limited data the product It_o is constant with the exception of the ∿1 μA case. This result indicates that the signal decay begins after some critical number of electrons have been incident upon the sample. Interestingly, the room temperature data may also be fitted by the same equation except that t_o for the 1 μA beam current has decreased by a factor of about 25. This preliminary data indicates that there is an initial residence time that is strongly temperature dependent, while the decay process appears to be relatively independent of temperature. If the assumption is made

that the residence time is controlled by a thermally activated process, then an activation energy of the order 0.04 eV, a surprisingly low value, is obtained.

It is emphasized that after each electron irradiation dose, the original surface composition (i.e., Na) could be restored by ion milling for approximately 5-10 minutes to remove the disturbed surface layer. Figure 9 provides a depth profile for a spot on the commercial glass surface after electron irradiation at 110°K. The beam current during irradiation was 5 μA. After the signal decayed to 20% of its original value (80 sec) the electron beam was turned off. Ion milling was initiated. To prevent further perturbation of the sodium ion concentration profile, only the Na peak was recorded. Each AES measurement took less than 10 seconds. It is indicated that the sodium concentration increased rapidly with ion-milling time. The affected surface layer is approximately 240Å thick.

Figure 10 shows a plot of the peak-to-peak heights, normalized to the peak-to-peak height at zero time, for the Na signal from the phase-separated invert soda-lime-silicate glass (surface prepared as described above) as a function of the time of exposure to the exciting electron beam and for both room temperature and for 110°K. The beam current utilized was approximately 5 μA with a beam diameter of approximately .5 mm.

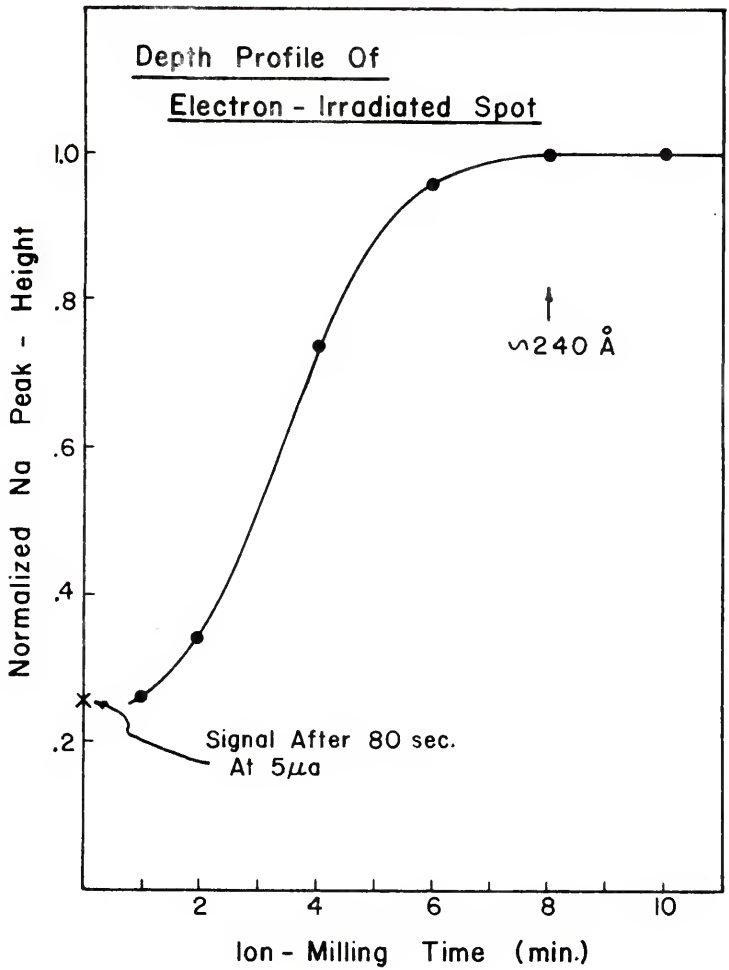

Figure 9. Sodium-depleted surface layer resulting from electron irradiation.

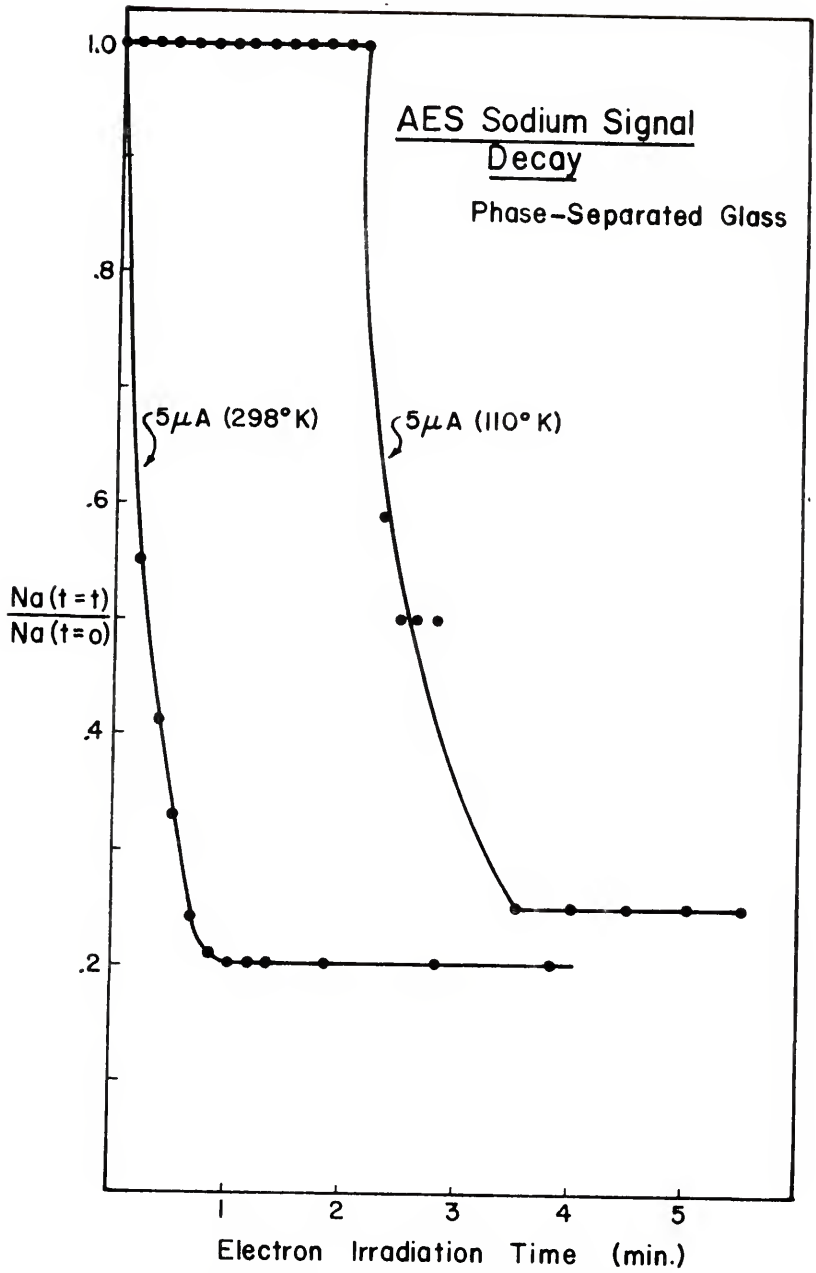

Figure 10. Sodium signal decay measured on phase-separated bioglass at both room temperature and 110°K.

At room temperature, the Na signal decreased markedly within 60 seconds but then stabilized at a value equal to 20% of its original value. Continued exposure did not affect the sodium signal.

Upon cooling the sample with liquid nitrogen, a residence time of 2 minutes was observed during which the sodium signal remained unchanged. This is similar to the effect noted previously for the commercial glass. The increased residence time here is most likely a reflection of the increased beam diameter, i.e., beam current density After 2 minutes of electron irradiation the Na signal decays rapidly, with approximately the same rate observed at room temperature. Again, the Na signal stabilized to a constant value, in this instance equal to 25% of its original value.

Comparison of the two curves in Figure 10 reveals that independent of temperature, the sodium signal decays to 20-25% of its original value and stabilizes. However, a residence time during which no decay is observed occurs at 110°K. Inspection of this specimen after electron irradiation revealed a blackish spot on the sample where the electron beam impinged the surface.

Qualitative Assessment

The disappearance of sodium (or any atomic species) at the surface can be due to either its escape into vacuum

or its migration into the solid. Lateral migration is ruled out in the present case by the large distances (beam diameter) over which the ion must move in order to result in measurable signal loss. Desorption from the surface or migration into the surface would produce the measurable signal decays observed.

Electron irradiation of alkali-silicate glasses during electron microprobe (EMP) analysis also results in the loss of alkali at the surface [49-53]. This observation tends to exclude the hypothesis that sodium loss at the surface is a result of volatization or electron stimulated desorption. The conclusion is based upon the fact that EMP analysis requires a metal overlayer on the surface. The hypothesis is further substantiated by the work of Hayami and Wakabayashi [53]. They compared the EMP alkali signal decay from glass samples with and without the surface coating. The results indicated that at moderate beam current densities, and for low alkali glass, the decay was observed to be independent of the presence of a coating. Upon imposing extremely high beam current densities, the alkali signal increased with electron irradiation. The latter effect is not completely understood but is perhaps a result of local melting at the surface and consequent alkali segregation. The beam current densities required to induce this particular effect are 2-3 orders of magnitude higher than those used in previous EMP

studies and the present AES study. Hence, although this latter effect is not clearly related to the present observations, it does indicate that significant temperature rises occur at the point of electron irradiation.

A study of chlorine contamination in thin SiO_2 films using AES [39] also reported the observation of unstable signals, in this case for the mobile Cl ion. In contrast to the alkali loss reported here and in the EMP studies, the chlorine concentration was found to increase at the surface during electron irradiation. Upon rising to a peak value, the concentration then decreased. The authors suggested that under electron irradiation the chlorine becomes positively charged, moves to the outer surface under the influence of an electric field and is released into vacuum. (During electron irradiation, chlorine was observed in the residual gas spectrum.) The time required to observe the peak and subsequent decrease in chlorine concentration was shown to depend upon the film thickness. This implied that the decrease in chlorine corresponds to its exhaustion in the film. The authors did not rationalize the production of positively charged chlorine nor the origin of the electric field. Nonetheless, the observations suggest that under conditions where desorption of ions is verified, a pile-up of the ions at the surface is detected by the AES analysis. This simply indicates that the desorption step

is occurring at a slower rate than migration of chlorine to the surface. A particularly interesting result of this work was the observation of a 90°C temperature rise in the vicinity of electron irradiation. Subsequent cooling of the sample to 77°K retarded the chlorine pile-up at the surface. It is clear, however, that chlorine responds to electron irradiation during AES analysis in a fashion which is similar to that observed for sodium, although a pile-up rather than depletion at the surface occurs.

In the absence of the EMP results, it could be argued that sodium migrates to the surface at a slower rate than it is desorbed there, resulting in its depletion. Considering all the observations, however, the discussion presented above has excluded the possibility that sodium is lost via its escape into vacuum. This leaves only one alternative. Namely, the sodium becomes ionized and migrates into the glass surface under the influence of an electric field. The dependence of the signal decay upon microstructure (Figure 10) supports the hypothesis that sodium is migrating within the solid. With regard to the chlorine migration discussed above, the sodium appears to migrate in the opposite direction. The sign of the field produced is probably the same in both studies. Since sodium undoubtedly becomes positively charged on ionization, it seems likely that contrary to the reported interpretation, the chlorine must become negatively charged.

This is certainly the more likely situation. The field may be produced according to the Lineweaver mechanism [54]. His model indicated that electrons impinging an insulator are buried in the surface upon some plane defined by the penetration depth of the electrons. The field produced by this space charge is then capable of attracting alkali ions away from the surface. Hence, alkali is depleted at the surface during electron irradiation.

Under the driving force of this electric field, the rate of signal loss, and its dependence upon temperature and beam current density must be rationalized. Similarly, the origin and behavior of the observed residence time must also be considered.

Discussion of Results

Results similar to those presented above were reported previously by Vassamillet and Caldwell in a study of the influence of the electron beam using EMP measurements of potassium-containing glasses [49]. They measured the alkali-ion X-ray intensity as a function of time, temperature and electron flux. The curves they reported are amazingly similar to those shown in Figure 8. The form of their decay curves is approximately consistent with the logarithmic decay noted in the present case. The EMP measurements were made at room temperature and temperatures

as high as 83°C. In that regard, it is surprising that they could measure residence times comparable to those measured here at liquid nitrogen temperature. However, that is most probably a reflection of the increased surface sensitivity of AES analysis in comparison to EMP analysis. EMP analysis averages compositional changes over a much thicker surface layer than does AES analysis and is therefore less sensitive to these changes. Hence, longer times or higher temperatures are required to obtain measurable changes. Nonetheless, the changes in residence time with both temperature and electron flux are consistent with the present work. Vassamillet and Caldwell qualitatively rationalized their data on the basis of the Lineweaver mechanism. Recently, Goodhew and Gulley [52] reported similar decay curves for EMP analysis of alkali metals in glass measured as a function of electron beam energy. At higher accelerating potentials, the residence time increased while the decay rate decreased. They interpreted the reduced effect to be a result of the deeper penetration of electrons at higher voltages. According to classical physics, however, the electric field for this geometry is independent of charge separation. The present study is aimed at a more quantitative explanation for the observed sodium migration. The similarity in the decay curves measured during AES and EMP analysis of alkali-containing silicate glasses suggests a common mechanism.

The depth profile presented in Figure 9 indicates sodium depletion within a rather distinct layer near the surface. This suggests that when a measurable migration is taking place, the signal decay observed is primarily due to sodium ions moving out of the range of detection. This model is represented schematically in Figure 11. Sodium ions move into the surface with some drift velocity characterized by the ion mobility and electric field gradient. Owing to a lack of depth resolution (both AES and ion milling) and the possiblity of back diffusion, the appearance of the measured profile (Figure 9) is in only qualitative agreement with the model. The profile indicates a sodium-depletion layer approximately 100-150Å. This is an overestimation of the expected escape depth (30-60Å) and suggests that if the model is valid, the ion-milling rate is in error. This is certainly a likely possibility. The ion-milling rate may be in error by as much as a factor of 2 (Chapter IV) and may therefore account for this discrepancy. More importantly, the Na signal does increase approximately exponentially with ion-milling time. This is to be expected upon removal of a thin depleted layer and further substantiates the model. The prediction of the model with regard to the measured Na signal decay is considered next.

The electron escape (and penetration) probability decreases exponentially with depth below the surface. If

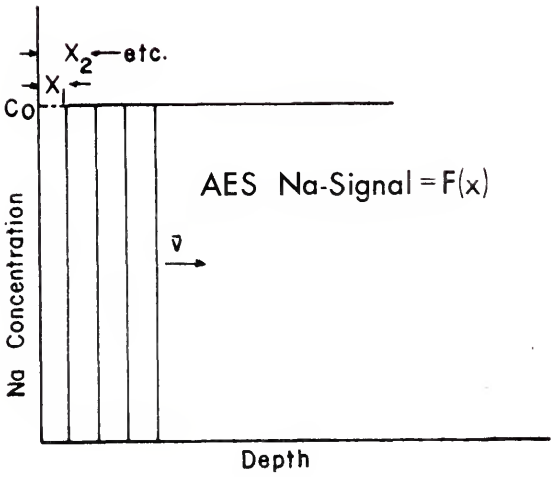

Figure 11. Model for AES sodium signal decay.

it is proposed that the sodium ions are migrating at a constant velocity away from the surface, the AES signal should decrease exponentially with time. This is expressed analytically as

$$Na_t = Na_0 \, e^{-\bar{v}t/\lambda} \qquad (3)$$

where Na_t and Na_0 are the sodium concentration (i.e., signal strength) at time t and time zero, respectively, $\bar{v}$ is the sodium ion drift velocity and λ is the sampling depth. (Because of the scatter in the measured data points an exponential, as well as the logarithmic, dependence indicated in equation (2) may be used to describe the decay curves.) It can be seen immediately that as the sampling depth increases the time constant for this decay process increases. Hence, the longer residence and decay times observed by EMP analysis are perhaps a reflection of its increased sampling depth. During the AES measurements the sampling depth, λ, is a constant. Hence, differences in signal decay rate are a reflection of changes in $\bar{v}$. $\bar{v}$ may be a function of (1) mobility, (2) field strength, or (3) rate of ionization. The mobility and ionization rate may be expected to depend upon temperature, whereas the field strength should depend upon the amount of buried charge. Through careful measurements of the specimen current, Lineweaver found that the field was established within a few seconds of irradiation [54].

Undoubtedly, the most difficult portion of the model to formulate concerns the dependence of the residence time upon a number of the experimental variables. The AES measurements indicate a dependence of residence time upon temperature, electron flux, and microstructure. The EMP measurements indicate a dependence of residence upon temperature, electron flux, electron energy, composition and concentration of alkali. The AES measurements were not made as a function of composition and concentration of alkali.

The dependence of residence time upon electron flux is internally consistent for both the AES and EMP measurements. The residence time multiplied by the electron flux gives the total amount of incident charge. For a given temperature, composition and concentration, the total incident charge prior to decay is found to be constant. If it is assumed that this charge is buried in the surface as suggested by Lineweaver, an electric field is set up between the surface and this layer of buried charge. Assuming the charge lies upon a single plane and recalling Gauss' law [55], the field, ε, is given by

$$\varepsilon = \frac{\tau}{2\varepsilon_0 \varepsilon_r} \tag{4}$$

where τ is the charge per unit area, ε_0 is the permittivity of vacuum and ε_r is the dielectric constant. Using the AES

data to provide $\tau(It_0$ per unit area) a field of about 10^{13} V/cm is indicated. This is obviously well in excess of the usual dielectric breakdown strength reported for this glass. Within the small volume of glass being considered, it is not clear whether or not the concepts of macroscopic dielectric breakdown are applicable. Furthermore, the model is greatly oversimplified, particularly with regard to the assumption that the charge lies upon a well defined plane. However, the calculation does provide an upper limit on the possible field strength, thereby indicating that extremely high fields may exist in the surface. Motion of sodium ions probably prevents fields from building in excess of the intrinsic breakdown field for the glass ($\sim 10^7$ V/cm). This is provided, of course, that sodium ions are capable of motion. Consideration of the ionic mobility may clarify this point.

Utilizing the dc-electrical conductivity data of Douglas and Rana [2] permits a calculation of diffusion coefficients, D, for this glass. At room temperature (298°K) $D = 3.5 \times 10^{-17}$ cm^2/sec while at low temperature (110°K) $D = 1.3 \times 10^{-38}$ cm^2/sec. The Einstein relation [56] provides the ionic mobility, μ, as

$$\mu = \frac{De}{kT} \qquad (5)$$

where D is the diffusion coefficient, e is the electronic

charge, k is Boltzmann's constant and T is the temperature. Substitution of the corresponding values gives $\mu(298°K) = 1.36 \times 10^{-15} cm^2/v\text{-sec}$ and $\mu(110°K) = 1.37 \times 10^{-36}$ $cm^2/v\text{-sec}$. Assuming the electric field to be 10^7 V/cm (approximately the intrinsic breakdown strength) [57], the velocity of sodium ions at room temperature (298°K) is 1.36 Å/sec. This is a reasonable value for the observed signal decay at room temperature. If the escape depth (1/e distance) for sodium Auger electrons is taken to be 33Å and the drift velocity, $\bar{v}$, is 1.36 Å/sec, the sodium AES signal should attenuate 63% in 24 seconds (equation (3)). This is in extremely good agreement with the experimental data in Figure 8 (1 μa, 298°K).

In contrast, the velocity, $\bar{v}$, of sodium ions under an identical field at 110°K is 10^{-21} Å/sec. Obviously, a sodium signal decay is not expected within the time scale of normal measurements. Due to the lowered thermal energy of the glass, the sodium is locked to the structure and cannot respond to the field. Under this condition, it is perhaps likely that the field may increase in magnitude to the value predicted by equation (4), 10^{13} v/cm. Physically, then, a situation exists at low temperature in which sodium atoms in a very high field must be ionized in order to migrate out of the surface and cause the observed signal decay. Obviously, an increase in the thermal energy of the system provides a higher probability for ionization.

This is reflected in the diffusion coefficient for sodium and suggests that a rise in temperature is required to make sodium ion migration observable. Local temperature rises during electron irradiation are well known. The work of Almasi et al. [58] predicts a temperature rise on the order of 25°C for the conditions of this work. This change in temperature increases the sodium ion mobility by 6 orders of magnitude. The work of Chou et al. [39] which has been described above, measured directly temperature rises of 90°C in the vicinity of electron irradiation. This temperature change increases the mobility by 16 orders of magnitude. The temperature rise in this case was measured relative to room temperature.

A second mechanism exists which may account for the response of sodium to the electrostatic field at low temperature. This involves the process of tunnelling [56], whereby very large fields essentially strip the sodium atom of its electron. Once ionized, it can respond to the field. The physics of this situation are very unclear. Since it has been established that temperature rises do occur, thermal activation provides both a higher probability for ionization and consequently a higher mobility, and therefore seems to be the more likely mechanism.

A Model

The discussion presented above suggests the following model for sodium ion migration during AES analysis.

Electron irradiation upon the glass surface produces an electrostatic field in the glass surface which is sufficient to attract sodium ions. Although the Lineweaver mechanism for this field production is perhaps oversimplified, it is qualitatively correct. At room temperature, sodium ions immediately respond to a field approximately equal to the intrinsic breakdown strength of the glass. The field does not increase to the value predicted by equation (4) because migrating sodium ions and the negatively charged oxygen ions left behind act to compensate the electron space change. Figure 12 provides a comparison of the experimental data with this model, predicted by equation (3). The sampling depth for sodium Auger electrons is taken as 33 $\mathring{A}$ ($\sqrt{E_{Na}}$) [59]. $\bar{v}$ is 1.36 $\mathring{A}$/sec, dictated by the temperature (298°K). The fit is not bad considering the assumptions made.

When the glass is initially at 110°K, the observed decay can be rationalized if local temperature rises occur during electron irradiation. The time, t_o, at which a measurable concentration change is observed probably corresponds to the attainment of some critical temperature and perhaps critical field. At this critical point, the ion velocity may change from thousandths of angstroms per second to tens of angstroms per second. Furthermore, since the ion velocity changes exponentially with temperature,

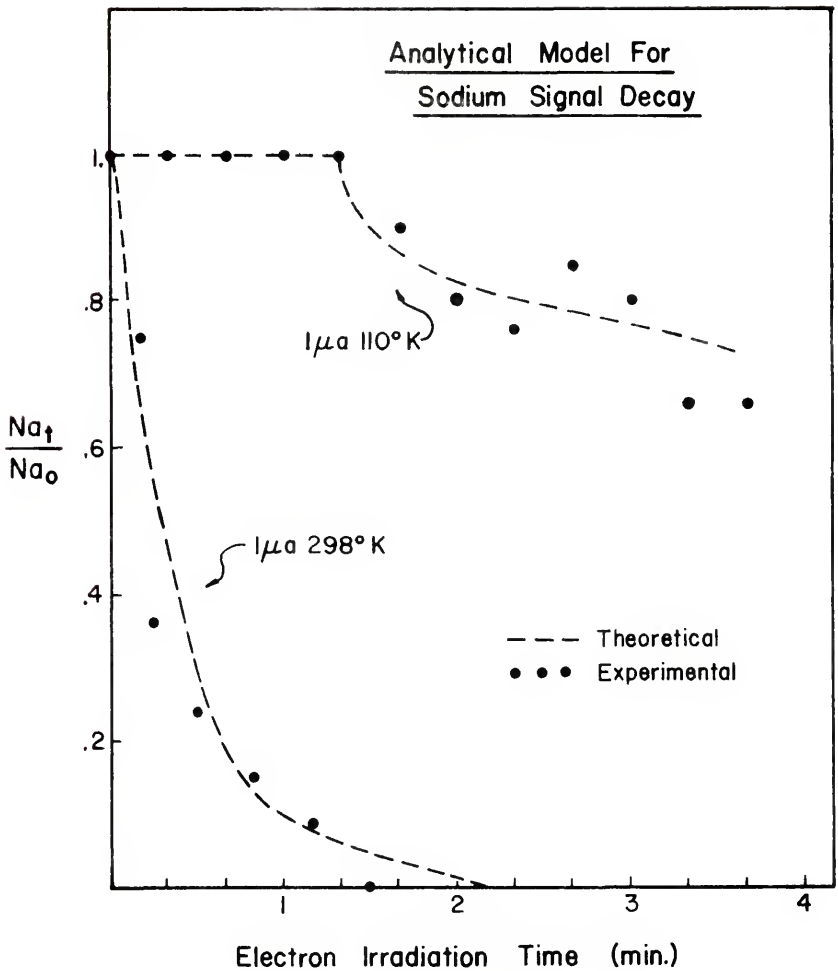

Figure 12. Comparison of the experimental data to the predictions of the proposed model for sodium signal decay.

significant temperature rises are not required to produce the abrupt transition. Hence, the residence time is very temperature dependent. This also gives rise to its linear dependence upon beam current (power input).

Considering equation (3), then, the following sequence of events is indicated. With the glass initially at 110°K, $\bar{v}$ is so low that $Na_t = Na_o$ (equation (1)). Since the sodium ions cannot respond significantly, the charge incident upon the surface (It_o) may continually increase the field as predicted by equation (4). During electron irradiation, the temperature increases locally. This temperature rise, even if linear with time, results in an exponential increase in $\bar{v}$ with time (equation (5)). When some critical temperature is reached, however, the exponential term, via a time-dependent change in $\bar{v}$, becomes important. A decay is observed whose rate is dictated by $\bar{v}$. The 25°C temperature rise indicated by the incident beam conditions (1 μA) probably occurs within 1-2 minutes. This would imply that the local temperature is changing at a rate of approximately 12°/min during the first 2 minutes of irradiation. Utilizing equation (3) under this assumption provides the theoretical curve in Figure 12. The experimental data is shown for comparison. The field strength utilized is predicted by equation (4). Conversely, if the local temperature increases are of the

order obtained by Chou et al. [39] (100°C), the same decay curve is predicted using considerably lower field strength. If the beam current (power input) increases, the equilibrium temperature rise, and probably the rate of temperature rise, increases. This results in shorter residence times and increased decay rates as the beam current increases. These conclusions are also in agreement with the EMP data, although the dependence upon alkali concentration is not clear.

A Test of the Model

This model implies that a critical temperature exists. Once the temperature is attained, a measurable migration of sodium ions occurs. Furthermore, the critical temperature is associated with the residence time. It seems likely that the point at which measurable decay is initiated may correspond to the attainment of the critical temperature. Vassamillet and Caldwell [49] have tested the critical temperature model for EMP analysis by measuring the residence time at different temperatures and beam current densities. The data extrapolated to a common temperature at zero residence time, indicating that a critical temperature is reached when decay begins. This hypothesis may be further tested by comparing the effect of continuous irradiation with intermittent

irradiation during AES analysis. Figure 13 presents such data for two beam currents, 4 μA and 9 μA, with the beam diameter at 400-500 μm. Samples are cooled with liquid nitrogen. Each dose of irradiation is at least 10 seconds but not more than 15 seconds. Waiting time between doses is 1 minute.

At the 9 μA beam current, a residence time of between 10 and 15 seconds is observed during continuous electron irradiation. In comparison, intermittent doses of 10-15 seconds do not produce an observable decay for up to 40 seconds. Thereafter, a decay is observed. Although the points are scattered and no curve fitting has been attempted, it can be seen that the rate of decay is slower than that observed during continuous electron irradiation. In contrast, the residence time observed for continuous irradiation at 4 μA is about 40 seconds. Intermittent doses of 10-15 seconds do not result in observable decay after a total of 180 seconds of electron irradiation.

The data presented above supports the critical temperature hypothesis. When the electron irradiation dose is close to or greater than the residence time the critical temperature can be attained and a measurable decay can occur. The rate of decay observed will depend upon the time per dose and to some extent the waiting time

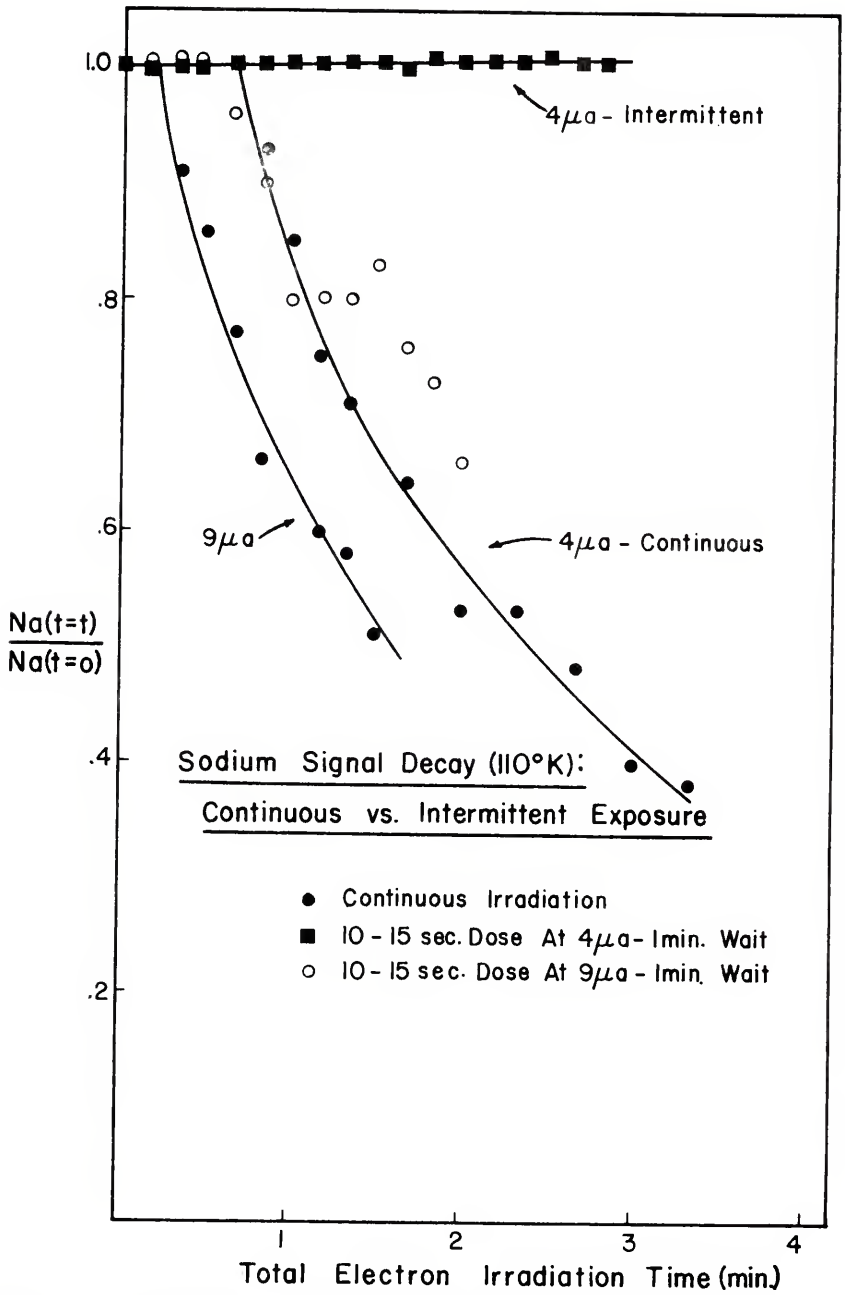

Figure 13. Effect of continuous vs intermittent electron irradiation upon sodium signal decay.

between doses. This situation is analogous to the 9 μA data presented above. Conversely, if the intermittent doses are much shorter than the observed residence time, the critical temperature cannot be attained. Measurable decay cannot occur under such conditions. This is analogous to the 4 μA data presented above. The observed residence time at 4 μA is 40 seconds, which is greater than the electron dosage time. Hence, the critical temperature is not reached during electron irradiation and no measurable decay occurs. This is observed in Figure 13. The analytical test of this model, which was presented previously in Figure 12, indicates the critical temperature to be about 25°C above the initial temperature. The initial temperature measured for these glasses cooled by liquid nitrogen is 110°K. This would indicate a critical temperature of 135°K or -138°C. However, if the measured initial temperature is in error, the indicated critical temperature is also erroneous. In practice, the best indication of the critical point is provided by measuring the residence time under the desired beam conditions. The initial temperature of the glass surface is determined by the specific sample and cooling configuration utilized. Hence, the allowable temperature variation, i.e., residence time, permitted can vary. Maintaining each electron irradiation dose below the observed residence time is most

suitable. This implies that in practice, each Auger measurement should take less than the residence time.

The work of Vassamillet and Caldwell also suggested a critical temperature for measurable alkali signal decay during EMP analysis. The temperature they reported was considerably higher than that indicated for the AES data. The difference is not unexpected, however. It was pointed out previously that EMP analysis requires migration of sodium ions over greater distances than AES analysis in order to observe a signal decay (equation (3)). To cover a greater distance in a comparable period of time requires that the drift velocity be increased. This would require a higher temperature, or for the same temperature, longer residence times. Hence, the present model is at least in qualitative agreement with the EMP data.

Summary

1. The absence of sodium at the surface of soda-lime-silicate glass during room temperature AES analysis is a result of its migration into the surface under the influence of an electric field produced by the electron beam.
2. During low temperature measurements, the migration is preceded by a residence time during which the sodium is relatively immobile.

3. At a given temperature, the residence time is proportional to the rate at which electrons impinge the surface.
4. The signal decay can be modeled assuming

$$Na_t = Na_o \, e^{-\bar{v}t/\lambda}$$

The drift velocity of sodium ions is primarily mobility dependent. When the sample is initially at low temperature, a critical number of incident electrons (residence time) act to raise the temperature (mobility) locally, thereby providing measurable migration rates.

5. It is possible to determine experimental conditions which permit AES analysis of mobile ions.
6. An analytical technique for compositional analysis of soda-lime-silicate glass has been developed.
   a. Cool the sample with liquid nitrogen during analysis.
   b. Maintain beam current density below $\sim$.01 amps per cm^2.
   c. Measure AES spectra within the observed residence time.

CHAPTER IV

ATMOSPHERIC EFFECTS UPON GLASS SURFACE COMPOSITION

Due to the extreme surface sensitivity of AES analysis, it is possible to investigate reactions between a gaseous environment and a glass surface, i.e., weathering. In particular, AES analysis provides a means for studying surface compositional changes in the very early stages of interaction even under conditions which result in only moderate reactivity. Of particular interest is the class of reactions which result in attack and general degradation of the surface. These reactions will be due primarily to an interaction between the surface and adsorbed water picked up in the ambient atmosphere. Charles [16] has suggested that reaction between an alkali-containing glass surface and water vapor is initiated by a sodium-hydrogen ion exchange between the sodium at the surface and in the subsurface and hydrogen from the adsorbed water vapor. To the author's knowledge, no direct experimental verification of that hypothesis has been reported for a glass-water vapor interaction. Furthermore, AES analysis of soda-lime-silicate surfaces, in general, will require

a recognition of this reaction since all surfaces prepared outside the vacuum will have been exposed to the ambient which is likely to contain water vapor.

During the course of analyzing a variety of soda-lime-silicate surfaces, a characteristic surface compositional profile has been observed. This is true, of course, providing that the surface has not received special chemical treatment of any kind. It is, however, observed for as-cast surfaces, mechanically abraded surfaces and fracture surfaces. This characteristic effect is believed to be the result of a glass surface reaction in the ambient environment of the type described above. The hypothesis is tested in this chapter by producing well characterized surfaces in vacuum and subsequently monitoring their compositional evolution *in situ*. Methods for semiquantitative analysis and structural interpretation of composition-depth profiles are presented.

(Semi)Quantitative Analysis

Estimates of surface composition can be made from the Auger spectra. The peak-to-peak height of the differentiated Auger signal for a particular element is known to be approximately proportional to the amount of the element at the surface [43]. Use of peak-heights as a measure of relative concentration requires that the peak shape is

not affected by the composition or chemical changes under study. The deleterious effect of intense electron irradiation upon the low-energy Si peak (Chapter II) represents such a situation. Peak-height interpretation for quantitative analysis is not valid under those conditions. In cases where peak shape changes occur, integration techniques are required to extract quantitative information [44]. Significant changes in peak shape have not been encountered as a result of glass-water reaction. Hence, the relative composition, C_x, in atomic percent, can be estimated by using the formula

$$C_x = \frac{I_x \cdot S_x}{\sum_x I_x \cdot S_x} \qquad (6)$$

where I_x is the peak-to-peak height of element x, S_x is the Auger sensitivity factor for the element, and the summation is taken over all detectable elements (not peaks) in the spectrum. The sensitivity factor calibrates the Auger transition signal strength for excitation cross-section and electron escape probability. Matrix effects are not included in the equation but may be accounted for in the measurement of S_x (see below). This method averages the composition over the entire sampling depth thereby obscuring, to some extent, the inherent depth sensitivity of the technique. When this is a major consideration,

peak-height comparison of high- and low-energy Auger transitions provide the necessary supplemental information.

The sensitivity factors for the various elements must be determined experimentally. One procedure for obtaining sensitivity factors is to measure the Auger spectra of pure elements, when possible, under identical conditions and to compare the peak sizes with respect to each other. This technique has been of value for analyzing relatively pure metals and metallic thin films. It is important to recognize, however, that a sensitivity factor for a particular element as defined here is not independent of the matrix in which it exists. For example, aluminum in aluminum metal does not have the same sensitivity factor as aluminum in aluminum oxide, owing to a difference in peak shape. For this reason, a better calculation of the sensitivty factors is obtained by measuring the Auger spectrum of the element in an environment that most closely approximates the sample in question. One alternative to the elemental standards, then, is to use pure oxide compounds such as SiO_2, CaO, Al_2O_3 and MgO. This accounts for the effects of compound formation upon excitation cross-section and peak shape, but a further correction is necessary to account for the electron escape depth which results upon fusing these compounds into a single solid. Therefore, it is more convenient to use sensitivity factors obtained by analysis

of the Auger spectrum of the multicomponent glass itself after extensive periods of ion milling (i.e., until peak-heights cease to change). Since the glass composition is known and extension ion milling exposes bulk glass, the sensitivity factors can be calculated more precisely on the basis of that Auger spectrum. This spectrum obtained after extensive ion milling has been found to be reproducible from sample to sample of the same composition. Also, except for the original surface, all spectra measured during compositional profiling are, of necessity, obtained from surfaces produced by ion milling. Hence, sensitivity factor determination utilizing the spectrum from an ion-milled surface also accounts for any differential ion-milling effects upon the measured surface composition.

It has been found convenient to convert the normalized peak heights to percentages of equivalent SiO_2, Na_2O and CaO constituents, i.e., molar concentration. This yields an approximation of the surface composition in a form which is readily comparable to the known bulk composition. In addition, this procedure permits a comparison to be made between the oxygen level detected and the level anticipated by the metal-oxygen ratios assumed above. Good agreement is found in most cases with occasional minor discrepancy occurring in a small region very close to the surface. This discrepancy can arise if other species such as adsorbed

water or hydroxyls are present which are not accounted for in the calculations. However, the excess or deficiency of measured oxygen levels has not been shown conclusively to be related to OH or adsorbed water because H cannot be directly measured by AES. The oxygen discrepancy could also be due to relatively small errors in establishing the metal ion concentrations.

Converting ion-milling time to depth requires an independent determination of ion-milling rate. This is most easily accomplished by measuring the time required to ion erode thin glass films of a known thickness. In the present case, the thickness of thermally grown SiO_2 films on silicon was measured using ellipsometry. A milling rate of 30 Å/min was determined for these SiO_2 films. This value is used for most silicate glass data in this work although it is possible that the milling rates may be somewhat different due to the presence of nonnetwork species.

Upon performing the above conversions, it is possible to obtain a plot of relative mole percent versus depth. This is most conveniently accomplished using computer calculations (Appendix I). Although such profiles are approximations, they provide a good, easily interpretable representation of surface concentration gradients which are readily comparable from sample to sample.

Experimental Procedure

A commercial soda-lime-silicate container* was sealed in a larger glass container immediately after it was annealed. The glass composition was approximately 74% SiO_2, 13% Na_2O, 12% CaO, 1% other (molar). The as-cast container surface was not further exposed to the external ambient environment except during a brief period for mounting and loading into the AES system. The inside surface of the container was analyzed. Extreme care was exercised to prevent the surfaces to be analyzed from being contacted by anything except air during handling. The surfaces were not subjected to cleavage or other mechanical treatment prior to examination.

AES analysis of this glass was carried out using the analytical technique developed in the last chapter. The samples were held at low temperature (cooled by liquid nitrogen), beam current was approximately 1 μA with a 250-350 μm diameter beam, and the beam energy was 3 keV. Measurements are made within the observed residence time of 80 seconds. Ion bombardment was carried out with 2 keV Ar ions in the presence of thermal electrons.

---

*Brockway Glass Co., Inc., Brockway, Pa.

Analysis of As-Cast Surface

The upper spectrum in Figure 14 represents the surface composition of the glass prior to ion milling. Peaks due to silicon, calcium, oxygen and sodium are evident. The lower spectrum in Figure 14 represents the surface composition after extensive ion milling. At this depth in the glass surface, no change in the AES spectrum is observed with continued ion milling. Hence, after extensive ion milling, it is assumed that the bulk glass has been exposed. Differences noted in the peak-height ratios between these two spectra indicate a difference in composition between the surface and the bulk, particularly with regard to sodium. The upper spectrum indicates a surface sodium concentration of 25%, while the lower bulk spectrum indicates 13% Na_2O (obtained using analysis presented above).

The AES spectra measured as a function of ion-milling times are presented in Figure 15 according to their peak-to-peak heights. Utilizing the method of analysis described previously, this "raw" data may be put on a semi-quantitative basis. The surface compositional profile which results from that calculation is presented in Figure 16.

The lower spectrum in Figure 14 represents approximately the data used to calculate sensitivity factors. The factors actually utilized, however, were determined using the average

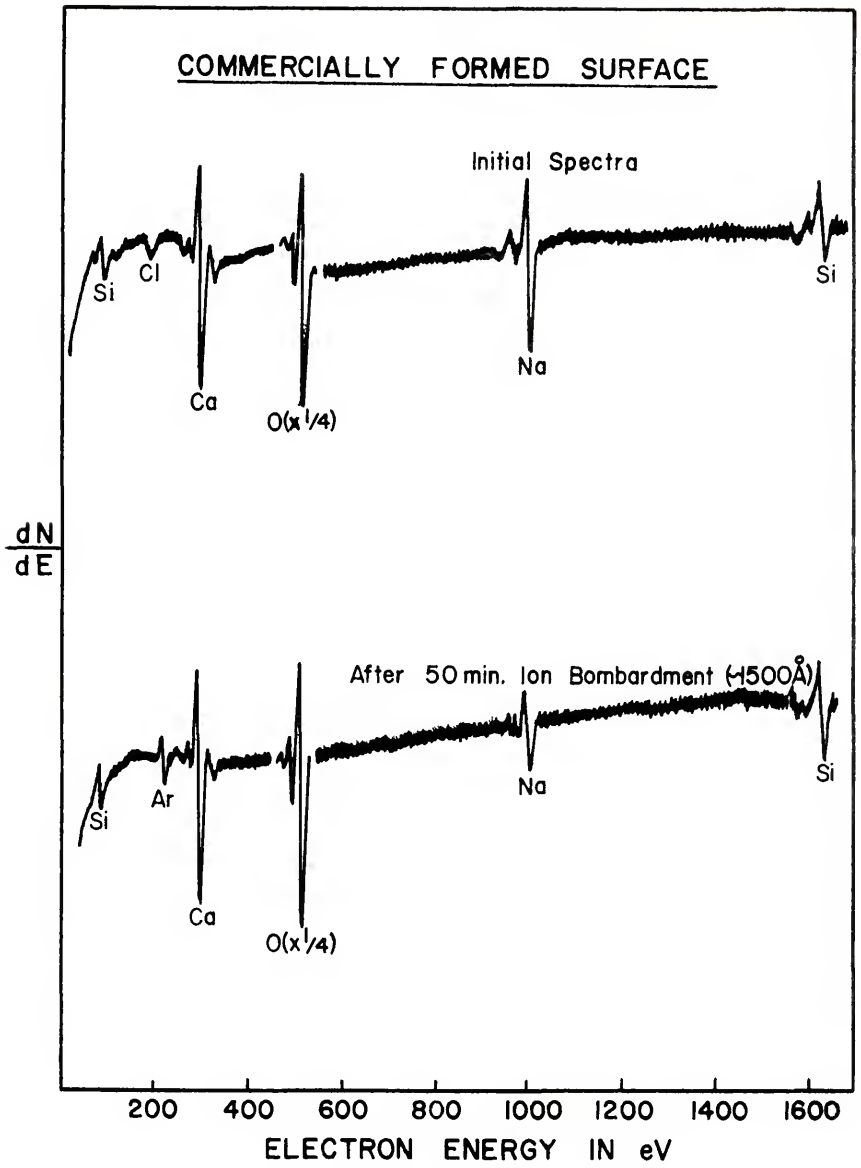

Figure 14. AES spectra for the inside surface of a commercial soda-lime-silicate glass container.

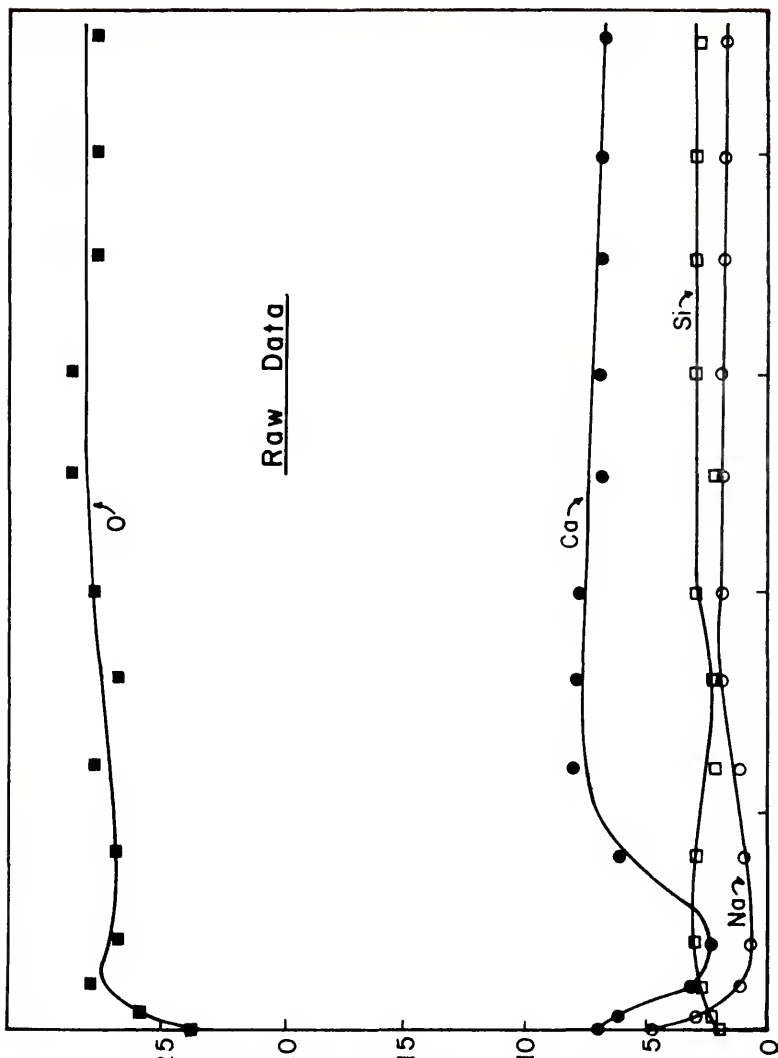

Figure 15. AES peak-to-peak heights vs ion-milling time for inside surface of a soda-lime-silicate glass container.

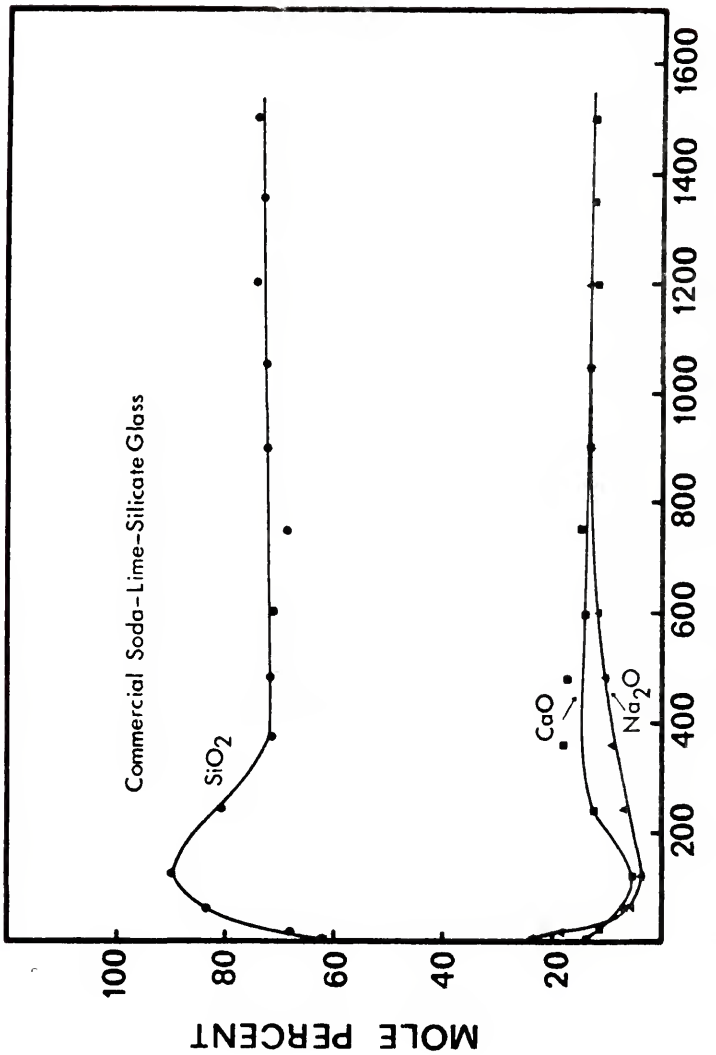

Figure 16. Compositional profiles for inside container surface, as cast.

spectrum measured on six different samples. The sensitivity factors obtained were O (KLL) 1, Si (KLL) 4.5, Ca (KLL) .3 and Na (KLL) 1.76. With the exception of the KLL-Si peak, these values are in approximate agreement with factors deduced by other methods [42]. The sensitivity to the Si (KLL) peak is quite low and is due primarily to the low beam current densities utilized for glass surface analysis. High-energy Auger peaks are, in general, quite sensitive to changes in the beam current density.

It may be recalled from the discussion of semi-quantitative analysis that the oxygen concentration measured during profiling does not always agree with the concentration anticipated by the measured cation concentrations. The correlation for the measurements presented here is about 90-95%. The measured oxygen concentration disagrees with the value dictated by the cation concentration on the average by 5-10% (plus or minus). Hence, the accuracy of the relative molar percent calculation is not better than 10%.

The surface layer of this glass is seen to be enriched in Na_2O and CaO with a corresponding depletion (silica-rich) zone below the surface. Chlorine is also detected on the surface. At a depth of approximately 900 Å, the bulk glass composition is reached.

The amount of Na_2O and CaO in the enriched surface does not account for the amount depleted in the silica-rich

zone. If the calculated compositions are accurate, the data indicates that Na_2O and CaO were lost from the surface during forming and annealing, creating the silica-rich zone. Manufactured glass can have varying degrees of surface alkalinity depending upon thermal history and the gaseous environment [10]. Glasses annealed in gas-fired lehrs have considerably better chemical resistance than those annealed in electric lehrs [61]. It is clear that the furnace gases play an important role in the surface durability. The widely accepted viewpoint is that sulfur gases present in the lehr can be responsible for dealkalizing the glass surface. No sulfur was detected on this surface, however. Furthermore, if dealkalization of the surface has in fact occurred, the outermost surface layer has since become enriched with sodium.

It has been found that for soda-lime-silicate glass surfaces which have not undergone special surface treatments, the presence of an alkali-enriched layer at the surface appears to be a common characteristic. (An interpretation of this characteristic profile in terms of a structural model of the surface is presented in a later section.) As pointed out previously, this is true for as-cast, abraded and fractured glass surfaces. The following experiments are designed to ascertain the origin of these characteristic profiles. After extensive ion milling,

the bulk glass can be exposed. The effects of reaction with the environment are determined by noting the changes which take place on that surface. Exposure to high vacuum conditions and to water vapor are considered below.

Reaction of Surfaces Prepared in Vacuum

A glass sample was ion milled for 60 minutes. The upper spectrum in Figure 17 is representative of that surface composition. This spectrum is assumed representative of the bulk glass composition as described previously in Figure 14. The resultant exposed bulk glass was allowed to stand in vacuum at room temperature. The total system pressure was 10^{-8} torr while a residual gas analyzer revealed that only a trace of water vapor existed; After 45 hours in vacuum, the AES spectrum given by the lower curve in Figure 17 was measured. No change in the peak-height ratios for the various elements can be detected. Hence, no alteration in the surface composition is indicated after aging 45 hours in high vacuum.

Figure 18 presents the compositional profile measured for this ion-milled surface after 45 hours exposure in vacuum. No change in calcium concentration is observed with ion milling. It can be observed, however, that a minor depletion of sodium has occurred in the subsurface. Since the AES spectrum measured prior to ion milling (Figure 17, lower

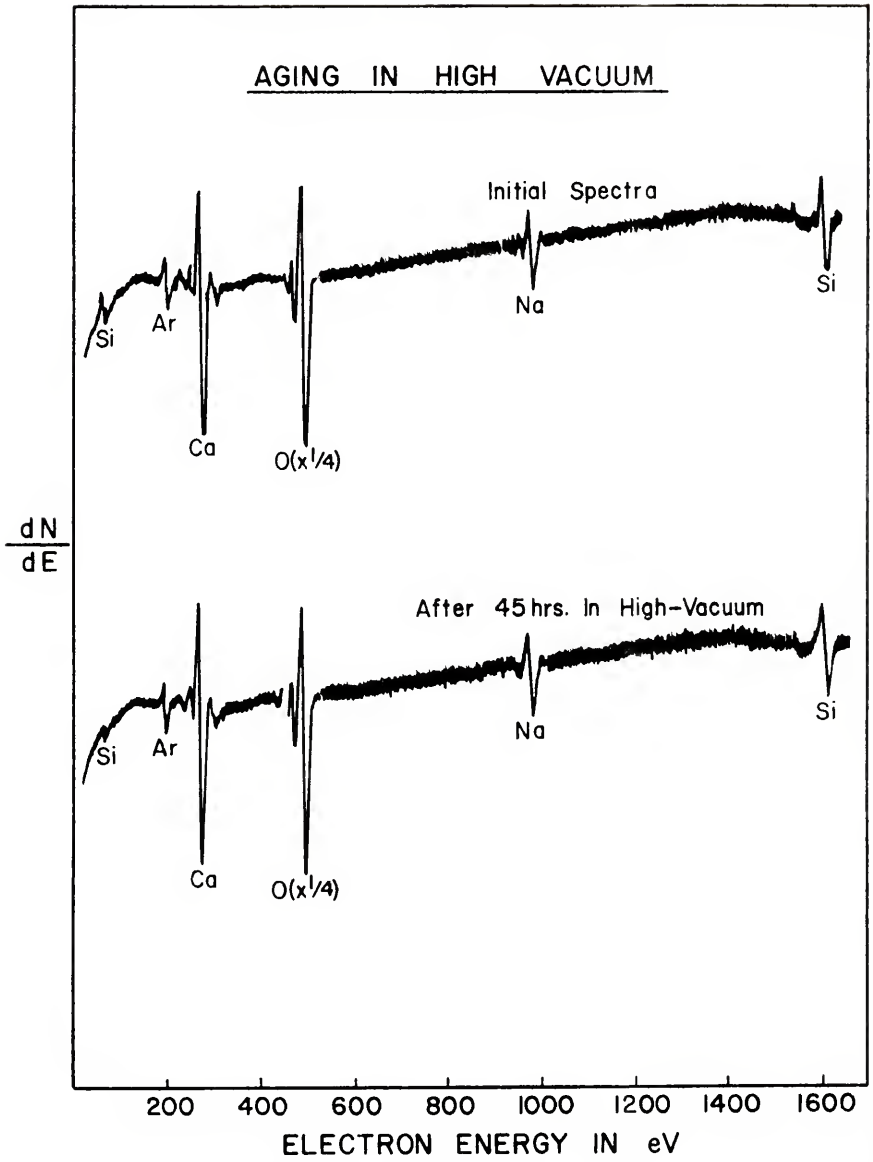

Figure 17. AES spectra for soda-lime-silicate glass surface produced and aged in vacuum.

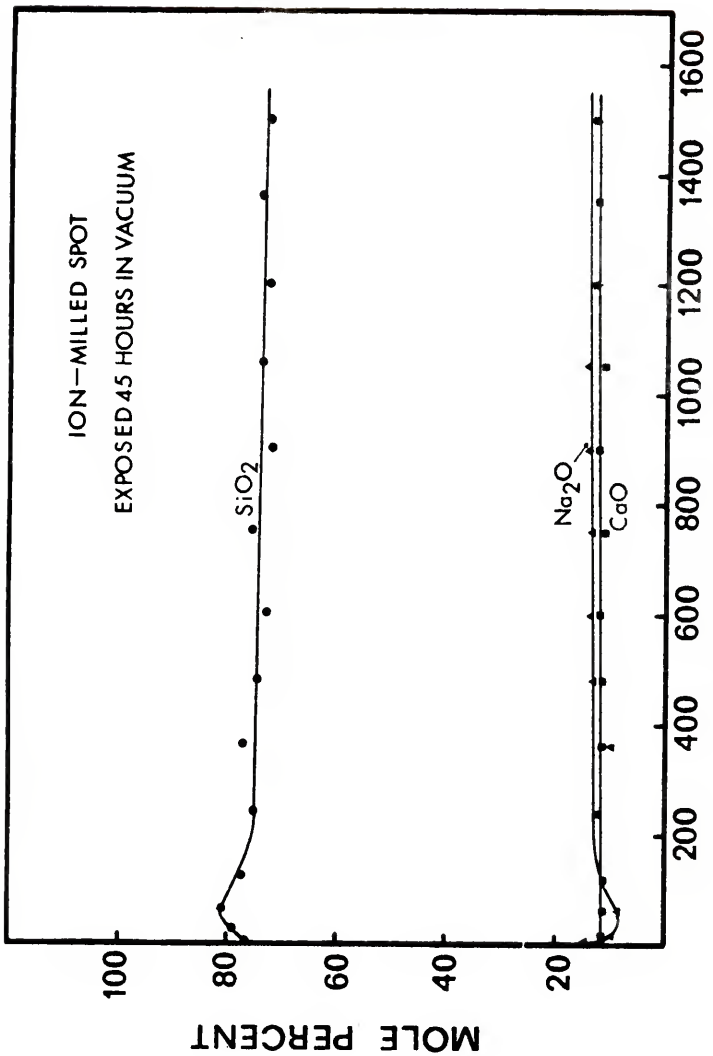

Figure 18. Compositional profiles for soda-lime-silicate glass surface aged 45 hours in a vacuum of 10^{-8} torr at room temperature.

spectrum) indicated no change in surface composition, it is difficult to understand the origin of this depletion on the basis of a surface chemical reaction. It is felt, therefore, that this effect may be due to the ion bombardment process. This point is discussed further below.

Again, the bulk glass was exposed by extensive ion milling. Exposure of such a surface to air at room temperature gave rise to much more pronounced changes than those observed after exposure to high vacuum. Figure 19 presents the AES spectra for surfaces exposed to air for both 5 minutes and 60 minutes. These spectra are to be contrasted with the upper spectrum for the bulk glass surface. Significant changes in the surface composition due to this exposure are indicated. In particular, the Na peak-to-peak height has increased. The increase is greater after 60 minutes' exposure than after 5 minutes' exposure. After 5 minutes in air, the surface soda concentration is 21% while after 60 minutes it is 27%.

Figure 20 represents the surface compositional profile which results due to the 5-minute air exposure. Figure 21 represents the surface compositional profile after 60 minutes in air. Note the general similarity when compared with Figure 14, the profile for the as-received glass surface. Hence, soda-lime-silicate glass is capable of reacting rapidly with the water vapor in air, which is

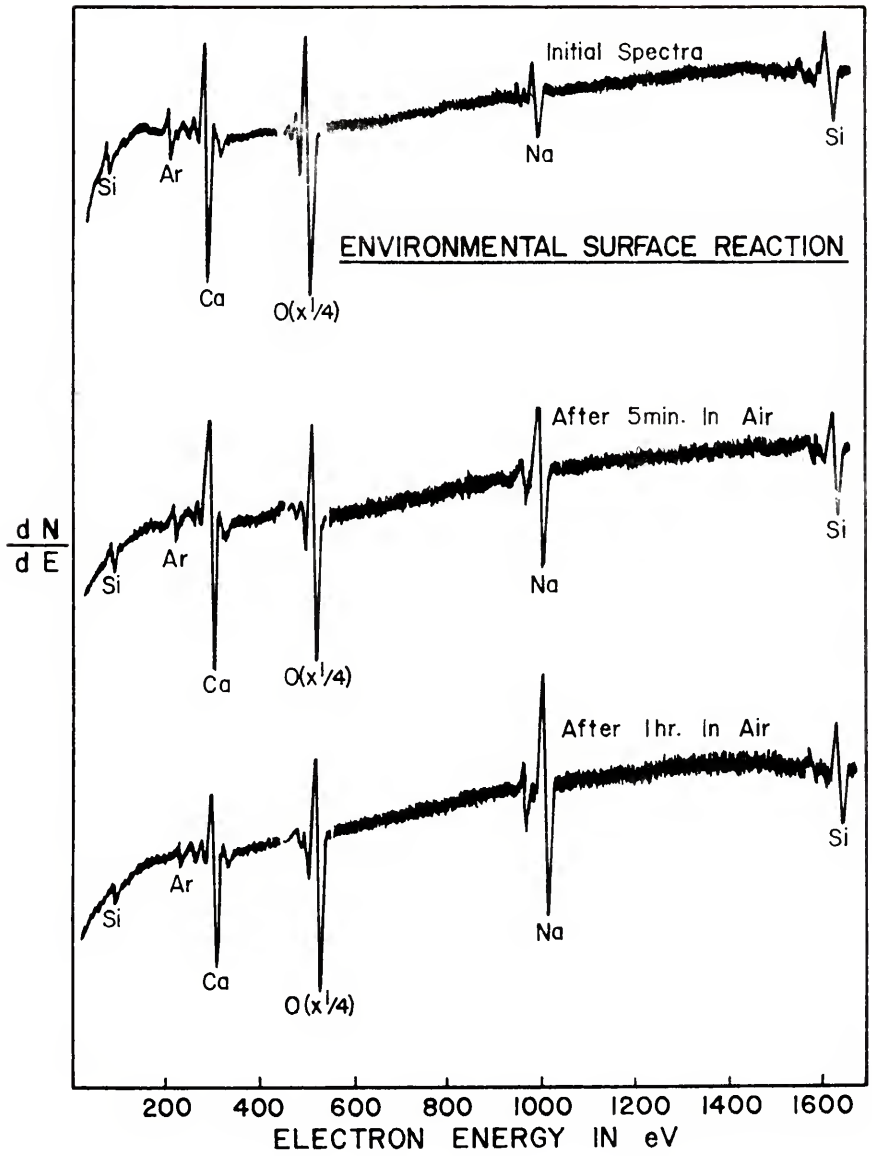

Figure 19. AES spectra for soda-lime-silicate glass surface produced in vacuum and subsequently exposed to air for 5 and 60 minutes at room temperature.

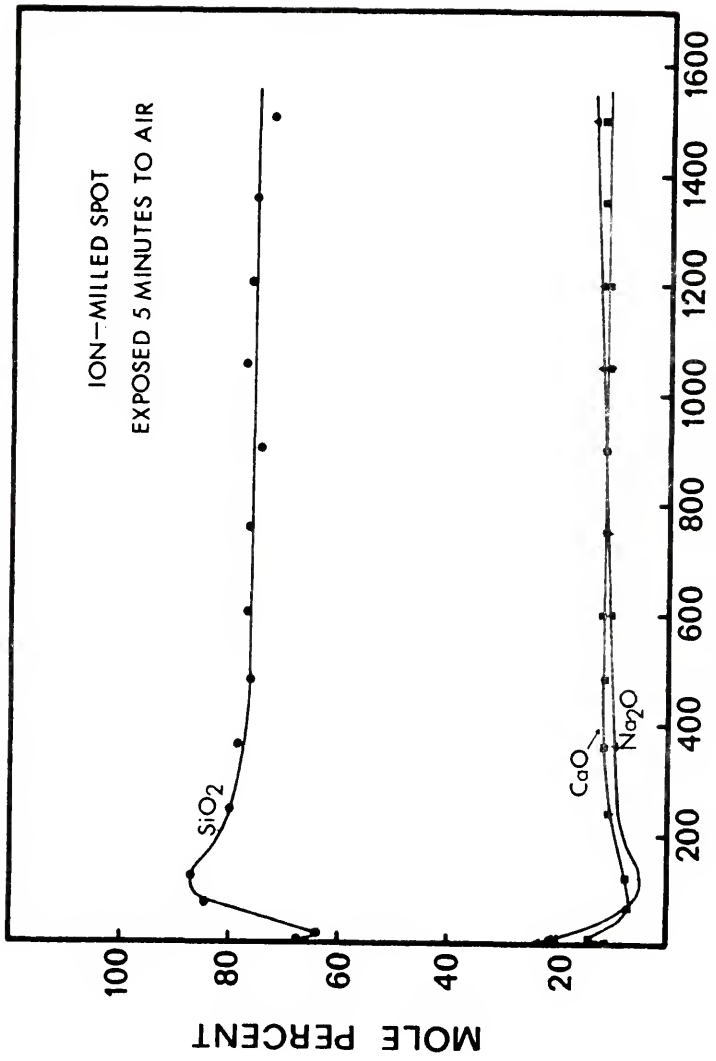

Figure 20. Compositional profiles for soda-lime-silicate glass surface after 5-minute reaction with air at room temperature.

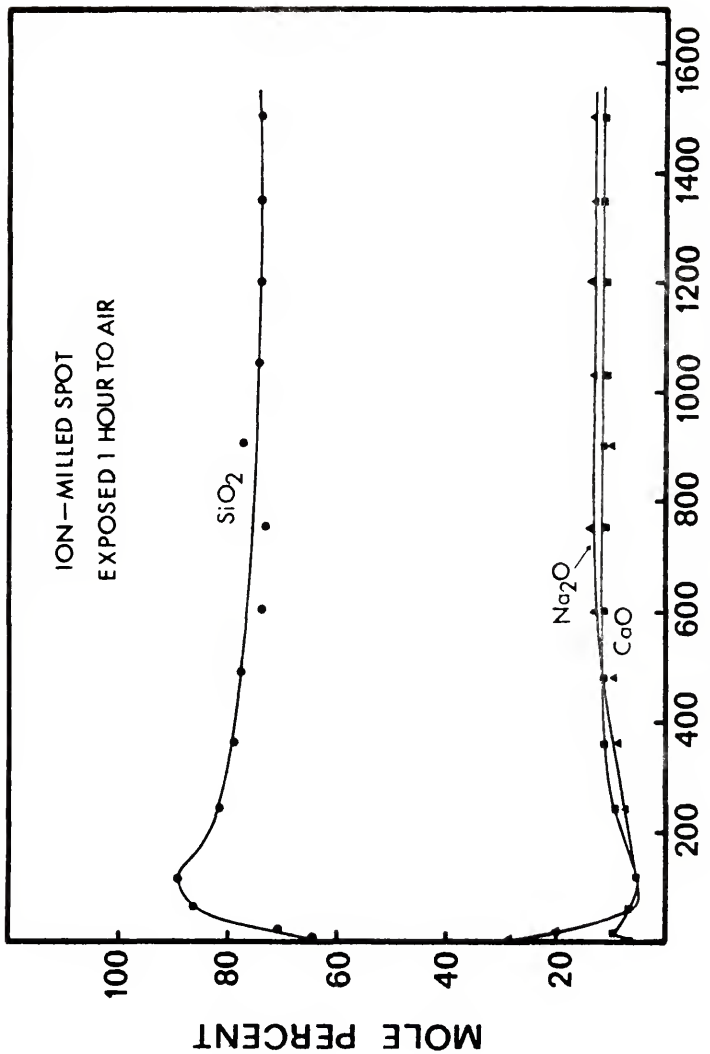

Figure 21. Compositional profiles for soda-lime-silicate glass surface after 60-minute reaction with air at room temperature.

sufficient to produce the characteristic profile observed initially. These enriched and corresponding depleted regions at the surface, then, will result whenever a soda-lime surface is exposed to water vapor, such as is found in ambient, provided the surface has not been specially treated.

The increased sodium concentration observed on the surfaces exposed to air is consistent with the hypothesis of Charles [16]. Ion exchange between the Na at the surface and in the subsurface with H from adsorbed water vapor results in a surface higher in sodium concentration than the bulk. This can be seen clearly in Figure 19. Under these conditions, the reaction appears to saturate within one hour. The representation of glass composition in terms of the starting oxide constituents is a convenience that is not meaningful at the outermost surface. Due to the presence of hydrogen and oxygen at the surface, the sodium enrichment at the surface most probably represents the formation of a hydroxide. This reaction gives rise to a depleted region beneath the surface which in turn tends to retard further reaction. Unfortunately, it is not possible to detect H by AES and another technique must be invoked in order to fully substantiate the above expectation. Although it is conceivable that the divalent Ca ions are subject to a similar reaction, enrichment of calcium at the surface is not observed. In fact, after 1 hour in

air, the calcium concentration on the surface decreases as a result of the sodium segregation there. The regions depleted of calcium below the surface are not understood. This matter is discussed below with regard to the ion-milling process.

In principle, it should have been possible to detect the presence of an adsorbed or reacted water-vapor layer by observing from the AES data whether a significant change in the oxygen level had occurred in the near surface region, but so far a definitive result has not been obtained.

It has been found that the excess sodium at the surface is water soluble and hence is readily removed by immersion of the sample in water. In this case, it is expected that the surface, which is now the Na-depleted region, is less able to react due to extended distance over which the sodium must diffuse to reach the surface. Hence, after immersion in water the profile denotes only a Na-depleted region at the surface since the dealkalized (Na-depleted) surface cannot initiate ion exchange (Chapter V).

During investigations of early-stage weathering on soda-lime-silicate glass using replica electron microscopy [17], Tichane suggested alkali enrichment at the surface. He hypothesized this because replicas were easily removed

from lightly reacted surfaces, although the replicas were featureless. In contrast, prior rinsing of the surface resulted in a tenaciously held replica.

Compositional Profiling

The measurement of an AES peak-to-peak height as a function of time of material removal by ion bombardment is directed at obtaining a compositional profile. In addition to procedures necessary to obtain quantitative composition data from the AES measurement, it is necessary to recognize a number of effects [62] inherent in the AES ion-milling process which complicate the complete extraction of composition versus depth data. Several distinct processes may be recognized.

1. The detected Auger electrons escape the solid with a probability which decreases exponentially with depth, typically 5-50 Å. Hence, this AES depth averaging tends to smear out edges in the compositional profile.
2. The incident electron beam illuminates an area of the sample which may be homogeneous in structure or separated into several phases that are removed at different rates by ion milling.
3. The ion bombardment process itself may give rise to a thin layer of modified surface composition [63].

This differential sputtering effect can lead to the accumulation or depletion of a particular species in this modified surface layer. In the case where a particular component has a higher sputtering coefficient than the homogeneous matrix (relative sputtering rate k is greater than 1), it is depleted from the surface. This process is rapid and will occur within fractions of a monolayer. Conversely, where k is less than 1, the speciesin question will accumulate in the surface. This latter process is slow and may extend over many atomic layers.

The influence of this on the Auger spectra can be minimized by calibrating peaks under conditions of ion bombardment. The effect of this upon composition profiles is much more complex and requires rationalization on the basis of the particular sample surface in question. Figure 18, for example, indicated a slight depletion of sodium in the subsurface which could not be rationalized on the basis of a surface chemical reaction in vacuum. Similar depletion regions are observed for calcium with no indication of a corresponding enrichment at the surface. Hence, it may be assumed that this depletion is a result of the preferential removal of modifying

ions. This is not unexpected when considering the spectrum of bond strengths in a multicomponent glass. Sodium, being a modifier ion, most probably has the weakest bond strength relative to the other glass constituents. Hence, it may be easily (preferentially) removed from the matrix. The AES spectra, then, would indicate a depletion of this species. (It has been shown in Chapter II that the elemental species Si and O which comprise the silicate network are not subject to such preferential effects during ion bombardment.) The subsequent increase in modifier-ion concentration back to its original value is not completely understood. It is known, however, that during thin film sputtering of multicomponent alloys, a period of surface conditioning is observed [62]. That is, the early stages of sputtering result in a film whose composition is not the same as the target. After a short period of sputtering, however, the film attains the correct composition. The minor depletion of sodium noted upon initiation of ion milling in Figure 18 is perhaps related to this surface conditioning process.

4. Kinetic effects occur that tend to smear out the measurement of sharp interfaces. In the case of an

adsorbed monolayer, removal by ion milling is not instantaneous. If the rate of removal of the adsorbed monolayer is written as

$$dN/dt = -NI\beta \tag{7}$$

where N is the number of adsorbed atoms/cm^2, I is the incident ion flux, and β is a cross-section for removal, then,

$$N = N_o e^{-I\beta t} \tag{8}$$

i.e., the rate of decrease of the number of atoms in the layer is exponential with time. Furthermore, if the substrate material has, for example, a much larger sputtering rate, then the AES signal would show the presence of atoms of the adsorbed species declining exponentially over many layers of removal of the substrate. Knock-on effects may also contribute to smearing of interfaces.

5. Ion-bombardment-induced migration of mobile species in thin, SiO_2 films may occur, as discussed by McCaughan et al. [38]. It is not clear, however, whether this process can operate during bombardment of a thick glass at low temperature such as in the present investigation.

6. In practice, depth resolution is further limited by the shape of the crater formed by the ion beam and by the roughness of the surface. Furthermore, the roughness of the surface may increase with ion milling.

Figure 22 schematically represents some of the effects noted above and shows how they might affect the AES-measured profiles. The effects must be considered before structural models of composition versus depth can be deduced from the measured-AES profiles.

In the present case of an ion-milled glass surface which has reacted with water vapor, the resultant profiles are quite reproducible and interpretable in terms of the above effects. Figure 23 shows a somewhat simplistic interpretation of the characteristic Na profile observed on the commerical glass surfaces. Certainly, the effects noted can be much more complex than those described in this sketch. However, in this case it can be qualitatively ascertained that a Na-rich film has formed on the surface. This has been extablished in Figure 18 without the perturbing effects of ion bombardment. The immediate decrease in the Na concentration at the surface implies either removal of a very thin layer or preferential removal ($k>1$) of the Na from within a surface film. The increased concentration of Na at the surface must necessarily result

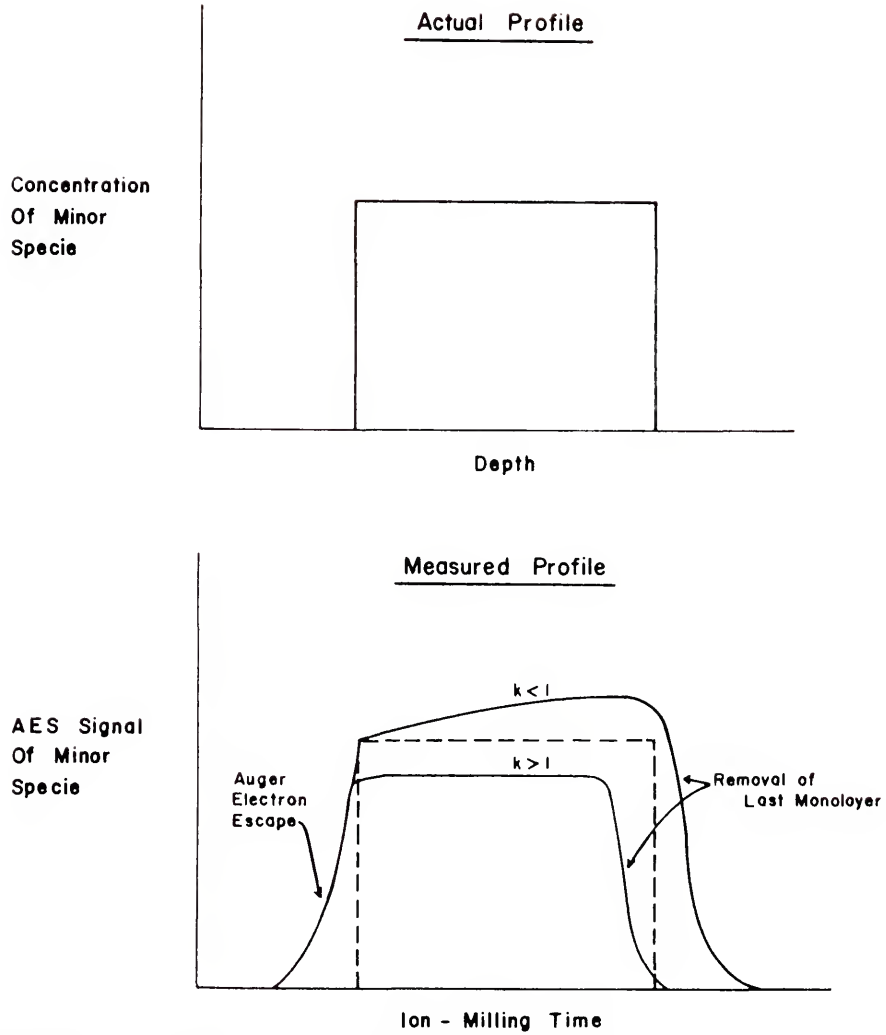

Figure 22. Schematic representation showing the distortion of a simple concentration profile when measured using ion-milling AES. The effects of Auger electron escape and differential sputtering are demonstrated, where k is the relative sputtering rate, k(minor species)/k(homogeneous matrix).

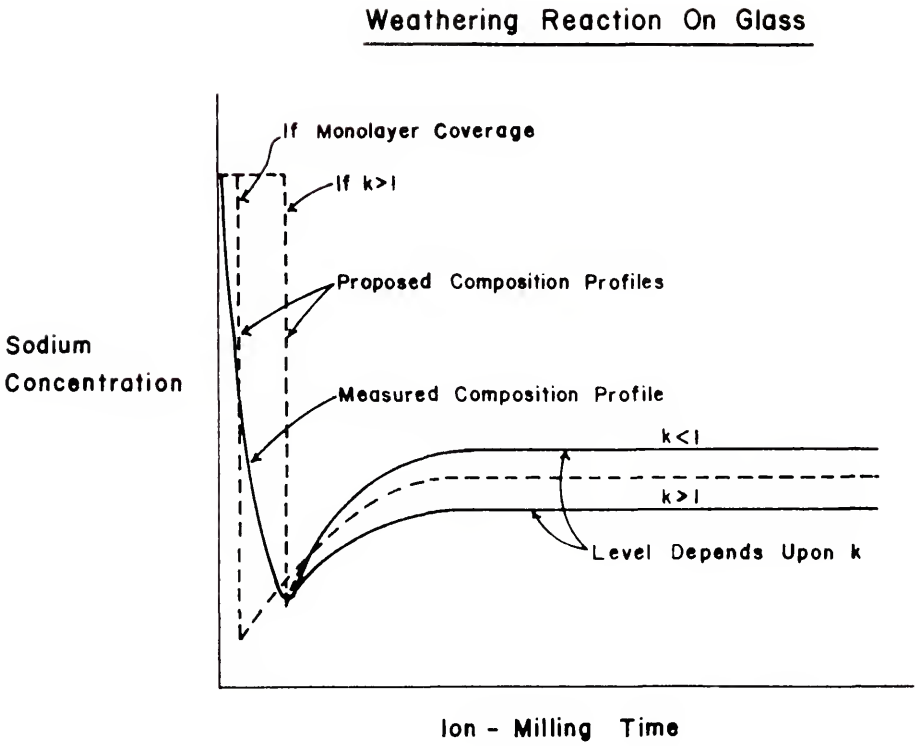

Figure 23. Schematic interpretation of the sodium compositional profile measured on the commercial glass surface. The declining sodium concentration into the surface can be interpreted with either of the two possibilities shown. k is the relative sputtering rate.

in a depleted region below the surface. The exaggerated minimumin the profile is due somewhat to preferential ion removal. Finally, the composition increases as the bulk glass region is approached. As shown in Figure 23, the actual level detected in the bulk is primarily dependent upon the relative sputtering rate k. In the absence of calcium enrichment on the surface, the region depleted in calcium in the subsurface must be interpreted as an ion-milling artifact.

In measuring compositional profiles at glass surfaces by the AES, ion-milling technique, the regions described above have been obscured as shown in Figure 22. While the determination of compositional profiles from AES data is a process involving a number of assumptions, qualitative results are more readily obtained. Hence, although the compositional changes observed at the surface of glasses may be readily followed by this technique, much work is needed before detailed quantitative composition versus depth profiles can be obtained with any precision.

Summary

1. The outermost surface of a commercially formed surface is rich in sodium relative to the bulk content.

2. Aging a bulk glass surface in high vacuum at room temperature for 45 hours does not induce changes in surface composition.
3. Exposure of a bulk glass surface to air containing water vapor at room temperature induces sodium enrichment at the surface.
4. The observation of sodium enrichment at a soda-lime-silicate glass surface upon exposure to water vapor provides the first direct confirmation of the Charles theory [16].
5. Surface compositional profiles indicated that a sodium-depleted region exists under the sodium-enriched surface.
6. Structural interpretation of surface composition profiles requires careful validation. In particular, the observation of subsurface depletion in the absence of surface enrichment is subject to doubt.

CHAPTER V

SURFACE COMPOSITIONAL CHANGES DURING COMMERICAL SODA-LIME-SILICATE GLASS-WATER REACTION

The interaction between soda-lime-silicate glass and pure water is governed by two processes [20]: (1) the leaching of modifier ions from the glass surface via an ion-exchange reaction with protons or hydronium ions in the water, and (2) the dissolution of the silicate network via the hydrolysis of siloxane bonds. (These two "processes" are referred to throughout the remainder of this chapter.) Clearly, the overall effect is dictated primarily by the relative rate at which the two processes occur. Because each reaction represents an independent function of temperature and solution composition, interpretation of experimental results has been difficult. In particular, the use of solution analysis to monitor the reaction requires measurable changes in the attacking medium. This solution modification, which is primarily a pH rise, then alters the reaction under investigation. This factor has been a primary deterrent in the determination of rate-controlling processes during glass-water reaction. Nonetheless, it is the best available method for

determination of glass decomposition products and the rate at which they appear in solution. Recently, IRRS has been used to monitor changes in the glass surface after aqueous exposure. This method can detect the presence or absence of a leached (silica-rich) layer on the glass surface, provided it is of the order 5000Å or greater in thickness. It does not provide a direct measure of the surface composition, although in simple binary systems this information may be obtained indirectly.

The present study is aimed at measuring directly the surface composition and surface composition profile of a soda-lime-silicate glass after reaction in static, aqueous solution. This is accomplished through the use of the AES ion-milling technique which has been developed. In addition to providing the first direct measurement of such surface composition profiles, this investigation should provide some answers to long-standing questions concerning the leaching and dissolution of soda-lime-silicate glass. The two processes cited at the beginning of this section can be easily distinguished by this method. By using large solution volumes and small surface areas, modifications in the solution chemistry can be prevented. Hence, the relative occurrence of the two processes can be investigated independently of solution effects. Clearly, the method provides a necessary supplement to the extensive studies which have already been carried out using solution analysis.

Although the conditions for reaction are chosen to be of general interest, each experiment is designed to clarify points raised previously in the absence of surface compositional data. In particular, the leaching of divalent cations (e.g., calcium), the dissolution of silica-rich films in neutral solution and the formation of steady-state surface compositional profiles are discussed. Also, the effect of temperature has been of interest with regard to accelerated tests of chemical durability. The ASTM method [64] for testing commerical soda-lime-silicate glass containers which is carried out at 121.5°C, is investigated in relation to its significance for ambient temperature reactions. This point has been the subject of previous investigations [65].

Experimental Procedure

Soda-lime-silicate containers obtained as described previously (Chapter IV) were used. All glasses considered throughout this work are from the same glass batch. The container is filled to 90% of overflow with the respective solution. This maintains a constant solution volume to glass surface area ratio throughout ($\sim$2ml/cm^2) and at the same time fulfills the requirements of the the ASTM durability test, C225, method B-W. In contrast to studies using crushed glass, this volume to surface area ratio provides almost

infinite dilution of the extract for this composition, thereby minimizing changes in solution chemistry. (Prior to filling, the container is rinsed twice with high-purity water.) The high-purity water is obtained by chemical ion exchange. The HF acid utilized is reagent grade.

The high temperature (121.5°C) exposures are carried out in an autoclave.* The temperature is obtained by maintaining the pressure at 14-15 psi. Except where noted, all tests are for one hour. After completion of the reaction the solution is removed and saved for solution analysis. The solutions were analyzed spectroscopically for Na, Ca and Si. The glass surface is rapidly dried via rinsing with high-purity (low-mobile ion grade) acetone. The samples are prepared and loaded in vacuum for AES analysis as soon as possible. The method of AES analysis has been described previously.

Surface Compositional Profiles at 37°C and 121.5°C

Figure 24 provides a comparison of the surface AES spectra for this glass before and after reaction in high-purity water at both 37°C and 121.5°C for one hour. The

*GCA/Precision Scientific, Model 67010

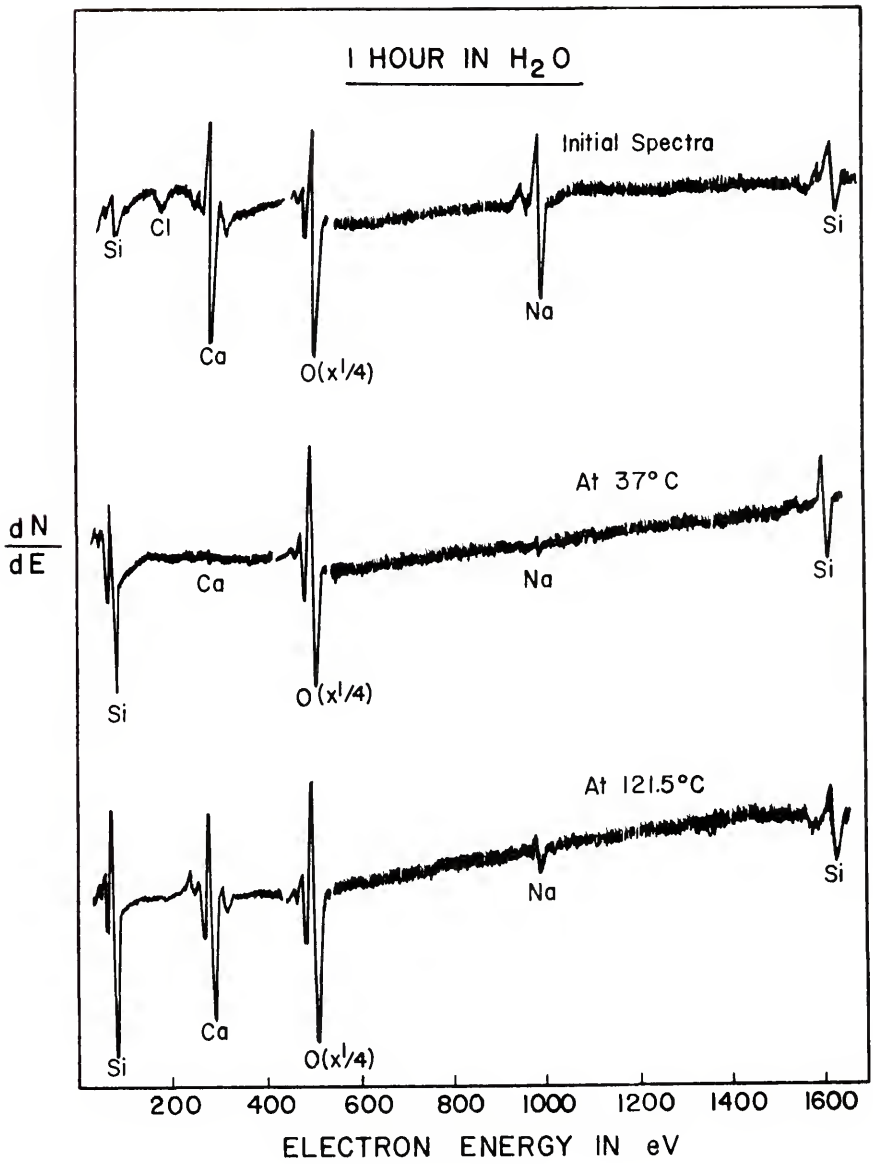

Figure 24. AES spectra for commercial soda-lime-silicate glass as received and after reaction in pure water.

middle spectrum indicates that after reaction at 37°C sodium and calcium have been exhausted from the surface. Only a trace of each species remains. The ratio of peak-heights for the low-energy (LMM) and high-energy (KLL) silicon signals has been significantly increased. This suggests an increase in the absolute (per unit volume) concentration of silicon at the outermost surface. This could result in one of two ways. If dealkalization were confined to 10 Å or less, the escape depth for the LMM-Si Auger electron, the LMM-Si signal would be enhanced without a proportionate enhancement of the KLL-Si signal (escape depth $\sim$ 40 Å). However, it is shown below that dealkalization extends to 100 Å into the surface. An alternative explanation, therefore, suggests that prior to dealkalization, sodium and calcium ions shielded the silicon atoms at the outermost surface. In that case, the low-energy silicon peak signal in particular would be greatly attenuated. Upon leaching the sodium and calcium, however, the silicon atoms are exposed at the outermost surface. In that configuration, the low-energy silicon peak signal is greatly increased while the high-energy silicon peak signal, which is representative of a considerably thicker surface layer, is affected to a much lesser extent.

It is clear, nonetheless, that sodium and calcium have been extracted from this surface, presumably through an ion exchange with protons or hydronium ions. The pH

remained neutral throughout the reaction. Hence, contrary to previous hypotheses [18], calcium can be leached from soda-lime-silicate glass even at neutral pH.

The lower spectrum in Figure 24 indicates that reaction at 121.5°C results in less drastic changes in the surface composition. This is perhaps surprising. In any event, sodium and calcium are still present at the surface, although the sodium concentration has decreased significantly. The low-energy silicon peak suggests an increased surface silica content has resulted although to a lesser extent than was observed at 37°C. Solution analysis indicated significant concentrations of all glass consituents in the solution. Further interpretation of these results requires the measurement of surface composition profiles.

The extent of dealkalization (leaching) can be examined using the compositional profiling technique. Figure 25 presents the profile resulting from the glass-water reactions at 37°C while Figure 26 presents the profile which results from reaction at 121.5°C. Analysis of the raw data provides the profile in mole percent vs depth. The same methods and sensitivty factors presented in Chapter IV are utilized here. The difference between the two profiles is significant.

Figure 25, the profile for the reaction at 37°C, indicates leaching of calcium to a depth of 100-200 Å.

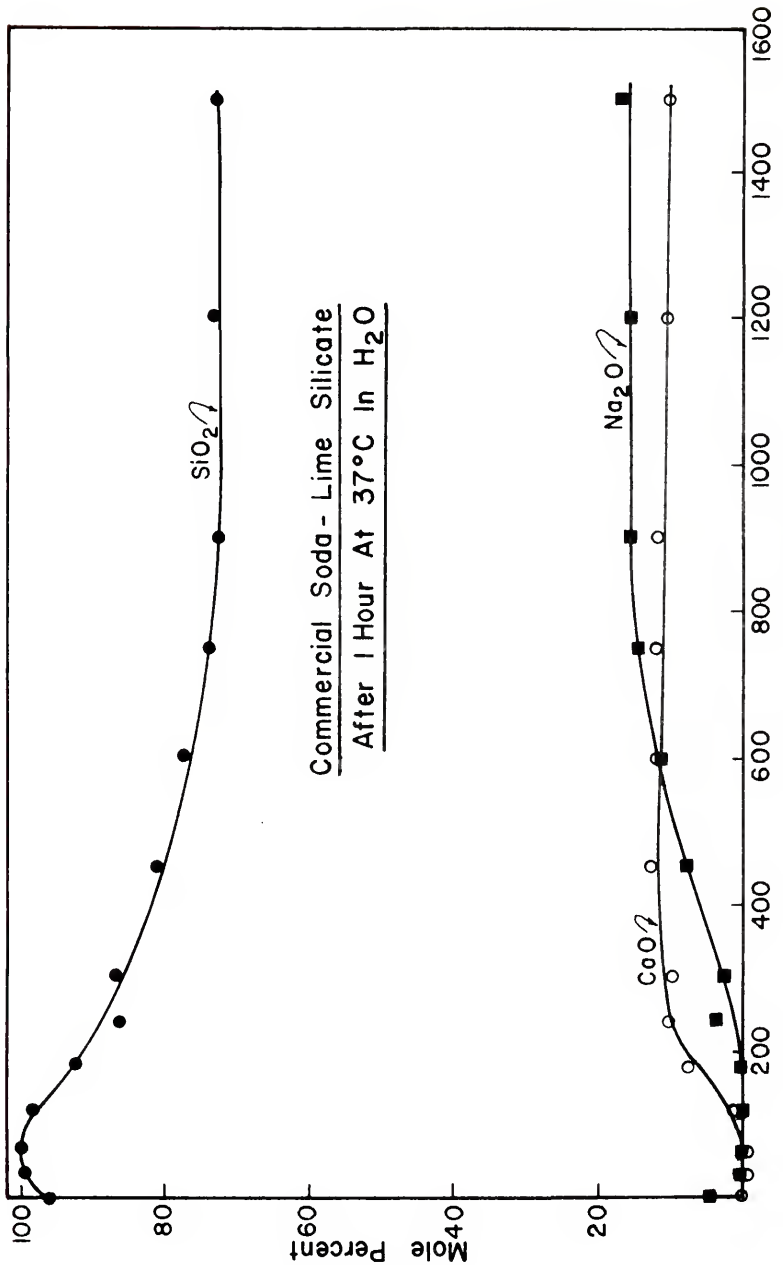

Figure 25. Compositional profiles for commercial soda-lime-silicate glass surface after reaction in pure water at 37°C.

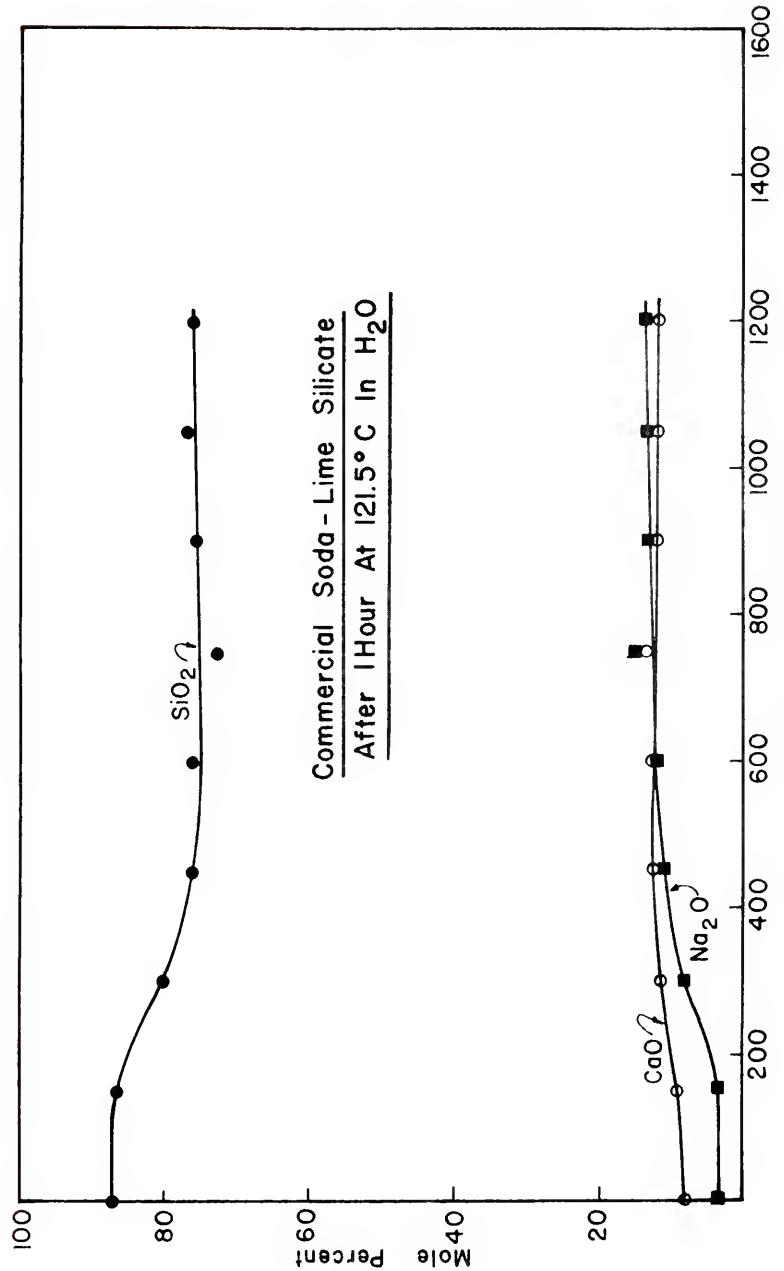

Figure 26. Compositional profiles for commercial soda-lime-silicate glass surface after reaction in pure water at 121.5°C.

Sodium, on the other hand, has been leached to a depth of up to 400-600 Å. According to previous reports, the leaching of modifier ions is largely a diffusion process [2]. Hence, the difference in the extent of leaching between sodium and calcium may well be proportional to their individual diffusivity coefficients. It is not possible to conclude from this data whether sodium and calcium are extracted simultaneously or alternatively that calcium extraction requires the prior removal of sodium. The structure through which each ion must migrate will determine the relative rates at which sodium and calcium are extracted. On the basis of the usual diffusion coefficients reported for sodium and calcium ions in glass [57], the profile is qualitatively correct. However, closer inspection indicates that for the observed sodium depletion, the calcium depletion expected should be negligible. This suggests the latter alternative to be correct; namely, the extraction of calcium requires prior removal of sodium. The opening of the silicate structure after sodium extraction may enhance the usual calcium diffusivity thereby providing greater calcium depletion than is expected.

A surface film approximately 100 Å thick, composed primarily of SiO_2 (and probably H), is apparent. Hence, the silica-rich layer at the surface probably corresponds to some form of hydrated silica left behind by the leaching of sodium and calcium.

Figure 26, the profile for the surface reacted at 121.5°C, is considerably different than the profile resulting from reaction at 37°C (Figure 25). The leaching of sodium, and to some extent, calcium, is decreased. In comparison to Figure 25, it can be seen that both surface dealkalization and extent of leaching are favored at the lower temperature (37°C) It is hypothesized that the dominant glass-water interaction has shifted from process 1 to process 2 simply on the basis of a temperature change. (A slight change in pH from 6.8 to 7.7 occurred during the high temperature test. It is demonstrated below that this pH change does not determine the observed profile.) This hypothesis obviously complicates the interpretation of accelerated durability tests which are usually carried out at 121.5°C.

Interpretation of Accelerated Durability Testing

The solubility of hydrated silica (mono-silicic acid) in neutral solution is quite low at 37°C. Published work, however, reveals that the solubility increases dramatically with temperature [66]. Hence, at 37°C, silicic acid is relatively insoluble in water of neutral pH and thereby forms a layer of hydrated silica on the surface. As sodium and calcium are leached into solution, the silica

layer thickens and the leaching profile extends deeper into the glass. As suggested by others [18], the rate of leaching probably decreases as the hydrated silica layer thickens. It is clear that this process (1) determines the glass durability in neutral solution at ambient temperatures.

At 121.5°C, the hydrated silica can enter the solution as silicic acid. Likewise, calcium and sodium are continually leached into solution. The relative rate at which these two processes occur determines the extent of leaching observed in the surface composition profile. Although previous studies of soda-lime-silicate glass dissolution have also recognized this, analysis of the solution indicates only the sum total effect of the two processes. Hence, the changes they observe cannot be ascribed to either temperature or solution modification alone. The present results indicate, however, that process 2 becomes operable during accelerated testing. Because process 2 does not occur significantly at room temperature, the test is not indicative of the long-term effects under ambient conditions. Consideration of the solution compositions may clarify this point.

Correlation Between Solution Analysis and Surface Composition

According to the solution data 4.6 mg silica were released to solution during corrosion at 121.5°C. The

presence of silica in the solution, then, substantiates the conclusion that dissolution of the glass network has occurred. After corrosion at 37°C, silica was not detected in the solution. Sodium and calcium were present in both solutions, considerably more being found in the solution produced by corrosion at high temperature. Hence, for the 121.5°C exposure, the sodium and calcium detected in solution are associated with both processes. The composition profiles indicate only minor preferential leaching of these constituents. Since the soda to silica ratio in the bulk glass is .17, and 4.6 mg silica were detected in solution

$$\left(\frac{Na_2O}{SiO_2}\right)_{bulk} = .17 = \frac{Na_2O}{4.6} \qquad (Na_2O = .78 \text{ mg})$$

.78 mg of soda in solution are associated with "total dissolution," (although it may not have dissolved simultaneously with the SiO_2) rather than preferential leaching. A total of 2.3 mg soda was detected in solution; hence, 1.5 mg soda in the solution correspond to preferential leaching. This is about 65% of the total amount of sodium detected in the solution.

Very simply, the extent of dissolution or leaching may be calculated on the basis of the solution analysis using

$$x = \frac{Q}{S\rho C} \qquad (9)$$

where x is the layer thickness (leached or dissolved), Q is the quantity of Na_2O, SiO_2, etc. found in solution, S is the glass surface area, ρ is the glass density and C is the bulk molar concentration. In this case, S is about 460 cm^2, ρ is 2.5 gm per cm^3, Q (SiO_2) is 4.6 and C (SiO_2) is .76. Hence, the quantity of SiO_2 detected in solution corresponds to the dissolution of approximately 600 Å. A similar calculation for the soda indicates a layer thickness of 1500 Å. The difference in these two values is 900 Å and should correspond to the thickness of the sodium-leached layer left on the glass surface (Figure 26). The discrepancy is most likely associated with inaccuracy in the solution analysis for silica, although the ion-milling rate may also be in error. Primarily, however, the analysis for these relatively low concentrations of silica in solution is most unreliable. Nonetheless, considering the number of assumptions made in the composition profiles and solution calculations the correlation is qualitatively significant and permits a meaningful interpretation of the reactions. To obtain a more quantitative correspondence between the profiles and solution analyses requires more accurate determination of the silica released to solution. This is because preferential leaching (or accumulation) is the only reaction process which is indicated in the surface composition profiles. Network dissolution can be monitored only by solution analysis.

Steady-State Dissolution

Boksay et al. [67] have shown that for a binary alkali-silicate glass the surface composition profile should approach a steady-state condition determined by the relative rate of leaching and dissolution. The theory is tested here for this relatively chemically resistant glass which was not amenable to investigation using their technique. The data in Figure 26 may represent the "steady-state" surface compositional profiles for this glass at 121.5°C in water. However, it may be argued that the minor changes noted in the solution pH are the primary criterion in determining the surface composition profile. This hypothesis was tested as follows. After reacting the glass surface for one hour in H_2O as described above in Figure 26, the solution pH was 7.7. The glass was quickly rinsed, and re-exposed for one hour to high-purity water. If the solution pH which is now lowered to 6.8 is significantly determining the surface composition profile, a change in the profile could result. In particular, one would expect increased preferential leaching of sodium and calcium at this more acidic pH. This should be reflected in both the composition profile and solution analysis. Figure 27 compares the Na and Ca profiles measured before and after this solution replenishment test. The peak heights are normalized to the oxygen peak height. These peak height ratios are

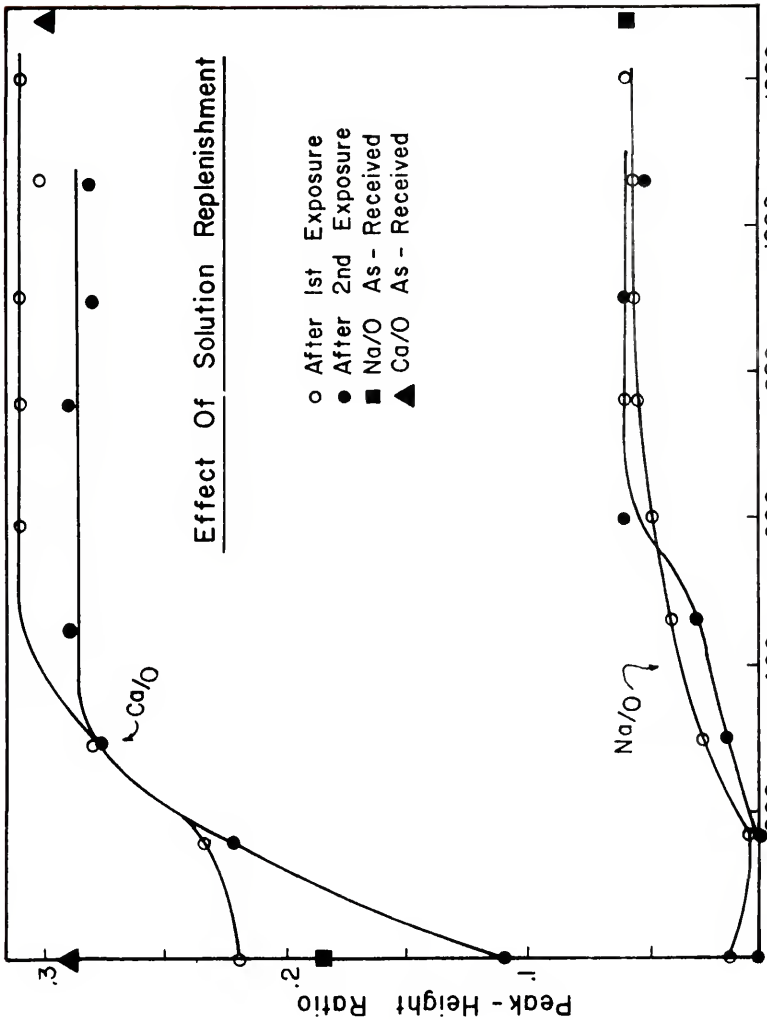

Figure 27. Comparison of depth profiles for soda-lime-silicate glass after reaction in pure water at 121.5°C before and after solution replenishment.

utilized here because the assumptions associated with semiquantitative analysis may obscure the small differences being sought.

In general, it can be seen that replenishment of the solution has had little effect upon the extent of the profile, although the sodium level in the leached layer was decreased to zero. The surface calcium content has been reduced by about 50% and hence may not have been "equilibrized" (dynamically) after one hour. The extent of the leaching profile, however, has not been altered. Solution analysis indicated slight preferential extraction of sodium, probably due to the 2 or 3% soda left in the leached surface after the first exposure. The dissolved layer thickness calculated from equation (9) is about 360 Å. No significant change in pH was observed. Hence, replenishing the solution and changing the pH from 7.7 to 6.8 has had little effect on the extent of preferential leaching. The test demonstrates, however, that dissolution of the glass is possible in the neutral pH range. This suggests that steady-state dissolution corresponds to a condition whereby preferential leaching and network dissolution are equally probable. For conditions of pH less than 9, the preferential leaching of modifier ions is clearly the more likely reaction. To render the two processes equally probable, therefore, requires the formation of a leached layer on the surface to

retard the further extraction of modifier ions. The extent of retardation is determined by the thickness of this layer, which is dictated by the temperature and solution composition for a given glass. The presence or absence of a third component in this layer, for example calcium, may also be a factor.

The condition of steady-state dissolution defined here probably corresponds to the extraction of alkali from the glass with a linear time dependence. Linear kinetics have been observed during solution analysis of glass-water reactions but are preceded by a period during which alkali extraction is proportional to the square root of time (2). This is often interpreted to be a result of diffusion-controlled ion exchange between hydrogen in solution and sodium ions in the glass. In the present context, then, the square root time dependence corresponds to the stage during which the steady-state surface composition profile (leached layer) is forming. This stage represents preferential leaching and may be expected to be diffusion controlled. Thereafter, a condition of dynamic equilibrium is reached (at 121.5°C in water of neutral pH) whereby the profiles in Figure 27 exist at the glass surface which is dissolving at about 360 Å per hour.

pH Effect

To further investigate the relationship between processes 1 and 2, 10ppm of HF were added to the water prior to corrosion. This lowered the pH from 6.8 to 3.3. With this increased hydrogen ion concentration in solution, enhanced leaching is expected even at 121.5°C. Figure 28 presents the leaching profiles for the sodium and calcium, normalized to the oxygen contents. In contrast to the leaching profile which results from reaction in pure water at 121.5°C, the extent of leaching in this case has doubled. Also, calcium is completely devoid at the surface to a depth of about 200 Å. (A small amount of fluorine was also detected in the depleted surface layer.) Solution analysis also indicated preferential leaching. Very little silica was found in solution yielding a soda (1.7 mg) to silica (.17 mg) ratio of 10 (bulk value is .17). Using equation (9), the sodium-leached layer thickness (corrected for 20 Å dissolved hydrated silica) is found to be 1160Å. This is in good agreement with the measured profile in Figure 28. In this case, preferential leaching is the predominant reaction process and hence can be clearly monitored by the composition profiles.

Lowering the pH has increased the extent of leaching and decreased the dissolution of hydrated silica. This is a direct result of the increased hydrogen ion concentration

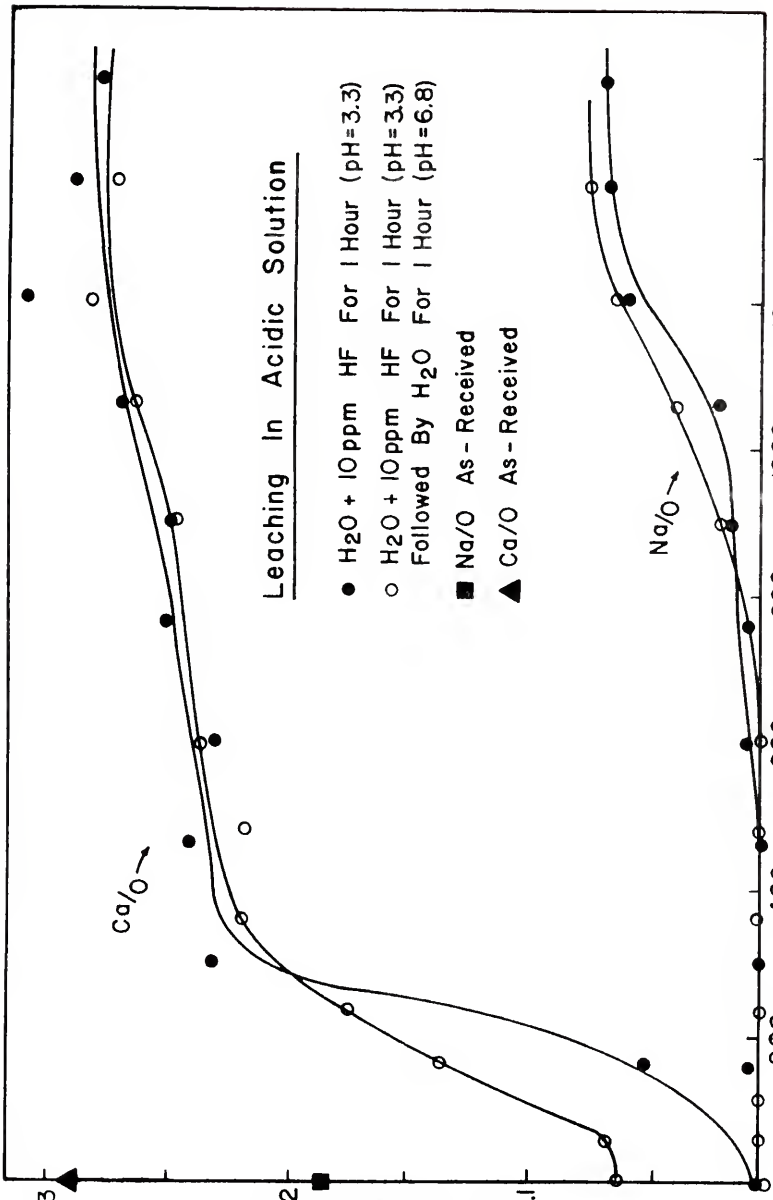

Figure 28. Comparison of depth profiles for soda-lime-silicate glass after reaction in aqueous solution of different pH.

in solution which increases the ion exchange flux between H^+ and Na^+. This also implies, however, that silicic acid is less soluble in this solution. To test that hypothesis directly, the acidic solution was replenished after 1-hour corrosion. The new solution, however, was pure water. On the basis of the hypothesis suggested above, the silica film on the surface should enter solution. The resulting composition profile is also given in Figure 28. It is indicated that the extent of leaching is decreased. This is a result of the dissolution of the silica-rich surface left by the acidic corrosion treatment. Again using equation (9), the dissolved layer is found to be 200-300 Å. Judging from the displacement of the calcium profile after replenishment (Figure 28), this is reasonable agreement.

Summary

1. In general, the measurement of composition profiles for soda-lime-silicate glasses exposed to aqeuous solution clearly indicates regions depleted of modifier ions near the surface.
2. Calcium can be leached from the silicate network. Hence, the presence of calcium in solution is not necessarily a consequence of network breakdown.
3. In pure water, the leaching of modifier ions is dominant at ambient temperatures, while at higher temperatures network dissolution is enhanced.

4. Accelerated durability tests carried out at 121.5°C in pure water do not monitor the process which determines the glass solubility at ambient temperatures. This test measures the steady-state dissolution of the glass at 121.5°C.
5. As expected, the leaching process is considerably enhanced in acidic solution.
6. Solution analysis results correlate with the interpretation of surface compositional profiles.
7. Surface compositional profiles of this kind must be interpreted with regard to the dynamic equilibrium they represent between leaching and dissolution.

CHAPTER VI

INVESTIGATION OF SURFACE FILMS FORMED ON "BIOGLASS" IN AQUEOUS SOLUTION

Previous work has established the rapid formation of surface films on particular invert soda-lime-silicate glasses during exposure to aqueous solution [68]. The approximate glass composition is 45 SiO_2, 24.5 CaO and 30.5 Na_2O (in weight percent). At the expense of Na_2O, P_2O_5 can be added in amounts up to 15% by weight. A glass with 6% P_2O_5 is termed "bioglass" owing to compatibility of the material with bone hydroxyapatite structures [24]. Several investigations have shown that this bioglass can bond to newly forming bone in animals, and transmission electron microscopy (TEM) studies have indicated that mineralization is initiated at a thin bonding layer between the bone and glass [25].

Solution analysis, IRRS and AES indicate the formation of silica-rich layers on the surfaces of all glasses investigated subsequent to their reaction in a simulated physiologic solution [68]. This silica-rich layer is believed to be a result of the leaching of sodium, calcium and phosphorous from the glass surface. AES-composition

profiles have revealed that as P_2O_5 is added to the composition, a second film rich in calcium and phosphorous forms at the surface [36, 37]. This second film appears to form at the SiO_2-rich film-water interface. The rate of formation of the calcium-phosphate film is accelerated as the P_2O_5 content of the bulk glass increases. When glasses are reacted under identical conditions, the thickness of the calcium-phosphate layer increases as the P_2O_5 content of the bulk composition is increased.

The work cited above aptly substantiates the usefulness of AES analysis of bioglass surface reactions. That work was restricted, however, by the lack of sodium data due to experimental difficulties discussed in Chapter III. A technique for sodium analysis has now been developed. Also, the previous study considered reactions between bioglass and buffered solution only. Since the resultant corrosion film formation is somewhat peculiar, the role of the organic buffering constituents in solution is not clear [69]. Reaction with pure water must be investigated, therefore, to provide a more familiar reference point. A mechanism for the calcium-phosphate film formation and its role in subsequent surface reactions has not been clearly established.

The aim of the present investigation is to characterize the compositional changes which occur during the early

stages of reaction. Sodium analysis is accomplished utilizing the developed technique. The composition profiles which result at the bioglass surface in both water and buffered solution are measured. The role of the glass microstructure in corrosion and film formation is discussed. In particular, the formation of the calcium-phosphate film and its effect upon subsequent reaction is defined.

Experimental Procedure

The composition of bioglass in weight percent is 45 SiO_2, 24.5 Na_2O, 24.5 CaO and 6 P_2O_5. A glass without phosphorous is also investigated. The glasses were prepared from reagent grade sodium carbonate, reagent grade calcium carbonate, reagent grade phosphorous pentoxide, and 5 μm silica. Premixed batches were melted in covered Pt crucibles in a temperature range of 1250 to 1350°C for 24 hours. Samples were cast in a steel mold and annealed at 450°C for 4 to 6 hours.

Bulk samples (∿1 x 1 x .1 cm) were prepared by wet grinding with 180-, 320-and 600-grit silicon carbide paper. All subsequent reactions of the samples were preceded by a final dry grinding with the 600-grit paper. Samples were reacted in 150-200 ml of solution. High purity water is obtained by chemical ion exchange (pH is 6.8-7). The

"simulated physiologic environment" is an organically buffered solution consisting of tris-hydroxymethyl-aminomethane and hydrochloric acid. A phosphate buffer made with monobasic and dibasic sodium phosphate is also used. For the latter two solutions, pH is 7.4 maintained at 37°C.

Due to the extreme surface sensitivity of AES, particular care is exercised in preparation of reacted samples for analysis. Specimens are dried, except in certain circumstances, by immersing the sample in electronic grade acetone. Upon removal, the specimen surface quickly dries with the aid of clean, dry air.

AES analysis is carried out using the techniques developed. The frail surface corrosion films required very low beam currents to prevent degradation. In some cases, dark spots formed on the surface under the electron beam, particularly on unreacted and lightly reacted specimens. These spots were believed to be associated with the high sodium contents in this glass. In the event that such spots were observed, the beam current was lowered and the experiment rerun at a different region.

The electron micrographs were obtained by replication of lightly etched fracture surfaces of bioglass.

Surface Compositional Response of Bioglass to Aqueous Solution

Simulated Physiologic Environment

It is clear that bioglass very rapidly responds to its solution environment via changes in surface composition. Figure 29 shows, for example, AES spectra for a bioglass surface before and after reaction in buffered solution. The surface was prepared by abrasion with 600-grit SiC paper. The initial condition of the surface is represented by the upper spectrum. It is apparent that all species in the glass are detected at the surface. The increased sodium content and decreased silicon content of this glass, in comparison to the commercial composition investigated earlier, are reflected in the relative peak-height changes. A small peak due to the phosphorous is also evident. The lower spectrum represents the surface composition after one-hour reaction in the buffered solution at 37°C. The resultant surface composition is hardly comparable to the bulk glass composition. After reaction, sodium and silicon are almost completely devoid at the surface. The phosphorous content has increased most dramatically, with little change in the calcium content. The calcium to phosphorous peak-height ratio was initially 28. After reaction this peak-height ratio is about 4.25. The spectrum indicates only Ca, P and O in significant quantity

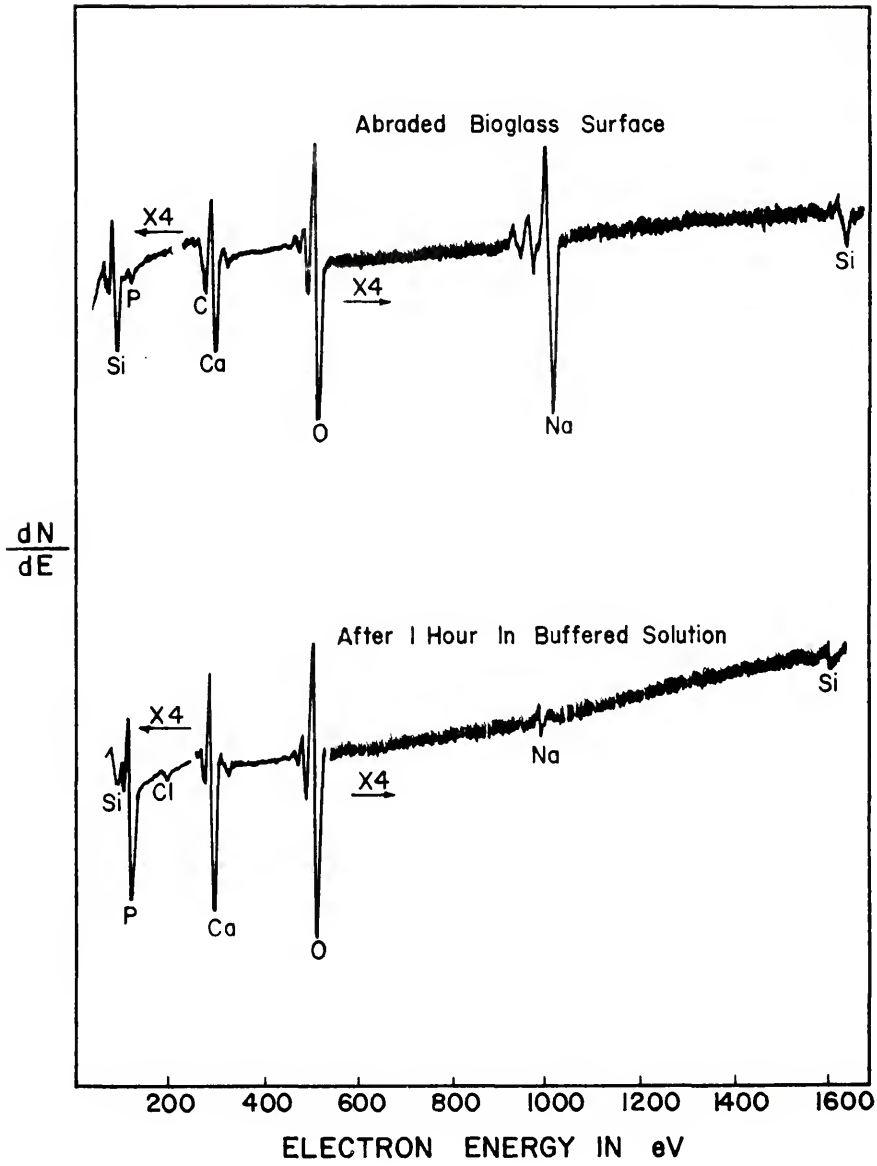

Figure 29. AES spectra for bioglass before and after reaction in simulated physiologic environment.

at the surface. This suggests the existence of a calcium-phosphate-rich film over the bioglass surface after reaction.

Figure 30 presents the surface compositional profile of the bioglass surface immediately after preparation (abrasion). The Auger peak heights have been normalized using sensitivity factors determined as described in Chapter IV. The general form of this profile is consistent with the conclusions drawn previously concerning environmental effects. Reaction with water in the ambient normal atmosphere after abrasion has resulted in the formation of a sodium-rich layer on the surface. The relative diffuseness of this particular profile is a result of the surface finish. The roughness of this surface in comparison to the as-cast surfaces examined previously, results in a smearing of the measured profile. In this case, micro-asperitites left on the surface by abrasion are oriented at a variety of angles to the ion gun. Hence the form of the measured profile is averaged over a longer ion-milling time.

The profile in Figure 30 is to be contrasted with the profile in Figure 31 which results after a 5-minute reaction in the buffered aqueous solution. The extensive leaching of the sodium and phosphorous, and the partial removal of the calcium from a region at the surface can be noted. In addition, a thin surface layer enriched in

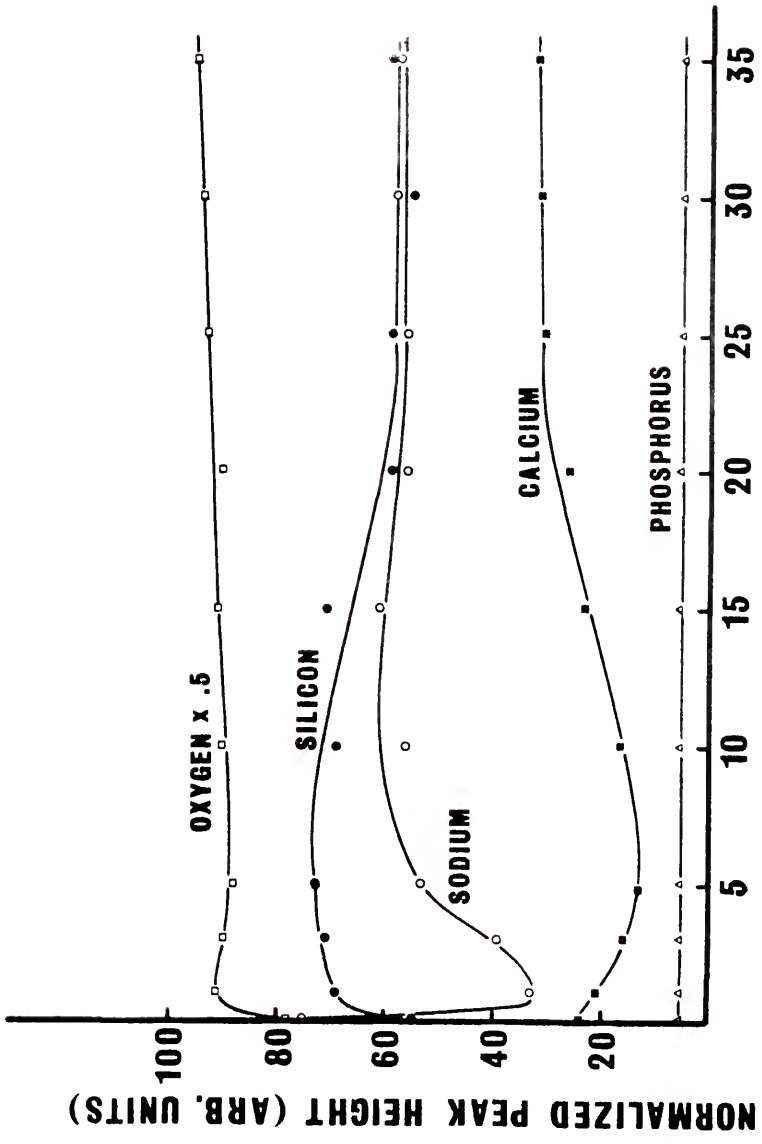

Figure 30. AES peak-to-peak heights (normalized to bulk composition) vs ion-milling time for the surface of abraded bioglass.

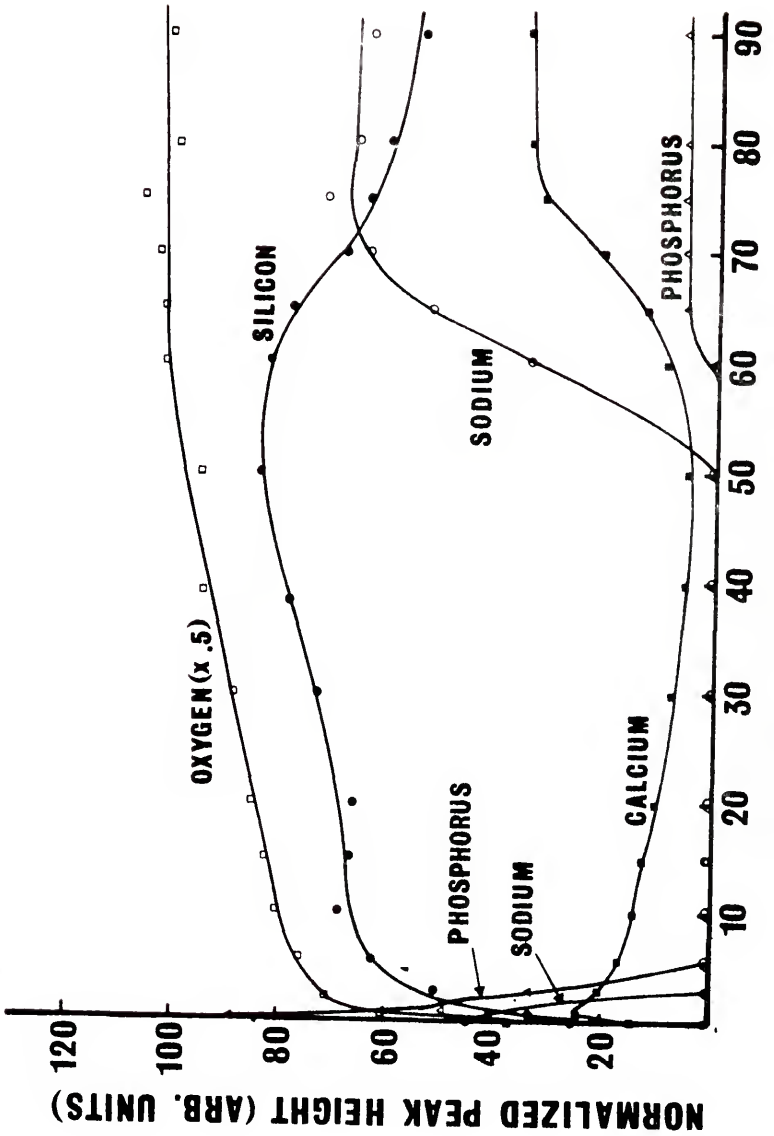

Figure 31. AES peak-to-peak heights (normalized to bulk composition) vs ion-milling time for surface of bioglass reacted 5 minutes at 37°C in simulated physiologic environment.

sodium and phosphorous and, to some extent, calcium can be seen. Estimates of the milling rate suggest this film to be about 6000 Å thick.

It has been suggested that removal of the alkali ions leads to a layer rich in silica having a porous, gel-like structure [68]. It was found that C, N, and Cl were also present in the Auger spectrum from the corroded sample. Figure 32 shows the peak-to-peak amplitudes of the differential spectra for these elements. The curve for sodium is also shown for comparison of signal levels and depth distribution. The curves indicate a penetration of C, N, and Cl (presumably from the organic buffer and from HCl) to a depth that corresponds very well with the region depleted of the alkali ions. Thus the alkali ions have been transferred to the solution from a surface layer and the organic constituent appears to have been able to penetrate into the resulting silica-rich zone. The sodium pile-up at the surface suggests that its transfer across the glass-solution interface is limited. Subsequent attempts to measure the surface sodium concentration for reaction times $\leq$ 5 minutes indicated it to be quite variable. For reaction times > 5 minutes, essentially no sodium is observed on the surface. Quite possibly when the leached layer is relatively thin (very early stages), a limited amount of weathering takes place in the atmosphere. Micro-porosity

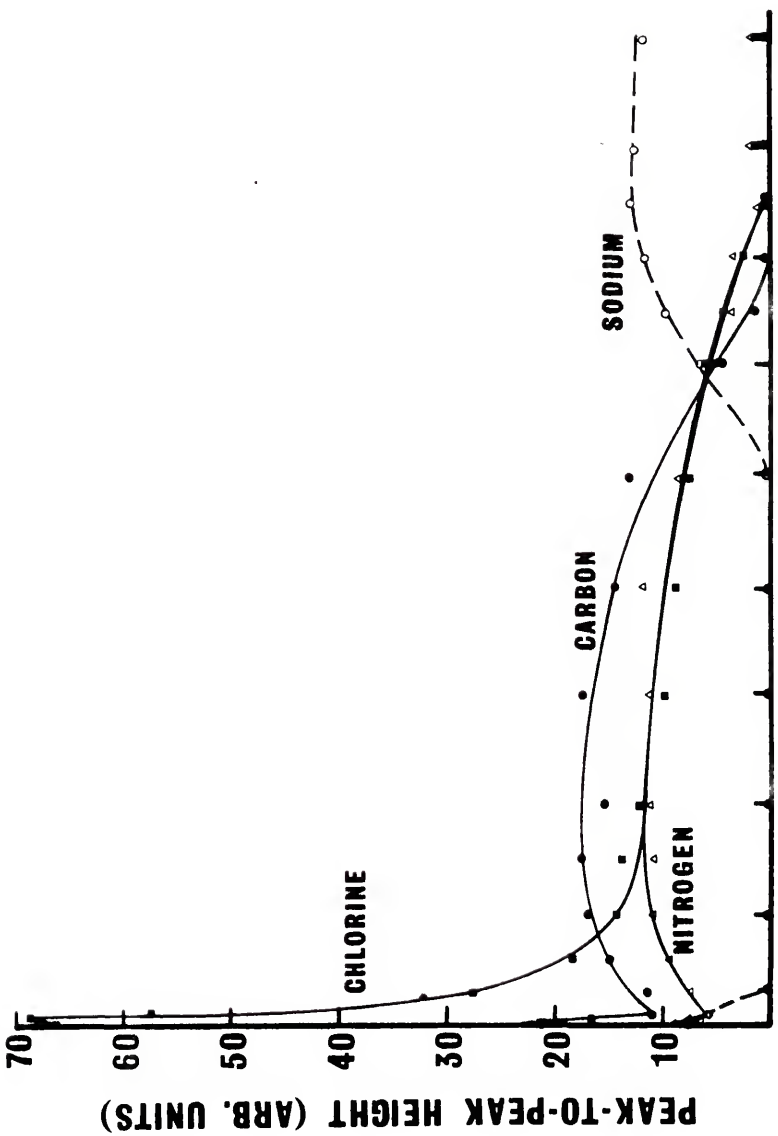

Figure 32. Relative AES peak-to-peak heights vs ion-milling time for Cl, C, N and Na at the bioglass surface reacted for 5 minutes.

which may exist in the leached layer could permit a limited amount of sodium transfer from the glass-leached layer interface to the air-leached layer interface. This is certainly not conclusive evidence, however.

Figure 33 presents the surface compositional profile which results after reaction in buffered solution for 1 hour. This data is presented in mole percent as a function of depth. It can be compared to Figure 31, the profile which is observed after 5 minutes. The leached surface layer, rich in silica, has grown considerably thicker. It can be seen that although sodium and phosphorous have been completely excluded in the silica-rich layer, a portion of the calcium still remains. This was also observed in the profile for the 5-minute reaction. It suggests that calcium provides the ionic bridge holding the silicate-tetrahedra chains together in this invert glass [70]. The rather thick leached layer observed is covered with another film rich in calcium and phosphorous. This calcium phosphate film apparently separates the silica-rich layer and solution. As indicated by the lower spectrum of Figure 29, it shields the underlying leached glass layer. The calcium-phosphate film thickness is approximately 600 Å.

Interestingly, if the sample is agitated vigorously just prior to removal from solution, the surface composition is altered. The AES spectrum which results is given in

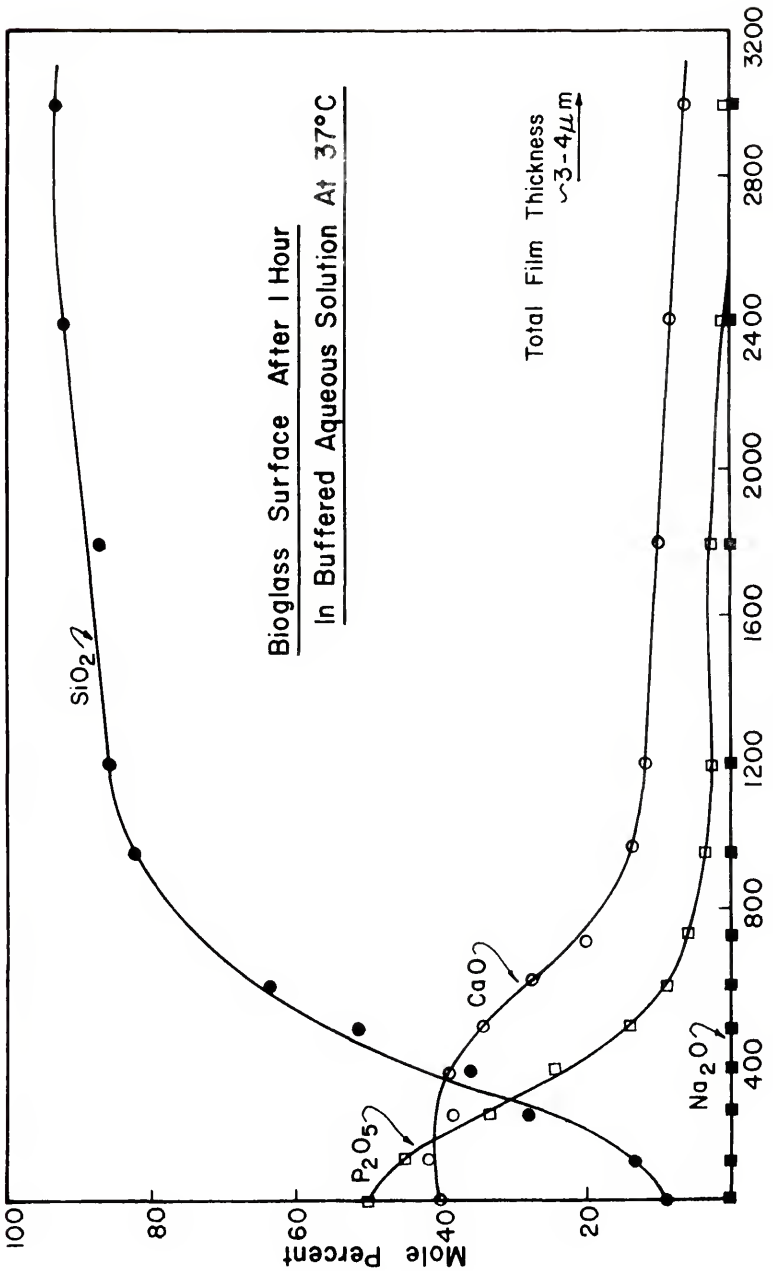

Figure 33. Compositional profiles for bioglass reacted in simulated physiologic environments for 1 hour.

Figure 34 (lower), and is compared to the spectrum which results upon carefully removing the sample (upper). An equivalent change is observed when the sample is rinsed with water or acetone after removal from solution. It can be seen that rinsing the sample surface has removed some calcium and phosphorous and exposed silicon. Significantly, the calcium to phosphorous ratio does not change as a result. Since the water, acetone and reaction solution itself all produced the same result, chemical solubilization of the film is ruled out. Hence, this indicates that vigorous agitation (rinsing) is sufficient to mechanically remove a portion of the film and reveal a fraction of the underlying silica-rich layer. The fact that the Ca/P ratio remains constant and that silica is detected after agitation can only be interpreted as the loss of a portion of the surface calcium-phosphate film. The amount of calcium-phosphate removed, relative to the amount of silica exposed is reproducible. This suggests that a portion of the calcium-phosphate film is adherent to the substrate (not removed by agitation) and other portions (removed by agitation) are not. It is quite possible that the calcium-phosphate which is removed by agitation merely resides over or at the surface in solution as a tightly adherent hydration layer, perhaps in the role of counterions to the negatively charged silica-rich layer.

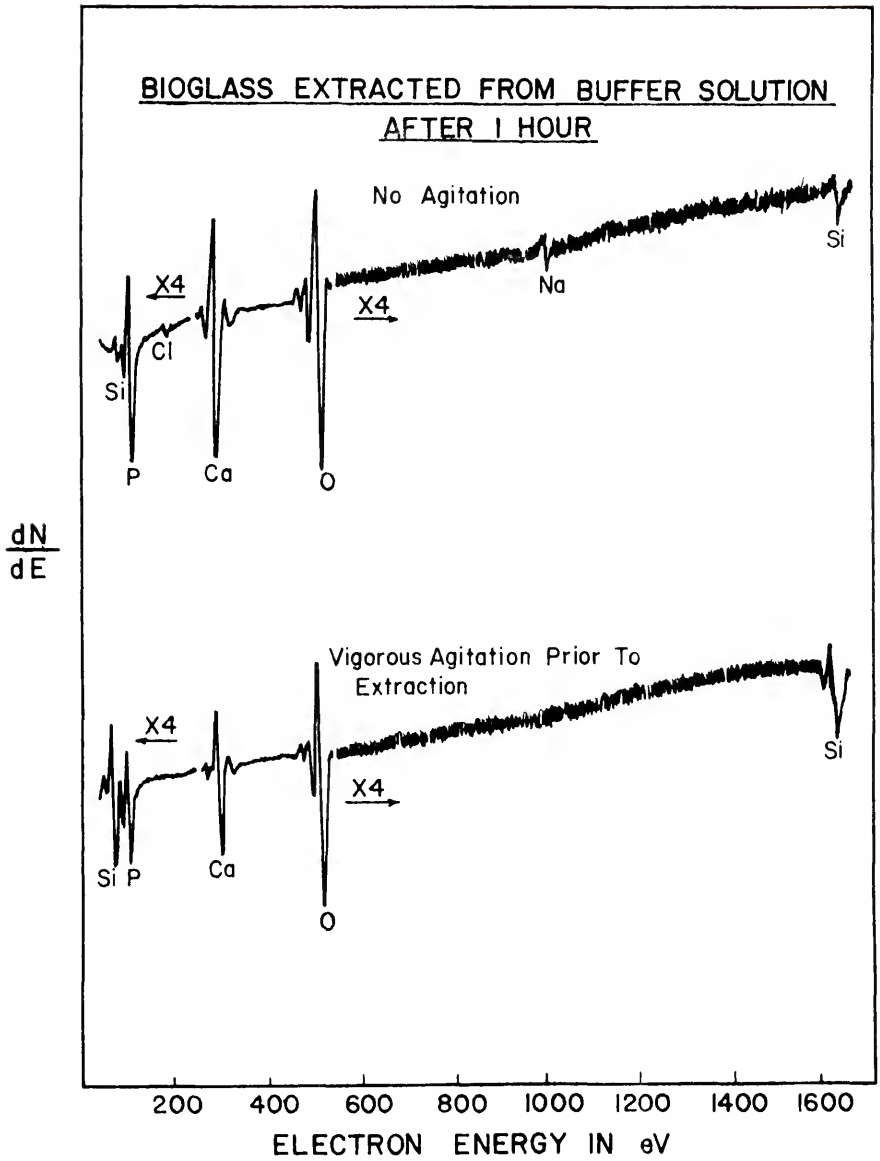

Figure 34. AES spectra for reacted bioglass surface illustrating the effect of solution agitation.

Pure Water

The surface compositional response of bioglass to pure water has also been investigated. Figure 35 gives the compositional profile which results after 1-hour exposure to pure water at 37°C. It can be seen that a calcium-phosphorous-rich film also forms on the surface in water. For comparison to the calcium to phosphorous peak height ratios observed after reaction with the buffer, the ratio here also is about 4.25 at the surface. A high concentration of sodium is observed at the surface. Below the surface and to a depth of about 2000 Å, sodium has been depleted. Interestingly, sodium is the only glass constituent which has been leached from the surface. The presence of excess calcium and phosphorous at the surface, however, suggests they are made available not by leaching them out of the glass but by total dissolution. This profile, therefore, must represent the steady-state surface composition profile for this glass during dissolution in water.

Further evidence for this is given in Figure 36. IRRS spectra before and after reaction of bioglass with pure water and the buffered solution are presented. When bioglass is reacted in water, the spectrumindicates total dissolution rather than preferential leaching, at least within the first hour of reaction. Hence, the AES profile indicates a relatively thin surface corrosion layer. The

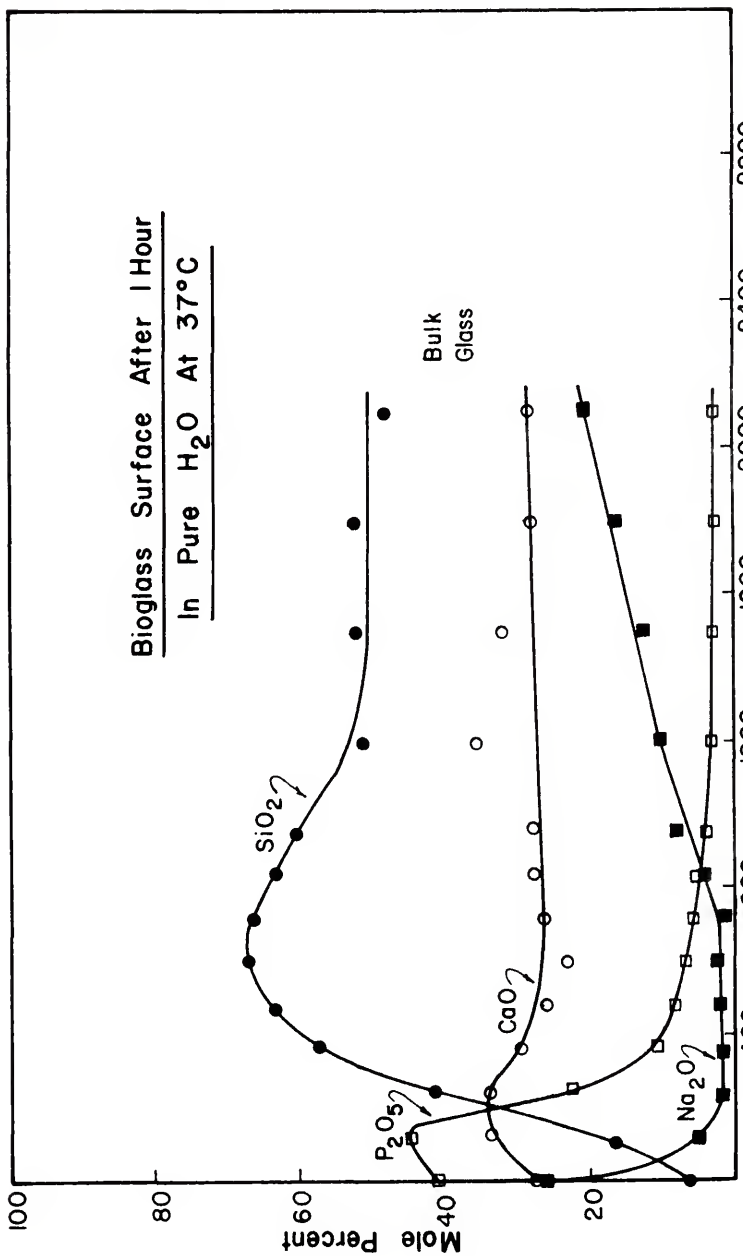

Figure 35. Compositional profiles for bioglass reacted in pure water.

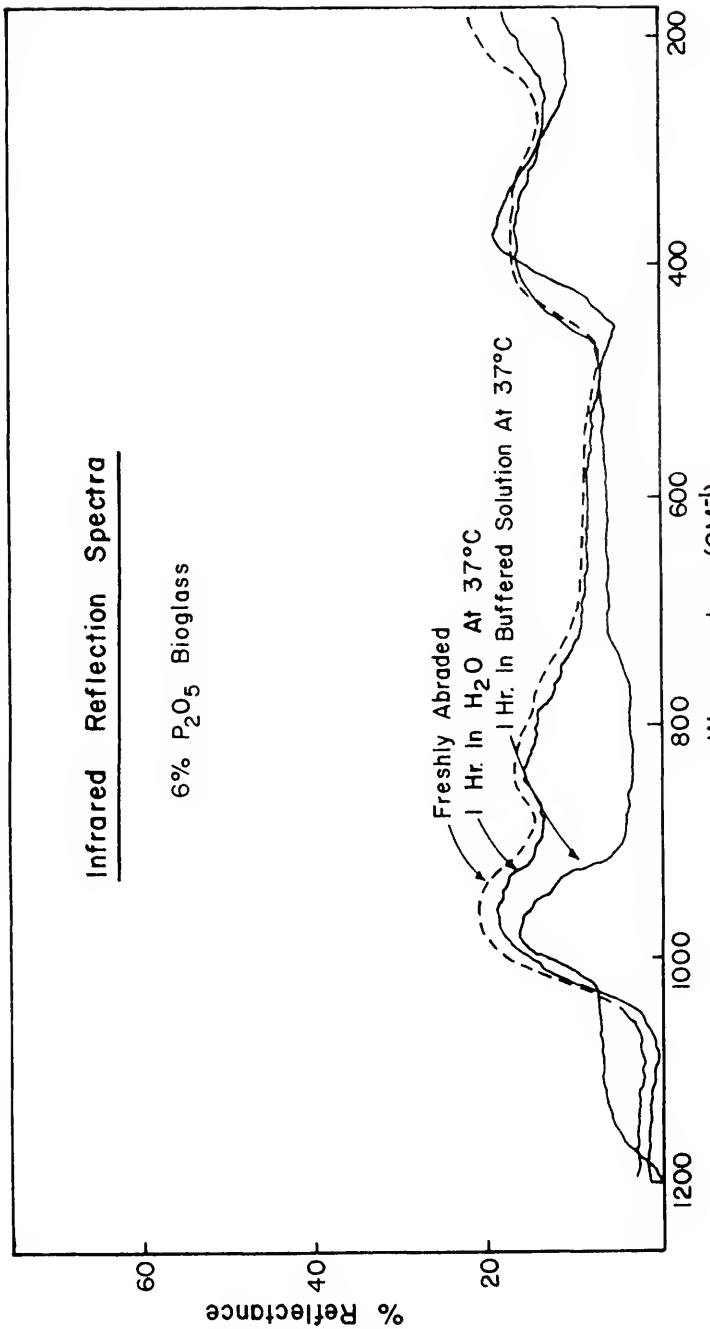

Figure 36. Comparison of IRRS spectra for bioglass surface reacted in both water and the simulated physiologic environment.

IRRS spectrum obtained after bioglass reaction in buffered solution indicates the formation of a silica-rich film on the surface. In this case, the AES profile indicated a leached surface layer 2-3 μm thick. The thin calcium-phosphate films detected by AES are not detected in the IRRS spectra due to a lack of sensitivity.

It is perhaps surprising that a silica-rich film of appreciable thickness forms on the surface in buffered solution but not in pure water. Differences in the sodium profiles for the two reactions are most apparent. It may be argued that signficiant changes in pH occur in the pure water. However, this was not observed. Approximately 1 cm^2 of glass in 150 ml of water, initially of pH 6.8, produced no pH changes in one hour. Hence, the differences in the profiles are not a result of pH. Perhaps, the organic species present in the buffered solution are adsorbed by a micro-porous suface silica layer. This may tend to stabilize the film both chemically and mechanically. Figure 32 indicated the presence of C, N and Cl solution species within the sodium-leached layer. In water, only protons, hydronium ions, hydroxyl ions and molecular water are available to fill the interstices. Probably, they may continue to break down the silica layer. Organics in the buffer may act to protect the silica layer.

In contrast, although the leached-silica surface layer varies depending upon the presence or absence of a

buffer, the surface calcium-phosphate film is present in either case. The difference in thickness may or may not be significant. The AES spectrum characteristic of this film which results after reaction in buffered solution is compared to the spectrum for synthetic hydroxyapatite* in Figure 37. The peak-height ratios are very similar. The bioglass surface film is slightly calcium-deficient in comparison. The similarity suggests that the calcium-phosphate film which forms on bioglass is compositionally similar to hdroxyapatite. Its immediate formation at the bioglass surface upon reaction in aqueous solution is significant in regard to the biocompatibility noted for this glass. Hence, the manner in which it forms and its effect upon subsequent surface reactions are of great interest.

Consideration of the Glass Microstructure

Figure 38 presents a replica transmission electron micrograph for a fracture surface on bioglass. The glass was given a 5-second etch in .05% HF. A plastic replica was then obtained from the etched fracture surface. A distinct two-phase structure can be seen. Judging from this micrograph, the approximately droplet-shaped particles are in the size range of .5-3.3 μm. Certainly the smaller droplets exposed at this fracture surface may represent

*$Ca_{10}(PO_4)_6(OH)_2$

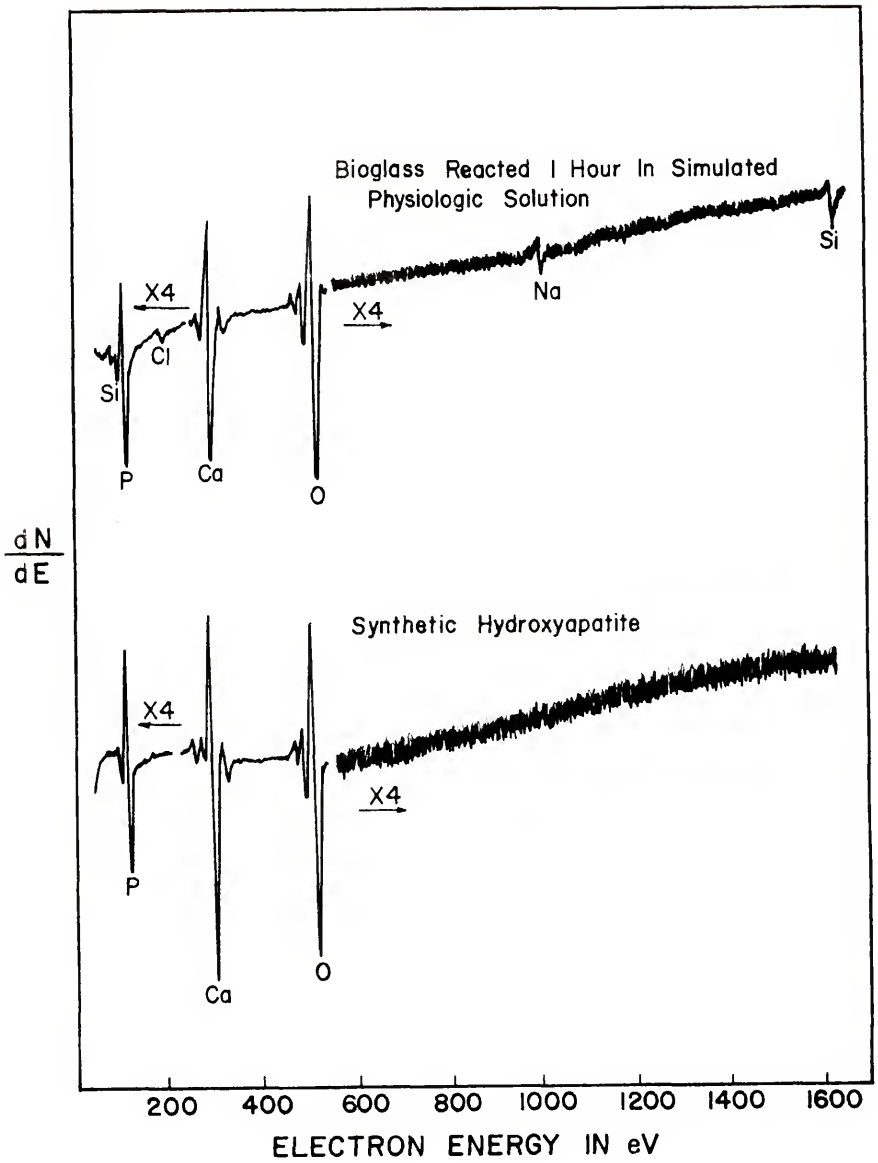

Figure 37. Comparison of AES spectra for reacted bioglass surface and synthetic hydroxyapatite.

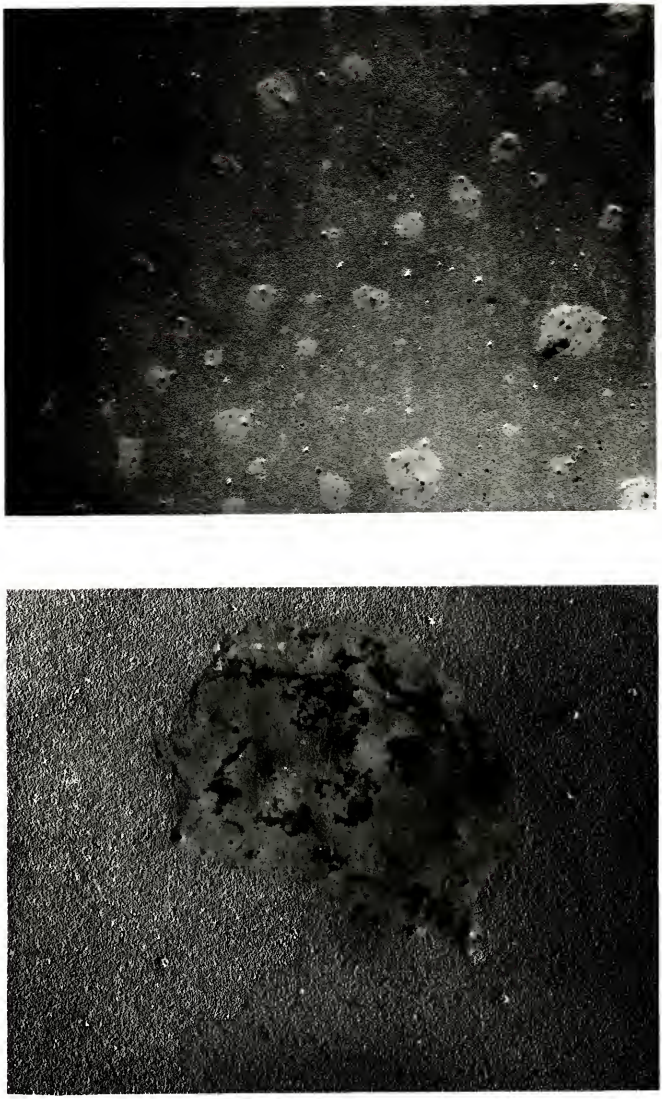

(a)

(b)

Figure 38. TEM replicas for bioglass fracture surface etched 5 sec in .05% HF: (a) 3,600x, and (b) 18,000x.

fractions of large particles and, hence, may not be representative.

The difference in roughness between these two phases indicates the relative chemical resistance of each to HF etching. According to previous investigations [68], this glass is expected to separate into a sodium-silicate phase and a calcium-phosphate phase. The micrograph indicates that the matrix is less resistant than the droplet phase. Hence, the matrix is probably sodium silicate. This data suggests that adherence of the overlying calcium-phosphate film should be heterogeneous in nature. This is consistent with the results discussed above concerning agitation of the glass prior to extraction from solution. Probably the loosely adherent portion of the film has covered the matrix portion of the substrate (originally sodium silicate) while the tightly adherent portion may well represent the calcium-phosphate rich droplets or some modification of them resulting from the reaction.

Calcium-Phosphate Film Formation

The available data indicates the rapid formation of a calcium-phosphate film on bioglass during reaction in both pure water and buffered aqeuous solution. This film may form in one of three ways: (1) precipitation from solution, (2) preferential sodium-silica attack which leaves calcium-phosphate behind, and (3) total dissolution with

accumulation of insoluble compounds at the moving glass-solution interface. These hypotheses are considered in this section.

Rate of Formation

The manner in which the initial calcium-phosphate film forms may be indicated by its rate of formation. Figure 39 provides a description of the rate at which the surface composition changes on bioglass in water. Peak-heights are plotted against reaction time. The very early stages are investigated. The Ca to P peak-height ratio is also presented. Within 5 to 10 minutes, the Ca/P peak-height ratio has decreased from 28 to 6.5. At that point, the ratio stabilizes between 5 and 7. The Ca/P peak-height ratios measured for hydroxyapatite and bioglass reacted in buffered solution are plotted for comparison. All ratios lie between 4 and 7. The surface sodium content as a function of reaction time is also presented. A dramatic difference is observed between water and buffered solution. In buffered solution, sodium is not present at the surface after 5-10 minutes' reaction. In water, sodium is present at the surface for up to 1 hour. This is further evidence that dissolution is enhanced in pure water while leaching dominates in the buffered solution. Note that the rate of change of surface sodium content with reaction time

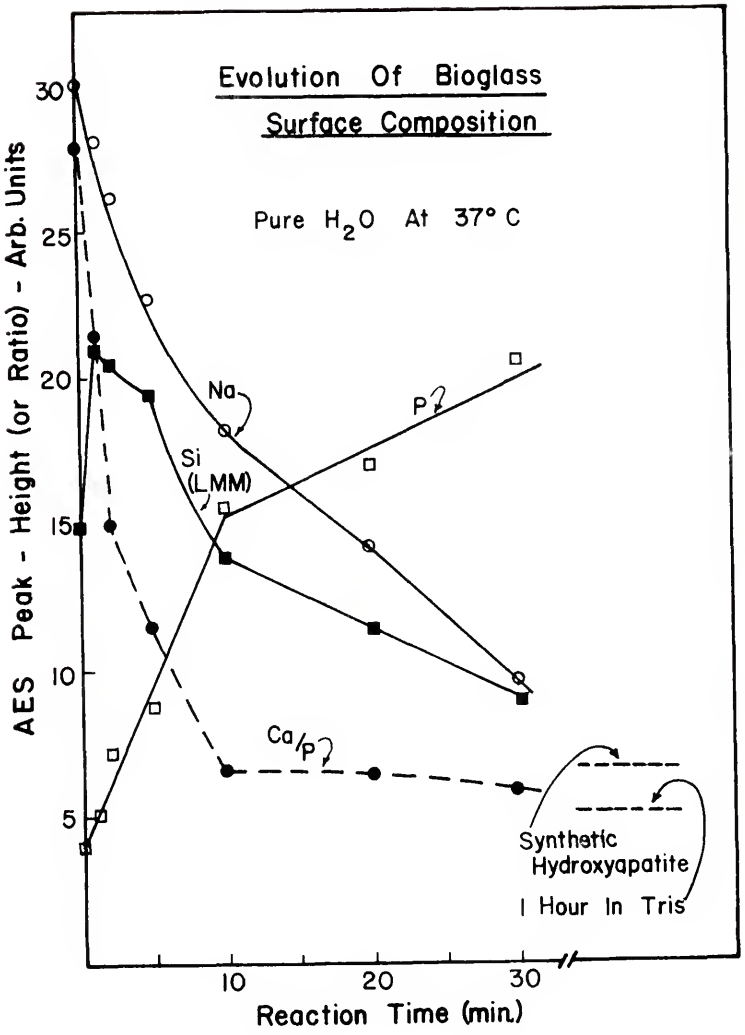

Figure 39. Change in bioglass surface composition during reaction in pure water. Changes in the calcium to phosphorous ratio are also presented.

changes once the Ca/P ratio reaches 5. Thereafter, the sodium disappears at the surface at an ever-increasing rate. This may correspond to thickening of the calcium-phosphate film.

It may also be observed that as the calcium-phosphate film is forming, the surface becomes enriched in silica. At the same time, sodium is depleted from the surface. This indicates that as sodium is removed preferentially from the soda-silica phase, the calcium-phosphate film is forming over it. This observation rules out previous conclusions [68] and hypothesis 2.

The drastic change in the Ca/P ratio seen in Figure 39 is due entirely to an increased phosphorous content at the surface. No change in the calcium peak-height is observed. Hence, it is phosphorous enrichment rather than calcium depletion at the surface which gives rise to this film formation. The source of this additional phosphorous is being sought.

Precipitation of Calcium-Phosphate

The possibility that the calcium-phosphate film precipitates on the glass surface in solution seems likely. This was tested as follows. Bioglass and the similar invert glass without phosphorous were placed juxtaposed in 200 ml of the buffered aqueous solution. After a 1-hour

reaction, the glasses were removed and subjected to AES analysis. The bioglass had a calcium-phosphate film on the surface as expected. The glass without phosphorous in the bulk composition did not indicate the presence of phosphorous on its surface. This was observed previously when reacting the 0% P_2O_5 glass in buffered solution. This result indicates then that the thin calcium-phosphate film which forms on the surface does not arise by precipitation from solution. (If, however, the glass is held in solution until the buffer is overriden, the pH increases and soluble P and Ca in solution spontaneously precipitate.)

It is surprising that considering the large amounts of calcium and phosphorous which are absent from the surface in Figure 33, the calcium-phosphate film has not grown thicker. Since solution analysis indicates the presence of P and Ca in solution within 1 hour, the precipitation model is further ruled out. It was pointed out above that calcium-phosphate does precipitate once the buffer is overridden and the pH rises. Hence, it is not clear whether the pH or ionic concentration of Ca or P determines the growth of the film. To obtain at least a qualitative indication, the bioglass was reacted in a phosphate buffer. The pH was 7.4 and temperature was 37°C. Hence, the only variation introduced here is the infinite availability of phosphorous in solution. The glass without phosphorous was also subjected to this test in order to provide a reference point.

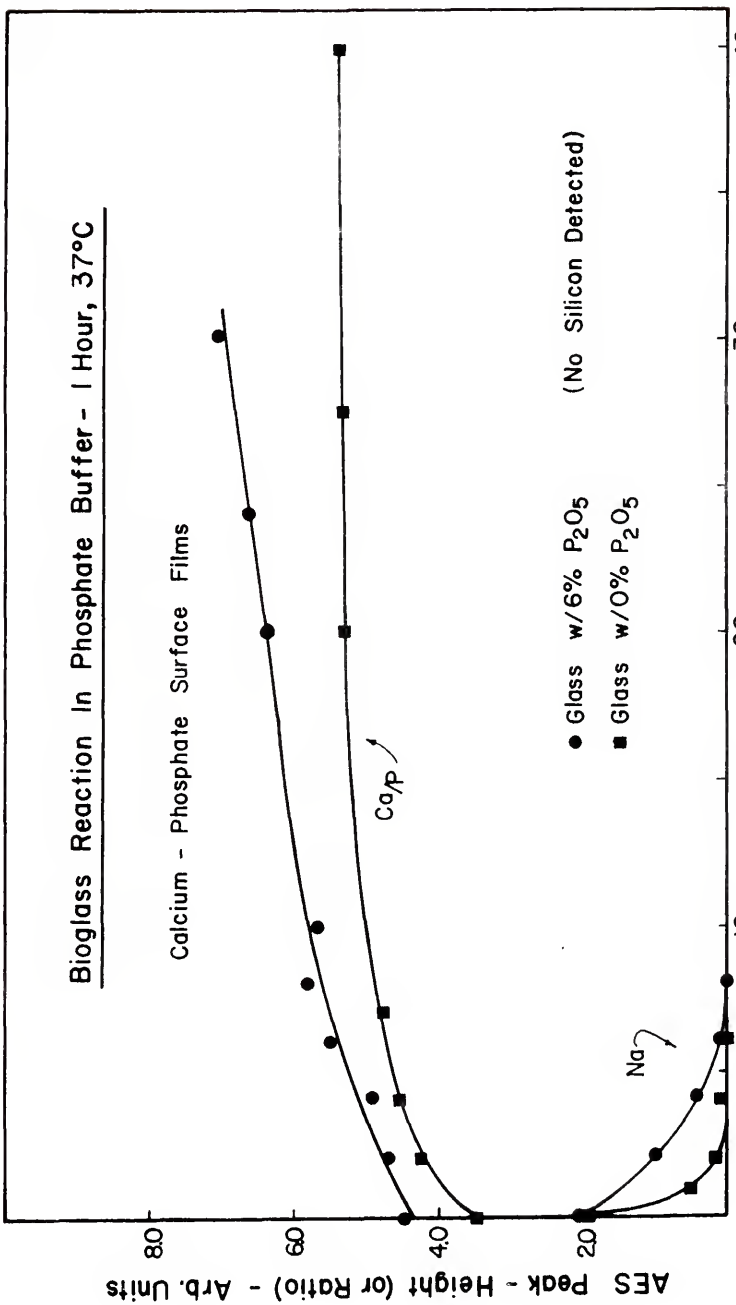

Figure 40. Depth profiles for bioglass and a similar glass without phosphorous reacted in phosphate buffer.

Figure 40 presents the resultant surface composition profiles. Only calcium, phosphorous and oxygen were detected at the surface. A minor amount of sodium is also detected. It can be seen that this calcium-phosphate film on the surface is quite thick. Approximately 90 minutes of ion milling ($\sim$2500-5000Å) was not sufficient to completely remove the film and reveal the underlying bioglass. The Ca to P ratio is approximately constant except for a region at the surface. Formation of this film is not particular to the glass with phosphorous, as a similar profile is observed on the 0% P_2O_5 glass. The significant result is that an alkaline pH is not required for calcium-phosphate precipitation. More importantly, the limitation in calcium-phosphate film growth is the availability of phosphorous. These profiles reveal that sufficient calcium is provided by the glass. The manner in which the calcium is transported from the glass to the film is not clear. Nonetheless, the formation of only a thin calcium-phosphate layer in water and buffered solution is due primarily to the lack of sufficient phosphorous. Finally, the formation of a calcium-phosphate layer is not dependent upon the presence of phosphorous in the glass. This suggests that previous conclusions that this thin calcium-phosphate layer acted as a nucleation site for subsequent calcium-phosphate precipitation are in error. Hence, the precipitation of calcium-phosphate from solution requires only that sufficient

phosphorous be present in solution (provided temperature and pH are appropriate). In addition to this phosphate buffer, this is also observed after reaction of bioglass in the overridden tris-buffer for 9-10 hours. It is clear, however, that the thin calcium-phosphate layer which forms in the early stages of bioglass reaction is not a result of precipitation. This excludes hypothesis 1.

The Accumulation of Calcium Phosphate

It has been demonstrated that neither preferential attack of the sodium-silicate phase nor precipitation from solution is responsible for calcium-phosphate film formation. It remains to be shown that the film forms through the accumulation of insoluble calcium-phosphate at a moving interface between the glass and water. The discussion presented in Chapter V indicated that a surface compositional profile resulting from a glass-water reaction represents the dynamic equilibrium between the leaching of modifier ions and dissolution of the silicate network, characteristic of the pH and temeprature of the test. Previous solution analysis of bioglass indicated that total dissolution is significant up until the solution pH changes ($\sim$9 hours). For the present purposes, total dissolution simply refers to the attainment of steady-state dissolution. Hence, the measured profiles represent the condition of the bioglass

surface as it is eroded. This implies that the phosphorous which is necessary is provided by dissolution. It is proposed that very rapidly this phosphorous complexes with calcium and forms an insoluble film on the surface. Although this model is highly qualitative, it is consistent with the experimental observations.

The discussion previously presented suggested that this glass tends toward total dissolution in aqueous solution. If the solution is buffered, dissolution is retarded and a silica-rich film is formed due to the leaching of sodium and to some extent calcium. Calcium is probably not completely removed because it must act to hold the short silicate chains together. However, the amount of calcium which is released is sufficient to form calcium-phosphate of the composition measured. (This conclusion is supported by the data of Figure 40, which results from reaction of bioglass in phosphate buffer.) The phosphorous or phosphate is made available by the initial dissolution of the glass. Hence, the rate at which calcium-phosphate accumulates at the surface will depend upon the velocity at which the surface is eroded and the phosphorous content in the glass.

This hypothesis is supported by a previous investigation which monitored the surface film formation as a function of P_2O_5 content in the glass [37]. If corroded

under identical conditions, the thickness of the calcium-phosphate layer increased with phosphorous concentration. Hence, the initial dissolution of the glass provides an increased amount of phosphorous for complexing with calcium at the surface. In contrast, if the P_2O_5 content is 3% by weight, insufficient phosphorous is present to form the insoluble calcium-phosphate. Leaching of the surface is observed in this case. A build-up of surface calcium-phosphate acts to shield the glass from the solution and hence further dissolution. The calcium-phosphate layer, therefore, acts as a semipermeable membrane through which ion-exchange reactions between the glass and the solution may take place.

In pure water, the species capable of ion exchange between the glass and solution are alkali and hydrogen (or hydronium) ions. The porosity of this reacted surface, however, probably admits molecular water and hydroxyl ions as well. In general, hydrogen ions may take the place of alkali ions while the hydroxyl continues to break down the silicate chains. Hence, the surface composition profile obtained after pure water reaction represents the steady-state dissolution of bioglass.

In contrast, the above reactions are modified by the buffered aqeuous solution. Ion exchange reactions are not limited to H^+ and OH^-. The data of Figure 32 indicate

a penetration of C, N and Cl into the sodium-leached layer. The C and N are associated with the tris-molecule which is $(HOCH_2)_3\ CNH_2$. The chlorine is derived from the hydrochloric acid. This suggests that under the buffering action of physiologic solutions similar penetration by organic species is possible. In stabilizing the corrosion of this glass, the organics also act to form a bridge between the inorganic glass and organic surroundings.

What could be the driving force for this mechanism? The formation or precipitation of calcium-phosphate is favored at high pH. Qualitatively, at least, it seems likely that the rapid solubilization of sodium may locally raise the pH at the surface. This may then provide the necessary conditions for complexing of calcium and phosphorous. Because sodium is always being released by the glass, a higher pH (>7.4) may continually reside at the glass surface. In water, it is observed that sodium exists at the surface even after the calcium-phosphate film has formed. This continues to favor breakdown of the glass and the leaching process is minimized. This is observed in the profiles (Figure 35). In contrast, sodium is very rapidly exhausted at the surface in buffered solution. The surface pH is perhaps the same as the bulk solution. Dissolution is minimized and hence leaching of modifier ions is favored (Figure 33). The continual dissolution of bioglass

in aqueous solution has been verified by solution analysis. It has been established in Chapter V that the form of the surface compositional profile is determined by the relative rates of leaching and dissolution. In the present case, the relative rates for these two processes are further influenced by the presence of insoluble calcium-phosphate at the surface. It is clear that the steady-state dissolution of the 6% P_2O_5 glass is sufficient to provide enough phosphorous for calcium-phosphate film formation and enough sodium to raise the pH locally at the surface.

The shielding action of the calcium-phosphate film which forms is clearly seen in Figure 41. These ellipsometry data indicate the corrosion layer thickness as a function of corrosion time. The measurements are made in situ, i.e., as the surface is reacting in a wet-cell. The buffered solution is utilized, the temperature varying from 37°C initially up to perhaps room temperature at the end of the test (in situ heating is not possible with the present arrangement). Data for the glass with and without phosphorous are presented. It is evident that the glass without phosphorous is rapidly leached thereby producing the silica-rich layer detected by the ellipsometer. The thickness appears to increase linearly with time at a rate of about 200 Å/min. In contrast, the glass with phosphorous is leached at a considerably slower rate although it

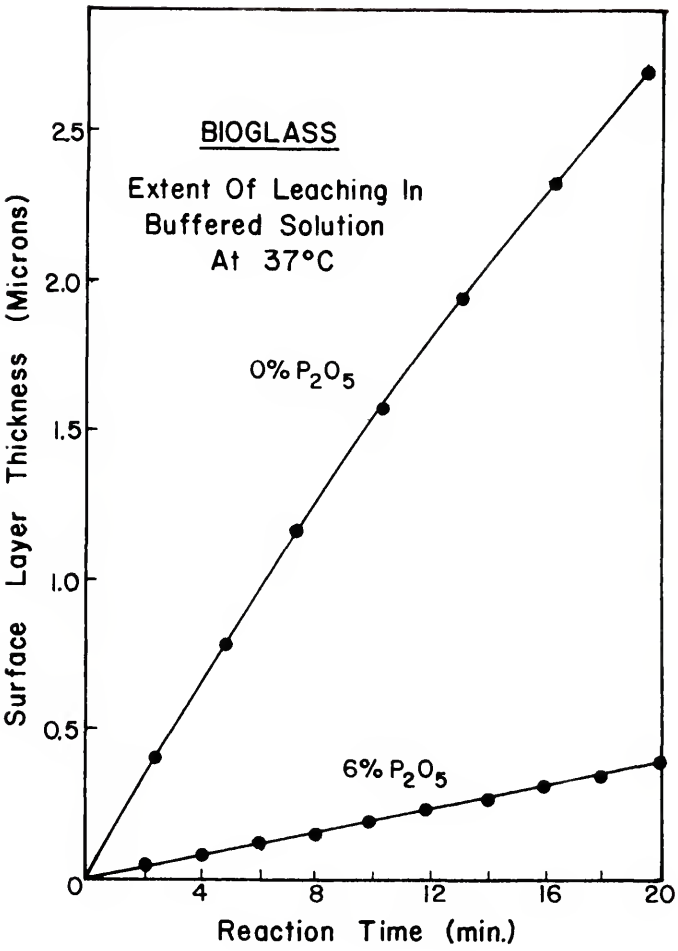

Figure 41. Ellipsometric measurement of reacted surface layer thickness vs reaction time.

is still linear with time. This indicates that the calcium-phosphate film which exists on the surface of the 6% P_2O_5 glass decreases the leaching rate between glass and solution. It is significant, however, that the calcium-phosphate film does not alter the time dependence of leaching; i.e., with or without the surface calcium-phosphate film, the growth rate is linear.

Summary

1. A thin calcium-phosphate film forms on the surface of bioglass when exposed to water or buffered solution within 5 minutes. The Ca/P ratio is comparable to that measured for synthetic hydroxyapatite.
2. Within 1 hour, a silica-rich layer forms beneath this film in buffered solution but not in water. It is suggested that the organic constituents present in the buffer solution act to stabilize the surface film. In a physiologic environment, they may form a bridge between the inorganic glass and organic environment.
3. Portions of the thin calcium-phosphate film are only loosely adherent to the surface. This is interpreted to be a result of the heterogeneous nature of the substrate.

4. A model is presented which suggests that the calcium-phosphate film observed forms through the accumulation of an insoluble calcium-phosphorous complex which forms during the glass dissolution.
5. Ellipsometric data have shown that the calcium-phosphate film alters the rate of silica-rich film growth but does not limit it.
6. More work is necessary to further interpret these results.

CHAPTER VII

CONCLUSIONS

A method of investigating the surface composition of multicomponent silicate glasses with Auger electron spectroscopy has been developed. It has been applied to the analysis of soda-lime-silicate glass surfaces which have reacted in aqueous environments. The results of the study are significant in regard to previous studies of the glass-water reaction which were not provided with surface composition information. In addition, a biocompatible soda-lime-silicate glass has been studied with regard to its peculiar surface compositional behavior in the aqueous physiologic (simulated) environment. Primarily, this study indicated the formation of a thin calcium-phosphate film on the surface upon exposure to aqueous solution. The film was compositionally similar to hydroxyapatite.

Chapter II considered the application of the usual AES procedure to measurements on glass. It was pointed out that particular problems arise due to the insulating nature of the material. In general, it was shown that stable AES spectra may be obtained for glasses utilizing

a 45° angle of incidence between the electron beam and sample surface. The results also indicated that the electron beam current density must be kept below a critical limit in order to prevent electron-induced dissociation of the silicate network. The major outcome of that study, however, was that AES analysis of soda-lime-silicate glass at room temperature perturbs the original surface composition, and in most cases indicates the absence of sodium on the surface. It was concluded that mobile ions at the surface are, in general, subject to perturbation by the electron beam.

Owing to the importance attributed to sodium in surface reactions of soda-lime-silicate glass, Chapter III considered in detail the behavior of mobile ions, such as sodium, under electron irradiation. It was shown that the absence of sodium at the surface of soda-lime-silicate glass during room temperature AES analysis is a result of its migration into the surface under the influence of an electric field produced by the electron beam. Careful measurements of the migration rate were made in order to determine experimental conditions which permit AES analysis of the mobile sodium. During measurements carried out at low temperature (sample cooled by liquid nitrogen) it was observed that the migration is preceded by a "residence time" during which the sodium signal is constant. A model

for this behavior suggested that the sodium ion is relatively immobile during the residence time at low temperature. However, during that time, a critical number of incident electrons act to raise the temperature locally thereby providing a measurable migration rate. This model was consistent with the observed signal decay, although a complete functional dependence of the migration rate upon the experiment variables was not established. Nonetheless, an analytical technique for compositional analysis of soda-lime-silicate glass has been developed: (1) cool the sample with liquid nitrogen during analysis, (2) maintain beam current density below $\sim$.01 amps per cm^2, and (3) measure AES spectra within the observed residence time.

The extreme surface sensitivity provided by this method allowed the investigation of glass-water vapor interactions. This study was carried out by producing clean glass surfaces in vacuum by ion bombardment and subsequently reacting them in situ. The results of Chapter IV indicated that exposure of a bulk glass surface to air containing water vapor induces sodium enrichment at the surface. The observation made is significant with regard to existing theories concerning the attack of glass by water vapor, particularly the hypothesis of Charles [16]. Surface compositional profiles indicated that under the sodium-enriched surface existed a relatively sodium-depleted region. This

supported the hypothesis that the increased sodium concentration on the surface resulted from ion exchange between the sodium at the surface and in the subsurface with hydrogen from the adsorbed water vapor.

In addition, Chapter IV discussed the extraction of semiquantitative information from the measured spectra. Empirical methods were devised to convert the ion-milling time to depth and the AES peak-to-peak heights to molar percentages of the constituent oxides. This yields an approximation of the surface compositional profile which is readily comparable from sample to sample. Considering the depth profiling technique, it was shown that the ion-milling process could adversely affect the compositional profile under analysis. It is emphasized, therefore, that structural interpretation of surface composition profiles requires careful validation.

Chapter V was devoted to a presentation of surface composition profiles which result upon reaction of soda-lime-silicate glass with static aqueous solution. The profiles clearly indicated regions at the surface depleted of alkali and alkaline earth species. The validity of the measured profiles was substantiated by the close correlation with the solution analysis. It was shown that divalent cations such as calcium can be leached from the silicate network. Hence, the presence of calcium in solution is not

necessarily a consequence of network breakdown as was previously suggested. The effect of temperature upon the surface composition profile was found to be significant with regard to accelerated testing of glass durability. It was shown that accelerated durability tests carried out at 121.5°C do not monitor the process which determines the glass solubility at ambient temperatures. In pure water, the leaching of modifier ions is dominant at ambient temperatures, while at higher temperatures network dissolution is enhanced. It was concluded that the reaction conditions lead to a steady-state surface composition profile and hence the test measures the steady-state dissolution of the glass at 121.5°C. It is emphasized that surface compositional profiles of this kind must be interpreted with regard to the dynamic equilibrium they represent between leaching and dissolution.

Finally, Chapter VI investigated surface films formed on the surface of "bioglass" in aqueous solution. It was shown conclusively that a thin calcium-phosphate film forms on the surface of bioglass when exposed to water or buffered solution within 5 minutes. The Ca/P ratio is comparable to that measured for synthetic hydroxyapatite. Within 1 hour, a silica-rich layer forms beneath this film in buffered solution but not in water. It is suggested that the organic constituents present in the buffer solution act to stabilize the surface film. In a physiologic environment

they may form a bridge between the organic glass and organic environment. Ellipsometric data indicated that the silica-rich layer thickens with linear kinetics, the rate of which is determined by the presence or absence of the calcium-phosphate film. However, it is significant that the calcium-phosphate film did not limit the silica-rich layer formation. This implies, at least, that the calcium-phosphate film provides a biologically compatible interface between the inorganic glass and its organic environment. However, the film does not hinder the exchange of ionic species between the two. This suggests that the film acts as an ion-selective membrane. Further investigation of this glass with that point in mind may prove to be useful.

Overall, it is emphasized that a method of investigating the surface composition of multicomponent silicate glasses has been developed. This method should be applicable to glass surface analysis in general when the composition effects are of importance. Moreover, the applicability of the technique is manifested by the successful study of soda-lime-silicate glass-water reactions. The ability to monitor this reaction should fill a gap in the list of techniques presently available for such investigations. (Since the initiation of this work, the methods of ESCA [71] and photon emission induced during ion sputtering [72] have also been applied to glass surface investigations.) It is hoped that

the significance of compositional effects at glass surfaces will provide sufficient impetus for further application of this method and its continued development.

APPENDIX

COMPUTER PROGRAMS (APL)

A. Data Input

```
     ∇ INDATA
[1]    ELEMENTS
[2]    NELP←1234
[3]    'ELEMENTS'
[4]    M←□
[5]    RR←⍴M
[6]    RAW←0,M
[7]    N←0
[8]    →MIME
[9]  OK:'NEW'
[10]   N←N-1
[11] MIME:'MIME'
[12]   M←□
[13]   →(0>M)/LAST
[14]   N←N+1
[15] REAL:'REAKS'
[16]   RKR←□
[17]   →(RKR=1234)/OK
[18]   →(RR=⍴RKR)/MAG
[19]   'LENGTH MISTAKE'
[20]   →REAL
[21] MAG:'MAG'
[22]   MAGN←□
[23]   MN←MAGN
[24]   →(RR=⍴GS)/ARC
[25]   'LENGTH MISTAKE'
[26]   →MAG
[27] ARC:RK←RKR÷GS
[28]   RAW←RAW,M,RK
[29]   →MIME
[30] LAST:RR←⍴M
[31]   NN←1+RR
[32]   WW←1+N
[33]   DATA←(WW,NN)⍴RAW
[34]   'ASSIGN NAME TO DATA NOW, AS NAME←DATA'
     ∇
```

B. Form matrix of raw or normalized peak-heights.

```
     ∇ RAWPEAK
[1]    PLEMENTS
[2]    'SAMPLE'
[3]    D←⎕
[4]    A←¯1+⍴D[1;]
[5]    B←D[1;1+⍳A]
[6]    B←¯1+⍴D[;1]
[7]    B
[8]    'WHICH ELEMENTS: YES=1,NO=0'
[9]    AA←⎕
[10]   BB←1,AA
[11]   COM←BB/D
[12]   'SENSITIVITIES:YES=1,NO=0'
[13]   S←⎕
[14]   →0×⍳S<1
[15]   AB←¯1+⍴COM[1;]
[16]   BB←COM[1;1+⍳AB]
[17]   MM←SENS[BB]
[18]   MMM←1,MM
[19]   M←((⍴COM)-1 0)⍴MMM
[20]   COM[1+⍳B;]←COM[1+⍳B;]×M
     ∇
```

C. Form matrix of peak-heights normalized to oxygen signal.

```
     ∇ OXR
[1]    'SAMPLE'
[2]    D←⎕
[3]    A←¯1+⍴D[1;]
[4]    B←¯1+⍴D[;1]
[5]    X←1
[6]    CALC←0
[7]    E←D[1;1+⍳A]
[8]    CALC←CALC,E
[9]    SS←SENS[E]
[10]   X←X+1
[11]   BBB←B+1
[12]   →(BBB<X)/LAST
[13]   M←D[X;1]
[14]   DK←D[X;1+⍳A]
[15]   DD←E÷0
[16]   CC←DK÷DK[DD]
[17]   CALC←CALC,M,CC
[18]   BB←⍴E
[19]   UU←1+BB
[20]   VV←1+B
[21]   →10
[22]   LAST:COM←(VV,UU)⍴CALC
     ∇
```

D. Calculate atomic percent.

```
     ∇ GO
[1]    O←8
[2]    'SAMPLE'
[3]    D←⍞
[4]    A←¯1+⍴D[1;]
[5]    B←¯1+⍴D[;1]
[6]    X←1
[7]    CALC←0
[8]    E←D[1;1+⍳A]
[9]    CALC←CALC,E
[10]   SS←SPNC[E]
[11]   X←X+1
[12]   BBB←B+1
[13]   →(BBB<X)/LAST
[14]   T←D[X;1]
[15]   PK←D[X;1+⍳A]
[16]   CC←100×PK×SS÷+/PK×SS
[17]   CALC←CALC,T,CC
[18]   BB←⍴E
[19]   UU←1+BB
[20]   VV←1+B
[21]   →10
[22]   LAST:COM←(VV,UU)⍴CALC
     ∇
```

E. Output RAWPEAK, OXR, and GO.

```
     ∇ GRAPH
[1]    ALL←1
[2]    'WHICH ELEMNTS(ALL OR SPECIFIED)'
[3]    NOW←⍞
[4]    →(NOW>1)/NEXT
[5]    NTAB←COM[1+⍳B;]
[6]    →TIME
[7]    NEXT:NOE←⍴NOW
[8]    O←COM[1;]⍳NOW
[9]    NTAB←COM[1+⍳B;1,O]
[10]   TIME:'MAX TIME, ALL OR SPECIFIED'
[11]   MX←⍞
[12]   →(MX=1)/DIM
[13]   MX←+/MX>NTAB[;1]
[14]   NTAB←NTAB[⍳MX;]
[15]   DIM:'DIMENSIONS'
[16]   NTAB[⍳B;1]←NTAB[⍳B;1]×30
[17]   DIME←⍞
[18]   (DIME[1],DIME[2]) PLOT NTAB
[19]   ' '
     ∇
```

F. Calculate molar percent.

```
     ∇ MOLE
[1]    GO
[2]    A←COM[1;]
[3]    C←(A≠8)/COM
[4]    B←(A=8)/COM
[5]    BB← 1 0 ↓B
[6]    CC← 1 1 ↓C
[7]    CCD← 0 1 ↓C
[8]    B←C[;1]
[9]    BBO←100
[10]   N←1
[11]   BBB←(B≠8)/B
[12]   MPP←0,BBB
[13]   Y←YY[BBB]
[14]   X←XX[BBB]
[15] ON:BO←BB[N;1]-+/((Y÷X)×(CC[N;]))
[16]   MP←(100×CC[N;]÷X)÷+/(CC[N;]÷X)
[17]   BBO←BBO,BO
[18]   MPP←MPP,MP
[19]   N←N+1
[20]   →(N≤ρBB[;1])/ON
[21]   MP1←1↓MPP
[22]   AA←ρCCD[;1]
[23]   AA1←ρCCD[1;]
[24]   ZZ←(AA,AA1)ρMP1
[25]   COM←B,ZZ,BBO
[26]   A←¯1+ρD[1;]
[27]   B←¯1+ρD[;1]
[28]   C←6
[29]   →
     ∇
```

G. Output MOLE.

```
     ∇ GRAPHM
[1]    ALL←1
[2]    'WHICH ELEMNTS(ALL OR SPECIFIED)'
[3]    NOW←□
[4]    →(NOW>1)/NEXT
[5]    NMAB←COM[1+⍳B;]
[6]    →TIME
[7]   NEXT:NOE←⍴NOW
[8]    C←COM[1;]⍳NOW
[9]    NMAB←COM[1+⍳B;1,C]
[10] TIME:'MAX TIME, ALL OR SPECIFIED'
[11]   MX←□
[12]   →(MX=1)/DIM
[13]   MX←+/MX>NMAB[;1]
[14]   NMAB←NMAB[⍳MX;]
[15] DIM:NMAB[;1]←NMAB[;1]×30
[16]   'SQUARE ROOT? YES(1) OR NO(0)'
[17]   PPP←□
[18]   →(PPP=0)/GEE
[19]   NMAB[;1]←(NMAB[;1])*0.5
[20] GEE:'DIM'
[21]   DIME←□
[22]   (DIME[1],DIME[2]) PLOT NMAB
[23]   →(PPP=0)/EEG
[24]   '                    SQ. ROOT OF'
[25] EEG:'                        DISTANCE'
     ∇
```

BIBLIOGRAPHY

[1] V. Gottardi, ed., "The Chemical Durability of Glass-A Bibliographic Review of Literature," International Commission on Glass, Institut du Verre, Paris, France (1972).

[2] R. W. Douglas and M. A. Rana, "The Reaction Between Glass and Water," Phys. Chem. Glasses, 2(6), 179-205 (1961).

[3] D. M. Sanders and L. L. Hench, "Mechanisms of Glass Corrosion," J. Amer. Ceram. Soc., 54(7), 373-378 (1973).

[4] G. Y. Onoda, D. B. Dove, and C. G. Pantano, Jr., "Some Applications of Surface Characterization Techniques to the Study of Glasses," In: Materials Science Research, Vol. 7 (Plenum: New York, 1974) 39-56.

[5] C. C. Chang, "Analytical Auger Electron Spectroscopy," In: Characterization of Solid Surfaces (Plenum: New York, 1974) 509-575.

[6] Y. J. van der Meulen, "Some Recent Studies of Very Thin SiO_2 Films," J. Vac. Sci. Tech., 11(6), 985-989 (1974).

[7] J. M. Morabito, "Selected Area and In-Depth Auger Analysis of Thin Films," Thin Solid Films, 19(1), 21-41 (1973).

[8] T. W. Haas and D. J. Pocker, "Some Applications of Auger Electron Spectroscopy to Metallurgical Problems," J. Vac. Sci. Tech., 11(6), 1087-1092 (1974).

[9] H. L. Marcus and P. W. Palmberg, "Auger Fracture Surface Analysis of a Temper Embrittled 3340—Stainless Steel," Trans. Met. Soc. AIME, 245, 1664-1666 (1969).

[10] P. W. Palmberg, "Use of Auger Electron Spectroscopy and Inert Gas Sputtering for Obtaining Chemical Profiles,' J. Vac. Sci. Tech., 9(1), 160-163 (1972).

[11] D. V. Mc Caughan and R. A. Kushner, "Impurity-Movement Problems in Analysis Methods Using Particle Bombardment," In: Characterization of Solid Surfaces (Plenum: New York, 1974) 627-640.

[12] L. Holland, "Surface Chemistry and Corrosion of Glass," In: The Properties of Glass Surfaces (Chapman-Hall: London, 1964) 102-192.

[13] W. A. Weyl and E. C. Marboe, "Surface Chemistry of Silicate Glasses," In: The Constitution of Glasses, A Dynamic Interpretation (Wiley: New York, 1969) 1010-1278.

[14] F. M. Ernsberger, "Properties of Glass Surfaces," In: Annual Review of Materials Science (Banta, Cal.), 2, 529-572 (1972).

[15] D. E. Clark, "A Durability Evaluation of Soda-Lime-Silicate Glasses Using Electron Microprobe Analysis, Infrared Reflection Spectroscopy and Other Techniques," Ph.D. Dissertation, Univ. of Fla., Gainesville, Fla. (1976).

[16] R. J. Charles, "Static Fatique of Glass. I," J. Appl. Phys., 29(1), 1549-1553 (1958).

[17] R. M. Tichane, "The Initial Stages of the Weathering Process on a Soda-Lime-Glass Surface," Glass Tech., 7(1), 26-29 (1966).

[18] C. R. Das, "A Review of the Chemical Resistance of Glass," Trans. Ind. Ceram. Soc., 24(1), 12-34 (1965).

[19] T. M. El-Shamy and R. W. Douglas, "Kinetics of the Reaction of Water with Glass," Glass Tech., 13(3), 77-80 (1972).

[20] T. M. El-Shamy and R. W. Douglas, "The Dependence on the pH of the Decomposition of Glasses by Aqueous Solutions," Glass Tech., 13(3), 81-87 (1972).

[21] L. Zagar and L. Schillmoller, "The Physico-Chemical Processes of Water-Leaching of Glass Surfaces," Glastechn. Ber., 33(4), 109-116 (1960).

[22] F. Y. Wang and F. V. Tooley, "Influence of Reaction Products on Reaction Between Water and Soda-Lime-Silica Glass," J. Amer. Ceram. Soc., 41, 521-524 (1958).

[23] C. A. Beckham, T. K. Greenlee, Jr., and A. R. Crebo, "Bone Formation at Ceramic Implant Interface," Calcif. Tissue Res., 8(2) 165-171 (1971).

[24] L. L. Hench, R. J. Splinter, W. C. Allen, and T. K. Greenlee, Jr., "Bonding Mechanisms at the Interface of Ceramic Prosthetic Materials," Biomed. Mater. Symp., No. 2 (Pt. 1) 117-141 (1971).

[25] L. L. Hench and H. A. Paschall, "Direct Chemical Bond of Bioactive Glass-Ceramic Materials to Bone and Muscle," Biomed. Mater. Symp., No. 4, 27-45 (1973).

[26] R. W. Douglas and J. O. Isard, "The Action of Water and of Sulphur Dioxide on Glass Surfaces," J. Soc. Glass Tech., 33(154), 289-335 (1949).

[27] H. R. Persson, "Improvement of the Chemical Durability of Soda-Lime-Silica Glass Bottles by Treating with Various Agents," Glass Tech., 3(1), 17-35 (1962).

[28] E. L. Mochel, M. E. Nordberg and T. H. Elmer, "Strengthening of Glass Surfaces by Sulfur Trioxide Treatment," J. Amer. Ceram. Soc., 49(1) 585-589 (1966).

[29] U.S. Patent 3,314,772.

[30] V. H. Rawson and G. Turton, "The Effect of Coatings in Reducing the Damage of Glass Surfaces," Glastechn. Ber., 46(2), 28-33 (1973).

[31] J. P. Poole and H. C. Snyder, "New Coating for Glass Containers," Glass Ind., 43, 175-208 (1962).

[32] B. Goldstein and D. E. Carlson, "Determination of the Composition of Glass Surfaces by Auger Spectroscopy," J. Amer. Ceram. Soc., 55(1), 51-52 (1972).

[33] J. P. Rynd and A. K. Rastogi, "Auger Electron Spectroscopy—a New Tool in the Characterization of Glass Fiber Surfaces," Amer. Ceram. Soc. Bull., 53(9), 412-413 (1974).

[34] R. A. Chappell and C. T. H. Stoddart, "An Auger Electron Spectroscopy Study of Float Glass Surfaces," Phys. Chem. Glasses, 15(5) 130-135 (1974).

[35] P. R. Anderson, F. R. Bacon, and B. W. Byrum, "Effect of Surface Treatments on the Chemical Durability and Surface Composition of Soda-Lime Glass Bottles," J. Noncryst. Sol., 19 (1976).

[36] C. G. Pantano, Jr., A. E. Clark, Jr., and L. L. Hench, "Multilayer Corrosion Films on Bioglass Surfaces," J. Amer. Ceram. Soc., 57(9), 412-413 (1974).

[37] A. E. Clark, Jr., C. G. Pantano, Jr., and L. L. Hench, "Auger Spectroscopic Analysis of Bioglass Corrosion Films," J. Amer. Ceram. Soc., 59(1), 37-39 (1976).

[38] D. V. McCaughan, R. A. Kushner and V. T. Murphy, "Ion Neutralization Processes at Insulator Surfaces and Consequent Impurity Migration Effects in SiO_2 Films," Phys. Rev. Lett., 30(13), 614-617 (1973).

[39] N. J. Chou, C. M. Osburn, Y. J. van der Meulen and R. Hammer, "Auger Analysis of Chlorine in HCl^- or Cl_2-Grown SiO_2 Films," Appl. Phys. Lett., 22(8), 380-381 (1973).

[40] W. T. Kane, "Application of the Electron Microprobe in Ceramics and Glass Technology,"In: Microprobe Analysis (Wiley: New York, 1973) 241-269.

[41] P. W. Palmberg, G. K. Bohn and J. C. Tracy, "High Sensitivity Auger Electron Spectrometer," Appl. Phys. Lett., 15(18), 254-255 (1969).

[42] P. W. Palmberg, G. E. Riach, R. E. Weber and N. C. MacDonald, Handbook of Auger Electron Spectroscopy (Physical Electronics Ind.: Eden Prairie, Minn. 1972).

[43] F. Meyer and J. J. Vrakking, "Quantitative Aspects of Auger Electron Spectroscopy," Surf. Sci., 33, 271-294 (1972).

[44] J. T. Grant, T. W. Haas and J. E. Houston, "Quantitative Auger Analysis Using Integration Techniques," Phys. Lett., 45A94), 309-310 (1973).

[45] J. E. Houston, "Retrieval of Electron-Excited Auger Structure by Dynamic Background Subtraction," Appl. Phys. Lett., 24(1), 42-44 (1974).

[46] D. B. Dove, "Surface Composition of Sputter Deposited SiO_2 Layers During Argon Ion Bombardment," IBM Research Report (IBM Thomas J. Watson Research Center: Yorktown Heights, New York, 1975).

[47] S. Thomas, "Electron Irradiation Effect in the Auger Analysis of SiO_2," J. Appl. Phys., 45(1), 161-166 (1974).

[48] J. Ahn, C. R. Perlebery, D. L. Wilcox, J. W. Coburn, and H. F. Winters, "Electron-Beam Effects in Depth Profiling Measurements with Auger Electron Spectroscopy," J. Appl. Phys., 46(10), 4581-4583 (1975).

[49] L. F. Vassamillet and V. F. Caldwell, "Electron-Probe Microanalysis of Alkali Metals in Glasses," J. Appl. Phys., 40(4), 1637-1643 (1969).

[50] M. P. Borom and R. E. Hanneman, "Local Compositional Changes in Alkali Silicate Glasses During Electron Microprobe Analysis," J. Appl. Phys., 38(5), 2406-2407 (1967)

[51] A. K. Varshneya, A. R. Cooper and M. Cable, "Changes in Composition During Electron Microprobe Analysis of K_2O-SrO-SiO_2 Glass," J. Appl. Phys., 37(5), 2199 (1966).

[52] P. J. Goodhew and J. E. C. Gulley, "The Determination of Alkali Metals in Glasses by Electron Probe Microanalysis," Glass Tech., 15(5), 123-126 (1974).

[53] R. Hayami and H. Wakabayashi, "Compositional Changes During Electron Microprobe Analysis of Alkali Silicate Glasses," Yogyo-Kyokai-Shi, 78(4), 138-147 (1970).

[54] J. L. Lineweaver, "Oxygen Outgassing Caused by Electron Bombardment of Glass," J. Appl. Phys., 34(6), 1786-1791 (1963).

[55] D. Halliday and R. Resnick, Physics (Wiley: New York, 1966) 686-700.

[56] P. G. Shewmon, Diffusion in Solids (McGraw-Hill: New York, 1963) 137-162.

[57] W. D. Kingery, Introduction to Ceramics, (Wiley: New York, 1960) 217-243.

[58] G. S. Almasi, J. Blair, R. E. Ogilvie and R. J. Schwartz, "A Heat-Flow Problem in Electron-Beam Microprobe Analysis," J. Appl. Phys., 36, 1848 (1965).

[59] C. J. Powell, "Attenuation Lengths of Low-Energy Electrons in Solids," Surf. Sci., 44, 29 (1974).

[60] F. R. Bacon and G. L. Calcamuggio, "Effect of Heat Treatment in Moist and Dry Atmospheres on Chemical Durability of Soda-Lime Glass Bottles," Amer. Ceram. Soc. Bull., 46(9), 850-855 (1967).

[61] G. Keppeler and M. Heckter, "Temperature Dependence of the Alkalinity of GLass Surfaces," Glastechn. Ber., 10(1), 37 (1932).

[62] J. W. Coburn and E. Kay, "Techniques for Elemental Composition Profiling in Thin Films," IBM Research Report (IBM Thomas J. Watson Research Center: Yorktown Heights, New York, 1974).

[63] H. Winters and J. W. Coburn, "Influence of the Altered Layer on Depth Profiling Measurements," Appl. Phys. Lett., 28(4), 176-179 (1976).

[64] "Standard Methods of Test for Resistance of Glass Containers to Chemical Attack," ASTM Designation C 225-65, Am. Soc. Testing Mater. ASTM Std., Part 13, 192-197 (1967).

[65] F. R. Bacon, "The Chemical Durability of Silicate Glass," Glass Ind., 49(10), 554-559 (1968).

[66] S. A. Greenberg, "Thermodynamic Functions for the Solution of Silica in Water," J. Phys. Chem., 61, 196-197 (1957).

[67] Z. Boksay, G. Bouguet and S. Dobos, "The Kinetics of the Formation of Leached Layers on Glass Surfaces," Phys. Chem. Glasses, 9(2), 69-71 (1968).

[68] A. E. Clark, Jr., "Solubility and Biocompatibility of Glass," Ph.D. Dissertation, Univ. of Fla., Gainesville, Fla. (1975).

[69] C. G. Pantano, Jr., D. B. Dove and G. Y. Onoda, Jr., "AES Analysis of Sodium in a Corroded Bioglass Using a Low-Temperature Technique," Appl. Phys. Lett., 26 (11), 601-602 (1975).

[70] J. D. Mac Kenzie, Modern Aspects of the Vitreous State, Vol. 1 (Butterworths: London, 1960) 188.

[71] J. H. Escard and D. J. Brion, "Study of Composition of Leached Glass Surfaces by Photoelectron Spectroscopy," J. Amer. Ceram. Soc., 58, 296-299 (1975).

[72] H. Bach and F. G. K. Baucke, "Investigations of Reactions Between Glasses and Gaseous Phases by Means of Photon Emission Induced During Ion Beam Etching," Phys. Chem. Glasses, 15(5), 123-129 (1974).

BIOGRAPHICAL SKETCH

Carlo George Pantano, Jr. was born in Paterson, New Jersey on December 17, 1950. Elementary education was obtained in Hawthorne, N. J. In 1968, he was graduated from St. Lukes High School, Hohokus, N. J. College education began at Newark College of Engineering where he was graduated magna cum laude in 1972 with a Bachelor of Science in Engineering Science degree. Subsequently, he entered the University of Florida, first as a Graduate School Fellow and finally working as a graduate research assistant. He received a Master of Engineering there in 1974, from the Department of Materials Science and Engineering. Since that time, he has been pursuing a Doctor of Philosophy degree in the same department.

His work at the University of Florida has included the design and construction of apparatus to carry out Auger Electron Spectroscopy; hence a strong familiarity exists with high vacuum equipment, electron energy analyzers, electron and ion guns, and the peripheral electronics. Research concerned with surface reactions, particularly on glass, has led to a knowledge of surface chemistry and its characterization using Auger Spectroscopy, Infrared

Spectroscopy, Electron Microscopy and the necessary wet chemistry. Work on a consulting basis has provided further experience in applying these techniques to a variety of problems; for example, metal and glass corrosion, commercial glass container surface treatments, microcircuit processing, as well as other surface or thin-film related problems.

He has published papers in research areas concerning Auger electron spectroscopy, glass surface reactions, biomaterials surface analysis and vacuum technology. He is a member of Sigma Xi honorary, Alpha Sigma Mu honorary, AIME, ASM, ACS and AVS.

I certify that I have read this study and that in my opinion it conforms to acceptable standards of scholarly presentation and is fully adequate, in scope and quality, as a dissertation for the degree of Doctor of Philosophy.

G. Y. Onoda, Jr., Chairman
Associate Professor of Materials
Science and Engineering

I certify that I have read this study and that in my opinion it conforms to acceptable standards of scholarly presentation and is fully adequate, in scope and quality, as a dissertation for the degree of Doctor of Philosophy.

D. B. Dove
Professor of Materials Science
and Engineering

I certify that I have read this study and that in my opinion it conforms to acceptable standards of scholarly presentation and is fully adequate, in scope and quality, as a dissertation for the degree of Doctor of Philosophy.

L. L. Hench
Professor of Materials Science
and Engineering and Head of
Ceramics Division

I certify that I have read this study and that in my opinion it conforms to acceptable standards of scholarly presentation and is fully adequate, in scope and quality, as a dissertation for the degree of Doctor of Philosophy.

E. D. Whitney
Professor of Materials Science and Engineering

I certify that I have read this study and that in my opinion it conforms to acceptable standards of scholarly presentation and is fully adequate, in scope and quality, as a dissertation for the degree of Doctor of Philosophy.

E. E. Muschlitz
Professor and Chairman of Physical Chemistry Department

This dissertation was submitted to the Graduate Faculty of the Department of Materials Science and Engineering in the College of Engineering and to the Graduate Council, and was accepted as partial fulfillment of the requirements for the degree of Doctor of Philosophy.

June, 1976

Dean, College of Engineering

Dean, Graduate School